Climate Trends and Future Projections in the Region of Peel

Technical Report

February, 2016

Prepared for:

Region of Peel
Working for you

Prepared By:

Toronto and Region Conservation for The Living City — ONTARIO CLIMATE CONSORTIUM — RSI RISK SCIENCES INTERNATIONAL

Contributing Authors

Heather Auld, RSI
Harris Switzman, TRCA/ OCC
Neil Comer, RSI
Simon Eng, RSI
Shelley Hazen, TRCA/OCC
Glenn Milner, TRCA/OCC

Recommended Citation

Auld, H., Switzman, H., Comer, N., Eng, S., Hazen, S., and Milner, G. 2016. *Climate Trends and Future Projections in the Region of Peel*. Ontario Climate Consortium: Toronto, ON: pp.103

TABLE OF CONTENTS

ACRONYMS

AR5	Fifth Assessment Report of the Intergovernmental Panel on Climate Change
CMIP5	Fifth Coupled Model Intercomparison Project
EC	Environment Canada
GCM	Global circulation model
GTHA	Greater Toronto Hamilton Area
IPCC	Intergovernmental Panel on Climate Change
ORM	Oak Ridges Moraine
PCCS	Peel Climate Change Strategy
RCP	Representative concentration pathway
SRES	IPCC's Special Report on Emissions Scenarios
SREX	IPCC's Special Report: Managing the Risks of Extreme Events and Disasters to Advance Climate Change Adaptation
SDII	Simply daily intensity index

FIGURES

TABLES

EXECUTIVE SUMMARY

Warming of Earth's climate system is unequivocal. Historical observations demonstrate that the atmosphere and ocean have warmed, the amounts of snow and ice have diminished, sea level has risen, and the concentrations of greenhouse gases have increased. Future global surface temperature change for the end of the 21st century is likely to exceed 2°C relative to 1850 to 1900 assuming business-as-usual emissions continue. This translates to increasingly frequent and more extreme weather events in the future, such as extreme heat days (*virtually certain)*, heat waves (*very likely*), and heavy rainfall events (*likely*) over many areas of the globe (IPCC, 2013).

The Region of Peel needs to be prepared, in part by understanding its regional climate conditions. The purpose of this study is to characterize recent trends and future projections in climate across an array of climate indicators of interest to Peel stakeholders. Meant to serve as the foundation for a variety of sectoral vulnerability assessments, this study emerged out of Peel's Climate Change Strategy in 2011.

This study uses state-of-the-science climate modeling recommended by the IPCC. The ensemble of global climate models used in the most recent IPCC assessment is used to obtain the future climate conditions for the period of 2011 – 2100 ("future periods"). Each variable is modeled for the future periods and presented as 2020s (short term), 2050s (medium term), and 2080s (long term) projections. Historical observations are also obtained for the baseline period (1981-2010) to examine to what extent Peel's historical climate is projected to change into the future. Future emissions scenarios, or Representative Concentration Pathways (RCPs), are provided to tell the potential range of Peel's future climate conditions. RCP4.5 illustrates a moderate radiative forcing (less extreme) future whereas RCP8.5 illustrates a high radiative forcing (more extreme) business-as-usual future which global greenhouse gas concentrations are currently following. While data were analysed out to 2100 for both RCP scenarios, this summary will focus on the RCP8.5 scenario and provide more details on the 2050s planning horizon, which was selected based on corresponding work on vulnerabilities in the Region of Peel (see Table ES-1).

Peel's Climate in the 2020s

Temperatures in Peel Region are very likely to increase in all seasons, with the greatest increases projected for winter and for minimum temperatures. Increases by the 2020s are modest in comparison with those further into the future, with mean annual temperatures expected to rise 1.4°C assuming business-as-usual emissions. Temperature extremes are also expected to increase in frequency and intensity. Days reaching above 30˚C, for instance, will very likely increase by 5 days per year by the 2020s. In fact, it is likely that the greatest temperature increases will occur in Mississauga and Brampton (away from the cooler north and lakeshore environments); where the urban heat island effect could exacerbate the intensity and frequency of these extreme heat events in Peel.

Total precipitation is likely to increase overall throughout the year by the 2020s with winter and spring seasons showing the greatest increase, while summer and autumn precipitation are projected to remain steady or slightly decrease. Instances of extreme precipitation are likely to become more severe and frequent on a regional scale, resulting in some shortening of return periods associated with historical storm intensities. For example, 1-day and 5-day maximum precipitation amounts (historically 37mm and 59mm, respectively) are expected to increase by 5% in the 2020s, and the worst 1% of extreme precipitation events (similar to July 8th, 2013 for example) are on track to increase by 20% in magnitude should business-as-usual emissions continue.

Peel Region will experience a longer growing season in the 2020s as well, which could extend up to 14 days longer in the short term. Historically, Peel's growing season has been increasing since the 1960s beginning earlier in the spring and ending later in the fall. With increases in the growing season come opportunities for higher value crops and greater yields. Corn heat units, for example, are likely to increase and present a valuable opportunity in Peel Region for agricultural systems; however, if accompanied by a lack of precipitation, this trend may not be beneficial to producers. Into the future, extreme heat events may compound issues of growing season water shortages without proper management practices. With warming temperatures and more days with extreme heat, drought and moisture deficit conditions are projected to increase.

Peel's Climate in the 2050s

In the 2050s, temperatures in Peel Region are very likely to continue increasing in all seasons, with the greatest increases still projected for winter and for minimum temperatures. Mean annual temperatures are expected to rise 2°C assuming business-as-usual emissions, with average winter temperatures rising faster by up to 2.2˚C and average spring temperatures rising slower by 1.8˚C. Temperature extremes are also expected to increase in frequency and intensity. Days reaching above 30˚C, for instance, will very likely increase by 14 days per year by the 2050s. Days above 35˚C, which have historically not been observed in the Region of Peel, are expected to occur twice per year by the 2050s as well (see Table ES-1). Spatially, higher mean temperatures are typically found in southern Peel rather than in the northwest regions. In the medium term, northern Peel can be expected to warm at a faster rate than southern Peel, with Lake Ontario remaining a critical driver of Peel's temperature into the future. It is also likely that the greatest temperature increases will occur in Mississauga and Brampton (away from the cooler north and lakeshore environments); where the urban heat island effect could exacerbate the intensity and frequency of these extreme heat events in Peel.

Table ES-1

FUTURE PEEL: WHAT TO EXPECT IN THE 2050S?

[Assuming business-as-usual emissions, or RCP8.5, for a *subset* of climate indicators]

Climate Indicator	Where are we now?	Where are we headed?	Trending
Mean Annual Temperature (˚C)	7.4	9.4	↑
➢ Winter	-4.8	-2.6	↑
➢ Spring	6.1	7.8	↑
➢ Summer	19.3	21.3	↑
➢ Autumn	9.1	11	↑
Number of Days Tmax ≥ 30˚C	12	26	↑
Number of Days Tmax ≥ 35˚C	0	2	↑
Number of Days Tmin ≤ -10˚C	44	23	↓
Number of Days Tmin ≤ -15˚C	19	8	↓
Total Precipitation (mm/yr)	852	926	↑
➢ Winter (mm/mo)	61	71	↑
➢ Spring (mm/mo)	68	78	↑
➢ Summer (mm/mo)	77	78	↔
➢ Autumn (mm/mo)	77	82	↑
1-Day Max Precipitation (mm)	37	40	↑
5-Day Max Precipitation (mm)	59	65	↑
Simple Daily Intensity Index (mm/day)	6.5	7.0	↑
Growing Season Length (days)	169	203	↑

Total precipitation is likely to increase overall by the 2050s along with the most increase in precipitation in the winter and spring seasons, while summer and autumn precipitation are projected to remain steady or slightly decrease. Annually, 74mm more per year is expected in the medium term, most of which will be delivered in the winter and spring months (see Table ES-1). Spatially, on a seasonal and annual basis, northwestern Peel is typically the wettest area within Peel Region while the southern portion receives the least precipitation. Into the future, the north-south gradient is likely to increase due to an increase in lake-effect precipitation with increasing ice free conditions over Lake Huron to the northwest. Instances of extreme precipitation are likely to become more severe and frequent on a regional scale, resulting in further shortening of return periods associated with historical storm intensities. For example, 1-day and 5-day maximum precipitation amounts (historically 37mm and 59mm) are expected to increase by 8% and 10%, respectively in the 2050s. The worst 1% and 5% of extreme precipitation events are expected to increase by 51% and 28% in magnitude, respectively, should business-as-usual emissions continue.

Peel Region will experience a much longer growing season by the 2050s as well, which is expected to be over a month longer (34 days). Historically, Peel's growing season has been increasing since the 1960s beginning earlier in the spring and ending later in the fall. With increases in the growing season come opportunities for some crops. Corn heat units, for example, are likely to increase and present a valuable opportunity in Peel Region for agricultural systems; however, if accompanied by a lack of precipitation, this trend may not be beneficial to producers. Into the future, extreme heat events may compound issues of lacking moisture in the growing season. For instance, the number of growing season days with temperatures exceeding 30˚C is expected to increase by 29% on average by the 2050s. Moisture indices calculated using the water budget (precipitation less evaporation) for the growing season demonstrates a likely overall drier season in Peel (changing from a 9.3mm water surplus historically to a water deficit of 19.5mm).

Peel's Climate in the 2080s

By the 2080s, uncertainty increases further with climate models, but so does the degree of change in climate predicted for Peel Region. Temperatures are anticipated to continue to increase over all seasons and throughout the year to rise by 4.9˚C annually. Winter temperatures, should business as usual emissions continue, are expected to average above freezing at 0.6˚C. Temperature extremes are expected to increase in frequency and intensity much more significantly in the long term. Over 60 days of the year Peel could have temperatures exceeding 30˚C. Days above 35˚C, which have historically not been observed in the Region of Peel, are expected to occur 14 times per year in 2080s as well.

Total precipitation is likely to increase overall throughout the year into the 2080s, similarly with greatest increase in precipitation in the winter and spring seasons, while summer and autumn precipitation are projected to remain steady or slightly decrease. Annually, 99mm more per year is expected in the long term. The north-south gradient in precipitation patterns in Peel Region is likely to increase due to an increase in lake-effect precipitation to the north. The frequency of rain versus snow will continue to increase. Instances of extreme precipitation may become significantly more severe and frequent on a regional scale, although, as always, extremes are less certain. For example, 1-day and 5-day maximum precipitation amounts (historically 37mm and 59mm) could increase by 22% and 17%, respectively in the 2080s. The worst 1% and 5% of extreme precipitation events could increase by 90% and 46% in magnitude, respectively, should business-as-usual emissions continue.

Peel Region could experience a significantly longer growing season into the 2080s as well, with an increase of up to 54 days per year projected. This could increase agricultural opportunities from some crops. Corn heat units, for example, are likely to increase and present a valuable opportunity in Peel Region for agricultural systems; however, if accompanied by a lack of precipitation, this trend may not be beneficial to producers. Into the future, extreme heat events may compound issues of lacking moisture in the growing season. With potentially significantly warmer temperatures and more days with extreme heat (particularly in the growing season), drought and moisture deficit conditions are projected to increase. What is still uncertain is the degree to which extreme precipitation events provide relief to extreme heat events, and

particularly the frequency of precipitation throughout the growing season to buffer issues of moisture deficits. Perhaps a prudent assumption is that on average, the summer is likely to be drier, but may be punctuated by heavy rainfall events.

Uncertainty still exists for predicting the precise magnitude of changes into the future for certain climate drivers. This uncertainty is the result of multiple sources of variability resulting from natural variation in the climate between locations and from year-to-year, the abundance of climate models and embedded assumptions with each, and multiple plausible future emission scenarios. For example, extreme precipitation events have more uncertainty in their future projections than temperatures since local scale convection drives much of the extreme events, which is not captured well by global or regional climate models. Furthermore, extreme winds are considered much more uncertain since historical data is unavailable in most locations and in general climate models can struggle to replicate historical windspeeds and extremes.

Recommendations from this study include the following. Firstly, to work with climate and subject matter experts to continually liaise and update this work as new climate model projections become available to contribute better information towards adaptation planning and similar initiatives in the Region of Peel. Secondly, to be conservative when estimating risk with the climate information contained in this report. Finally, to continue understanding and addressing the impacts of climate change, such as bolstering higher resolution and long term monitoring programs to support better adaptive management and planning.

1. INTRODUCTION

1.1. Purpose of This Study

The purpose of this study is to characterize recent trends and future projections in climate across an array of variables of interest to stakeholders involved in implementing the *Peel Climate Change Strategy (PCCS)*. In 2011, the partners involved in the PCCS committed to completing assessments of climate change risk and vulnerability for infrastructure, the natural heritage system, communities and human wellbeing within the geographic area of the Region of Peel. A critical component of any climate risk or vulnerability assessment is a characterization of the relevant climate conditions. In the case of climate change, this involves characterizing current climate conditions and how they are anticipated to change in the future, along with how they have changed in recent history. Within the broader definition of "risk" employed by the Intergovernmental Panel on Climate Change (IPCC) in its Fifth Assessment Report (AR5) and Special Report on Extremes (SREX), this characterization constitutes an assessment of the "hazard" or "event" to which a system is exposed.

Beyond risk and vulnerability assessments, there are many areas of decision-making in both public and private sectors that are informed by analyses of climate, and in which impacts of climate change are already perceived to be occurring. Examples include stormwater management, public works, agricultural production, emergency planning and response, and public health monitoring. The occurrence of shifts in the timing of seasons, along with more frequent and intense extreme weather events in the Region of Peel have been linked to climate change, however there is a need to provide stakeholders with more clarity around these trends and future projections.

1.2. Overview of Climate Variables Analysed

The variables analysed in this report were identified to be of relevance to a range of stakeholders consulted as part of the following two risk and vulnerability assessment pilot projects:

(1) Critical infrastructure and shoreline property in Port Credit, Mississauga; and,
(2) The Agricultural Sector in Caledon (risks and opportunities to cash crop production).

Input was also received by other stakeholders throughout the Region of Peel through a project advisory group. The variables analysed in this study area summarized in Table 1, and Section 2 provides technical details on and the rationale for the procedures used for producing localized information for the Region of Peel. In summary though, historical spatial and temporal trends for each variable in Table 1 were analysed for a baseline period of 1981-2010 using a combination of Environment Canada climate station and gridded time series data from the CANGRD product developed by McKenney et al. (2011). Future projections for the Region of Peel were derived using raw output from the ensemble of global circulation models (GCMs) used in the IPCC's

AR5 report. The IPCC's analysis of global climate change used in this study relies on a set of consistent modeling experiments coordinated under the Fifth Coupled Model Intercomparison Project (CMIP5), coordinated by the World Climate Research Program.

Table 1: Summary of climate indicators and datasets used for analysis.

Climatic Driver	Climate Indicator Produced[1]	Historical Raw Dataset	Future Climate Projection Raw Dataset[2]
Temperature	Average Monthly Maximum Temperature, T_{max} [°C]	EC monthly homogenized & CANGRD Daily	tasmax
	Average Monthly Minimum Temperature, T_{min} [°C]	EC monthly homogenized & CANGRD Daily	tasmin
	Average Monthly Temperature, T_{mean} [°C]	EC monthly homogenized & CANGRD Daily	Calculated from tasmin/tasmax
Precipitation	Total Monthly Precipitation [mm]	EC monthly homogenized & CANGRD Daily	pr
Windspeed	Average Monthly Windspeed [m/s]	EC monthly homogenized	Calculated from wind components: uas & vas
Humidity	Average Seasonal Specific humidity [kg/kg]	Not Available	huss
	Average Monthly Relative humidity [%]	EC historical archive	hurs
Growing Season	Annual Corn Heat Units [CHU]	EC monthly homogenized & CANGRD Daily	Calculated from ts
	Annual Growing Season Length (frost-free period)	EC historical archive & CANGRD	Calculated from tasmin

[1] Unless otherwise specified in the indicator description, all computations were done on the monthly basis

[2] The names of these datasets represent the raw climate model output from the CMIP5. Unless otherwise specified, datasets are available for the full CMIP5 ensemble for the scenarios of RCP4.5 and RCP8.5

Climatic Driver	Climate Indicator Produced[1]	Historical Raw Dataset	Future Climate Projection Raw Dataset[2]
	[days]		
	Annual Growing Season Start Date [date of year]	EC historical archive & CANGRD	Calculated from tasmin
	Annual Growing Season End Date [date of year]	EC historical archive & CANGRD	Calculated from tasmin
	Number of years in a normal period when both growing season precipitation and CHUs are between 5 and 10% ABOVE historical monthly [years]	EC historical archive & CANGRD	Calculated from pr and ts
Hot Days	Days per month with $T_{max} \geq$ 30°C, 35°C, 40°C [days]	EC historical archive & CANGRD	Calculated from tasmax
Cold Days	Days per month with $T_{min} \leq$ X, -5°C, where X = {-5, -10, -15,} [°C]	EC historical archive & CANGRD	Calculated from tasmin
Drought / lack of moisture	Days per month with no precipitation [days]	EC historical archive & CANGRD	Calculated from pr
Snow and Ice	Monthly Ice Potential: number of freezing rain events in a month, where freezing rain was defined as a day with precipitation AND where $T_{max} <$ 2°C and $T_{min} >$ -2°C [days]	EC historical archive & CANGRD	Calculated from pr, tasmin, tasmax
	Number of monthly freeze-thaw cycles, where $T_{max} \leq$ 0°C and $T_{min} >$ 0°C [days]	EC historical archive & CANGRD	Calculated from tasmax and tasmin
	Days per month with $T_{min} \leq$ X, where X = {5, 3, 0, -2, 1.7} [°C]	EC historical archive & CANGRD	Calculated from tasmin
Extreme precipitation	Annual 1-day maximum precipitation accumulation [mm]	EC historical archive & CANGRD	r1d[3]

[3] Raw data extracted from variables in the CLIMDEX experiment led by Environment Canada: www.cccma.ec.gc.ca/data/climdex/climdex

Climatic Driver	Climate Indicator Produced[1]	Historical Raw Dataset	Future Climate Projection Raw Dataset[2]
	Annual 5-day maximum precipitation accumulation [mm]	EC historical archive & CANGRD	r5d[3]
	Annual Simple daily Intensity index (SDII) [mm day^{-1}]	EC historical archive & CANGRD	SDII[3]
	Annual 95th Percentile Daily Precipitation [mm]	EC historical archive & CANGRD	r95t[3]
	Annual 99th Percentile Daily Precipitation [mm]	EC historical archive & CANGRD	r99t[3]

2. METHODOLOGY

2.1. Overview

Figure 1 provides a graphical overview of the steps used in this study, which are detailed further throughout this Section of the report. Historical trends in climate were analysed using a combination of gridded historical and climate station-based time series acquired from Natural Resources Canada and Environment Canada, respectively. These datasets were quality controlled using graphical methods and by comparing key climate statistics (See Section 2.2). For historical analysis recent trends in climate, three 30-year normal periods representing the 1970s (1961-1990), 1980s (1971-2000) and 1990s (1981-2010) were used for selected variables wherever dataset time series were long enough. Analysis was completed on daily time series data with respect to spatial, seasonal and long-term trends for each variable and as many normal periods as possible. A baseline period of 1981 to 2010 was then established for comparison of historical and future trends.

The future climate analysis was done by comparing the difference between historical and future modeled results, known as “deltas” (see Section 2.5). These delta values were processed into 10-year periods for each variable described in Table 1 and a variety of ensemble summary statistics were calculated for each period, including the mean, standard deviation and multiple quantiles. The source of future climate data was an ensemble of the full global climate model output available from CMIP5 for the grid cell best representing the Peel Region (See additional details on climate model ensembles in Section 2.3). An ensemble is a collection of individual model results, either from multiple different models or the same model run with different parameters. With respect the CMIP5, the members of the ensemble include multiple global climate models, in addition to multiple runs of the same model.

The CMIP5 ensemble used in this study is that the same dataset used by the IPCC in its AR5 report. For certain variables, higher resolution climate modeling output was available from the most recent Canadian regional climate model (CanRCM4) and this data was also included in the analysis, but does not represent an ensemble of localized projections.

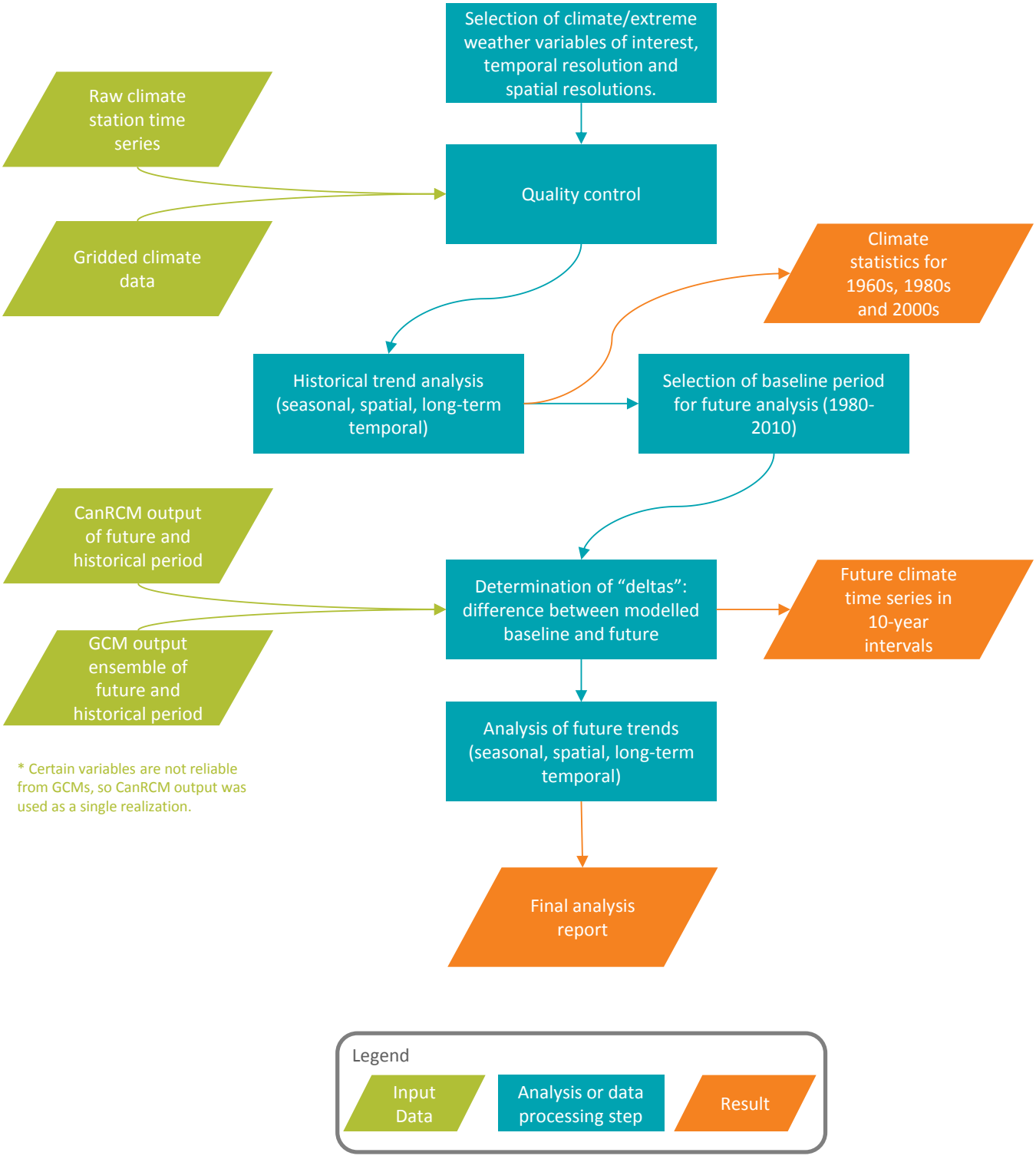

Figure 1: **Conceptual diagram of the data inputs, processing steps and outputs of this study.**

2.2. Historical Trend Analysis

Most of the variables analysed in this study required algorithms to generate time series of climate statistics based on daily or hourly records of temperature, wind velocity, precipitation, humidity or some combination thereof. Given the need to analyse long-term changes in climate over several normal periods of interest, it was necessary to rely on data with a long period of record to cover at least the two most recent normal periods of 1971-2000 and 1981-2010, and with minimal gaps. When these search criteria were applied to all Environment Canada, provincial, conservation authority, municipal and known private climate datasets in the Region of Peel, or within a 50 km radius of Mississauga and Brampton, the only two viable stations were Toronto Pearson Airport and Orangeville MOE (see Table 2 and Figure 2 for a map).

Table 2: Summary of station data available for historical trend analysis.

Station	**Daily Data**		**Hourly Data**	
	Variables	Period of Record	Variables	Period of Record
Toronto Lester B Pearson Int'l A (6158733)	T_{min}, T_{max}, T_{mean}, Heat Degree Days, Cool Degree. Days, Total Rainfall, Total Snowfall, Total Precipitation, Wind Velocity	1937 – 2013	Temperature, Dew Point, Relative Humidity, Wind Velocity, Air Pressure	1953 – 2013
Orangeville MOE (6155790)		1961 – 2013	Not available	Not available

In order to analyse spatial trends, and then calculate future "deltas", a spatially interpolated product with a resolution of approximately 10 x 10 km, called CANGRD, was used to map baseline temperature and precipitation. The CANGRD product was developed collaboratively by Natural Resources Canada and Environment Canada (Hopkinson et al, 2012; McKenney et al, 2011), and is a dataset of spatially and temporally interpolated daily temperature and precipitation data using Environment Canada station observations for the period of 1951 to 2010. This dataset has been used extensively within Canada and the interpolation techniques have been employed internationally as well. The CANGRD domain employed in this study is presented in Figure 2.

For this study, the most recent standard normal period of 1981-2010 was used to produce a baseline climate. Full details of the CANGRD interpolation procedure can be found in in Hopkinson et al. (2012) and McKenney et al. (2011), but a summary is provided in the following sub-section of this report.

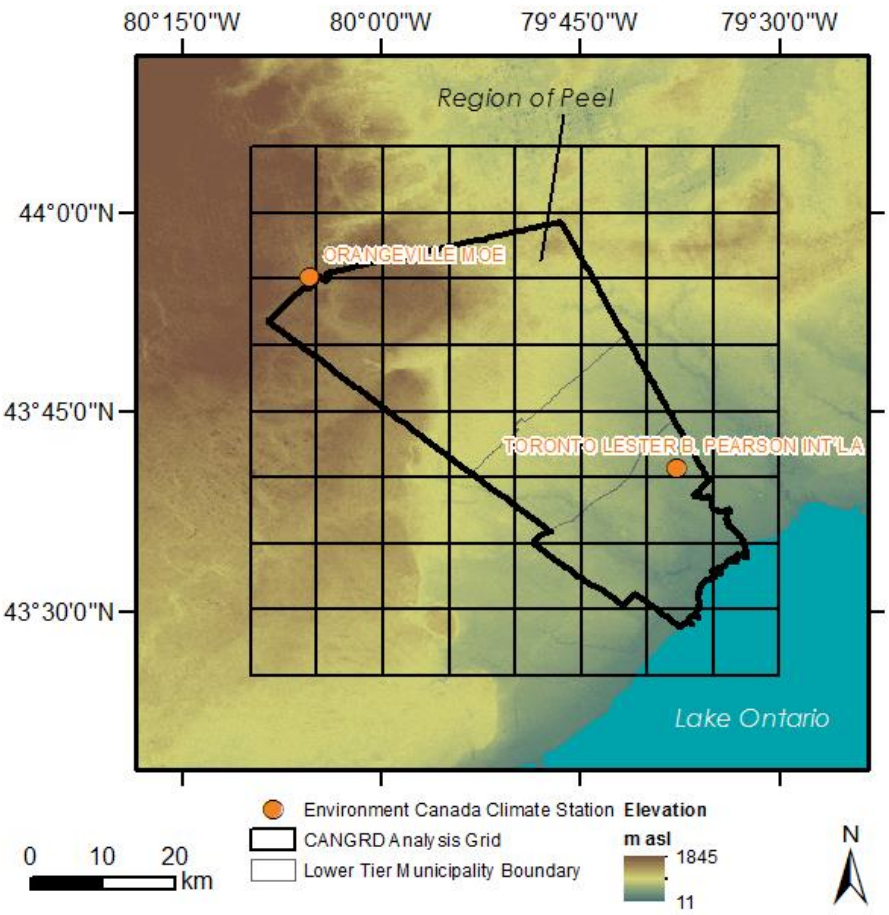

Figure 2: The Peel CANGRD points considered (64 are shown below on an 8 by 8 grid cell area of 10km).

CANGRD Overview

Observed daily station temperatures (maximum, minimum) and precipitation (including rain and snow) are used for the interpolation. A software package called ANUSPLINE uses a smoothing-spline technique to interpolate between stations to produce a continuous climate surface. Stations with data records greater than 5 years were included, and the procedure includes effects of station proximity and elevation. In general the CANGRD data represents the climate condition very well, but in data-sparse regions of Canada's north, the margin of error is large. This is not a factor in Southern Ontario, as the Environment Canada monitoring network is denser and more temporally consistent. Using a withholding technique (where 48 station observations across Canada were removed from the procedure), interpolated values showed average differences of 0.36°C, 0.66°C and 4.7mm compared to the observed maximum temperature, minimum temperature and total annual precipitation normals for 1971-2010. For the Region of Peel, CANGRD is a good representation of climate as shown for the Toronto Pearson Airport, location above. Figure 3 presents a timeseries comparison of annual average temperature and total annual precipitation for the period of 1981 to 2010 and demonstrates good agreement between the Environment Canada station and its overlapping CANGRD grid

point. There is similar agreement in Orangeville and McKenney et al. (2011) has validated the use of CANGRD across Canada.

(A) Average Annual Air Temperature (B) Total Annual Precipitation

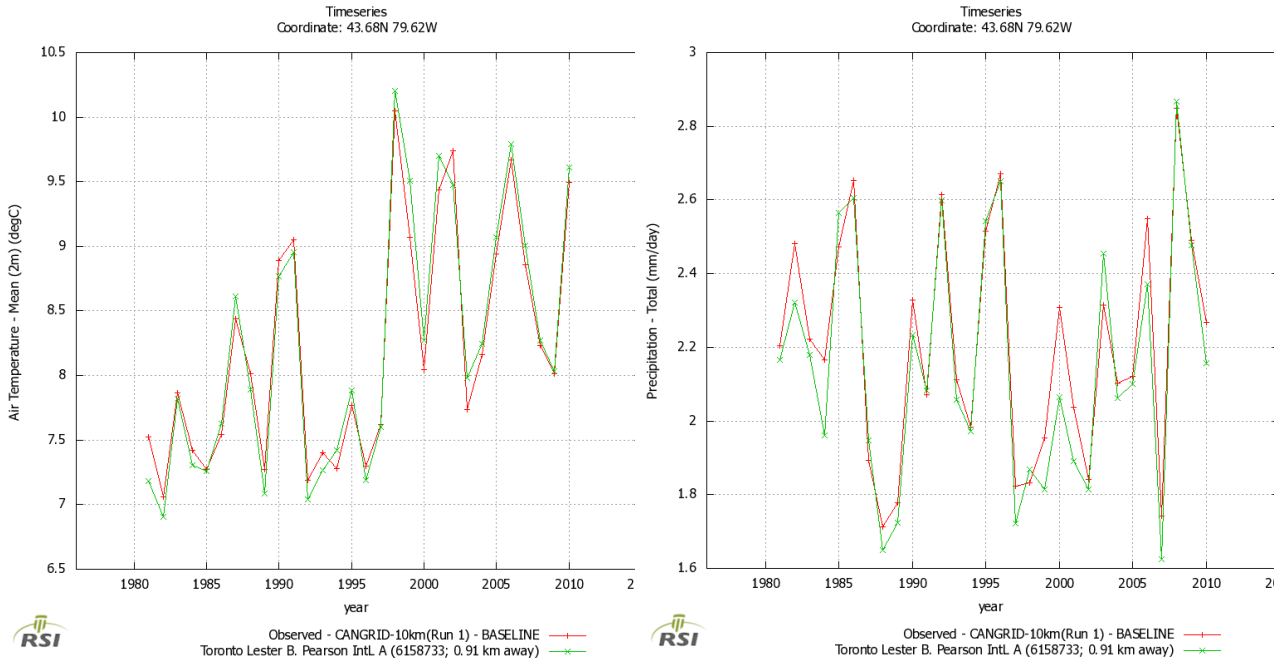

Figure 3: Comparison between Toronto Pearson Airport Station and its overlapping CANGRD grid point for 1981-2010 for the variables of (A) mean annual temperature and (B) total annual precipitation.

2.3. The Ensemble Approach to Climate Change Analysis

Since the Second IPCC Assessment was released in 1995, the number of international climate modelling centres contributing to global analysis of climate change, along with the quantity of models and their complexity, has increased. There are currently forty models which comprise the IPCC's AR5 ensemble, compared to eleven in 1995. With increased computing power, better refinement of atmospheric phenomena has been incorporated, and model spatial and temporal resolution has improved (Kharin et al. 2013). An important outcome of this increase in model availability is a greater ability to produce projections of climate based upon an 'ensemble' of many models.

The ensemble, or multi-model, approach to projecting climate has the advantage of capturing a full range of possible climate scenarios and representing those projections using a statistical distribution. Statistical distributions are useful because they allow the user to interpret trends probabilistically and assess the uncertainty associated with climate modeling. Research has

also indicated that the use of multi-model ensembles has the advantage of accounting for all possible biases associated with individual models and can therefore provide the user with the most robust analysis of overall trends in climate (IPCC-TGICA, 2007, Tebaldi and Knutti, 2007). Individual models represent climatological processes slightly differently and each has its own biases (Sheffield et al. 2013). The use of only one or two climate models can potentially introduce gross errors and lead to misinterpretation of future trends, given that certain individual model biases can become prominent. The use of numerous models, on the other hand, averages out the random errors in individual models. Once model biases are adjusted, the remaining signal provided by the ensemble is that associated with trends in climate change. Using ensemble projections from the family of global modelling centers therefore produces the most comprehensive estimate of climate change projections on a large scale (Sheffield et al. 2013; Gleckler et al. 2008). With the ensemble approach, individual biases tend to be reduced while the uncertainty associated with the overall modeling process is maintained and can be propagated through subsequent analysis and local-scale modeling (Giorgi et al. 2009; Gleckler et al, 2008). A key limitation with relying solely on GCMs however, is that their coarse spatial scale prevents them from capturing the effect of local features that can influence certain climatological processes at this scale (Giorgi et al. 2009). This is particularly the case in capturing the finer scale influences of inland features, or processes driven by local conditions such as convective precipitation in the Great Lakes region (AMEC 2014, Bürger et al. 2012) and land use influences (agricultural, urban, etc.) that occur at localized, highly seasonal scales. While regional climate models and certain downscaling procedures can better capture regional scale and topographical influences on climate, these approaches have their own limitations.

Both statistical and dynamical downscaling techniques rely on GCMs to drive local-scale modeling and analysis, and ideally the uncertainty associated with the GCMs should be propagated through the downscaling process (Wilby et al. 2004). Additionally, historical and downscaled local climate estimates of extreme events have been observed in many studies to lie within the uncertainty bounds of raw GCM ensembles (Peters et al. 2012). Finally, statistical downscaling relies on historical relationships among climate variables of various scales, and there is uncertainty as to whether these relationships will hold under evolving conditions associated with climate change.

Given that the quantification of uncertainty associated with future climate projections was a key element of the trend analysis required in this study, it was felt that using a full range of GCM projections in an ensemble was the most robust way of capturing the full range of uncertainty associated with climate projections in Peel Region. Future local studies could apply downscaled products either derived from individual members of the ensemble or ensemble statistics with an understanding of how these datasets fit within the range of future climate uncertainty.

Figure 4 provides a conceptual diagram of the sources of uncertainty associated with future climate modeling and highlights the elements captured explicitly in this study. All available CMIP5 model runs were used for as many of the variables as possible to capture the uncertainty associated with climate models. A full list of the climate models and their country of origin is presented in Appendix A. Two emissions scenarios were used to represent moderate and high forcing, and where possible, variability in monthly variables for each averaging period

was calculated to reflect uncertainty in the baseline climate. Section 2.4 provides a description of the emission scenarios used.

(A) Conceptual Diagram of Projection Uncertainty

(B) Sources of Global Projection Uncertainty (from IPCC 2013 p.979)

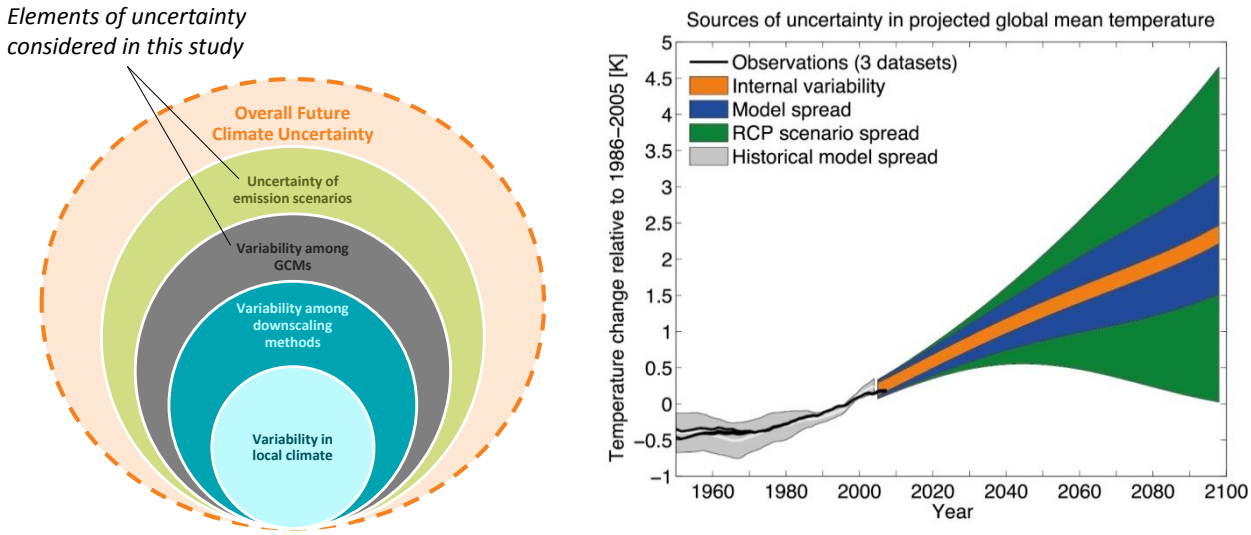

Figure 4: **Conceptual diagrams of the elements of uncertainty associated with future climate projection. (A) is a conceptual diagram of different sources of variability and (B) shows how they are manifested in the CMIP5 experiment from IPCC (2013).**

2.4. Selection of Emission Scenarios

A new initiative in the IPCC AR5 is the introduction of Representative Concentration Pathways (RCPs) to represent future emission scenarios. These scenarios represent future releases of greenhouse gases, aerosols, and other pollutants into the atmosphere, along with information on land and resource use which combine to provide inputs to drive climate change models that simulate different climate conditions (Taylor et al. 2012). The scenario of lowest climate forcing is RCP 2.6, which represents an increase of 2.6 W/m^2 in radiative forcing to the global climate system, while the highest RCP 8.5 represents an increase of 8.5 W/m^2 of energy (see Figure 5). There are also assumptions embedded in each RCP about how emissions will change over time and these are highlighted graphically in Figure 6. Any single radiative forcing pathway can result from a diverse range of socioeconomic and technological development scenarios. Factors influencing the RCP which might occur include population growth, economic growth, degree of urbanization, land use change, use of renewable versus carbon-based energy sources and any future international agreements on greenhouse gas (GHG) emissions, among others.

WHICH SCENARIO IS THE MOST EXTREME?

The RCP8.5 scenario represents the closest, most realistic, pathway to observed temperature trends historically, and additionally provides the strongest climate change signal which would be associated with extreme events. It aligns closely with the A2 scenario from the CMIP3 experiment used in AR4.

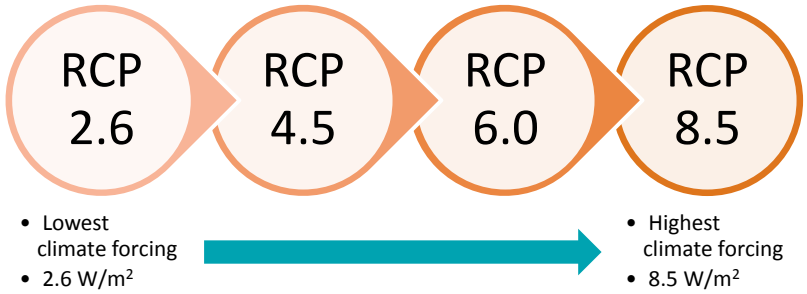

Figure 5: Summary of the climate forcing associated with the different CMIP5 scenarios.

The scenarios between RCP 2.6 and RCP 8.5 encompass a large range of possibilities associated with global climate change. It is unknown which of the RCPs will apply in the future, however it is important to note that historically, the GHG emissions have followed the highest (8.5) pathway (Peters et al. 2012) (see Figure 7). In the absence of a global agreement on GHG reduction, a conservative view to the future would suggest that it is prudent to assume this trend will be maintained in the near-term. Climate change projections indicate these trends will continue regardless of the RCP considered – simply that the change will be greater with the higher RCP8.5. The future projections between the two extreme RCPs begin to diverge significantly after the year 2050. Nevertheless, in this report, RCP 4.5 (moderate) and RCP 8.5 (high) emission scenarios are presented for each variable. Until the 2050s, projections for both scenarios are quite similar. This is consistent with IPCC findings. The number of models used for the ensemble varies with the RCP selected since not all international modelling centres generated model runs for all scenarios.

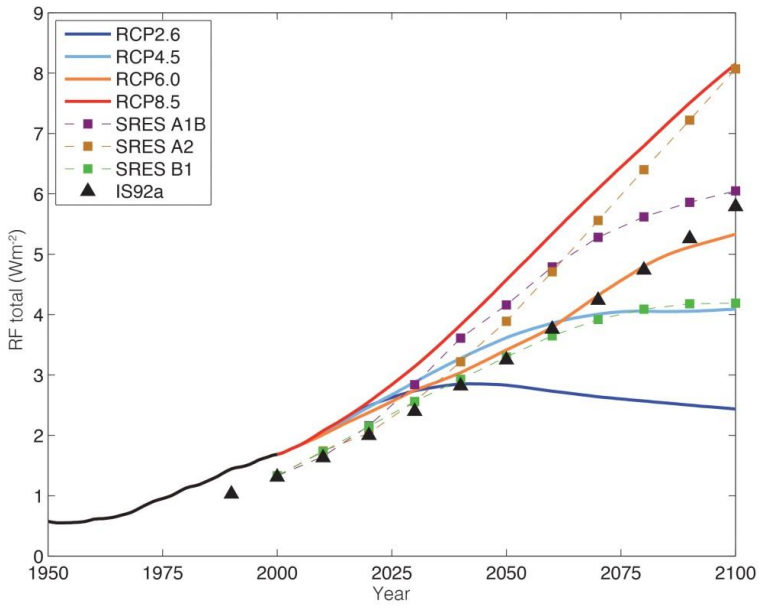

Figure 6: **Global greenhouse gas emission scenarios from CMIP3 (SRES Scenarios) and CMIP5 (RCP scenarios), expressed as Total Radiative Forcing over time (From IPCC 2013, Figure 1-15).**

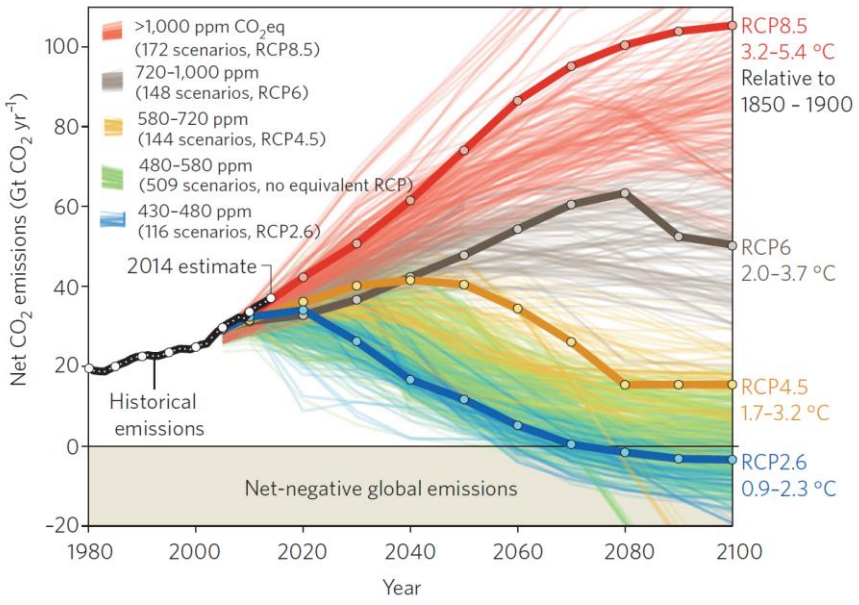

Figure 7: **Comparison of actual emissions to various RCP scenarios showing an estimate for 2014 tracking along the pathway of RCP8.5 (from Fuss et al. 2014).**

2.5. Delta Approach to Downscaling

This study uses a delta approach (sometimes also called 'climate change factor approach'), to obtain future estimates of climate variables for the local area in the Region of Peel. The delta approach has been commonly used as a simple way of adding spatial detail on historical climate to large-scale climate change projections (Bürger et al. 2012).

The delta approach is one of several methods which can be used to obtain projections of future climate. It is perhaps the simplest to obtain and to understand, and has been used widely because of its straightforward procedure and parsimonious approach. When this method is coupled with the use of a multi-model ensemble to generate climate projections, the result is a robust characterization of uncertainty compared to the use of a single model.

This is not to say that the delta approach is the only method available for climate change studies. Instead of using a delta ensemble approach, the delta approach could also be applied to a single model; however, the projection estimates would therefore rely on one's assumption that the single model employed was the ideal choice. In climate science there are tradeoffs between model complexity and expediency. Another approach is simply to run a very high resolution model once over the area of interest (so called 'dynamical downscaling'). In the simplest of terms one can either have 'many model runs at a coarse resolution' or 'few model runs at high resolution'. These high resolution models are called 'Regional Climate Models' (RCMs). There are RCMs available, but this data can be difficult to obtain and they still require a coarser resolution CMIP5 model or earlier model as an input. Over North America, the North American Regional Climate Change Assessment Program (NARCCAP) has assembled less than a dozen RCMs for various time periods (http://www.narccap.ucar.edu/) using the GCMs and emission scenarios employed in the IPCC's Fourth Assessment Report. Because these models are high temporal and spatial resolution (e.g., hours and 10s of kilometers), there are fewer available compared to the full suite of CMIP5 Global Climate Models. In addition, there are far fewer model runs from which to obtain an average climate change value. Furthermore, various studies indicate that the most important factor in the validation of these RCMs is the skill of their driving model (GCM) (e.g. EBNFLO Environmental AquaResource 2010; Deidda et al. 2013; Flato et al. 2013; Zwiers 2014).

Thus, to make scientifically robust and confident projections of the future climate, it first has to be demonstrated that global or regional climate models are sufficiently realistic in simulating the present climate. The level of agreement between model simulations and observations of the present climate is used as a method of assessing model reliability. It is assumed that models or ensembles which adequately simulate the present climate will provide more reliable projections of the future. Thus, for this study, the decision was to use many coarser models from which to obtain the climate change signal rather than fewer higher resolution models. The coarse projection 'delta' is then applied to a spatially distributed gridded dataset of the 1981-2010 baseline climate to create a geographic map of future climate.

There is also another method used in climate change studies to obtain future estimates of climate conditions known as 'statistical downscaling.' The main drawback of this technique is that climate projections can only be obtained from either specific observation stations that have sufficiently long data records, or from gridded climate data. This method calibrates historical climate observed at an observation station (for example Toronto Pearson Airport) or from gridded climate analyses for any location, with historical model data at a coarse scale (called 'predictors'), to obtain a statistical relationship. For example, perhaps the daily temperature observed is related to the modeled upper atmosphere wind direction. If one provides the future upper atmosphere wind direction from a gridded climate change model, it could then be used as one of the variables to predict the future temperature. The difficulty with this process even with pre-constructed software is that spurious associations based on pure statistics and not climatology can be applied which could produce unrealistic future conditions. This procedure would also have to be repeated for all station locations for which there was long term reliable station observation data to produce estimates of climate change for only those specific locations. An IPCC document entitled "Guidelines for Use of Climate Scenarios Developed from Statistical Downscaling Methods" (Wilby et al, 2004) further discusses these procedures.

The use of the delta method in this study can be summarized in the following 5 steps:

Step 1. Obtain a baseline climate condition (or 'average' climate). In this case, the CANGRD data is used to obtain these conditions for the 1981-2010 period at 10 x 10 km resolution.

Step 2. Using an ensemble of all available CMIP5 models, we obtain the model average climate for this same period – the average of all models for the grid covering Peel Region. However, each modeling centre does not use the same grid alignment and resolution, so a first step before obtaining the average of all the models is to re-grid them all to a common resolution. This re-gridding typically uses a scale representative of the resolution of the models, in this case approximately 200 by 200 km. In this project, the standard regular 0.5° grid used by the U.S. National Oceanic and Atmospheric and Administration (NOAA) National Centers for Environmental Prediction (NCEP) was employed (Figure 8). Each CMIP5 GCM was re-gridded to the NCEP grid using a linear interpolation algorithm. For this study, the NCEP re-gridding results in 2 cells covering Peel region (one in the northern portion and one in the southern portion). This result necessitated the investigation of the climate change signal difference between the 2 neighbouring cells, since it is not advisable to split this signal based upon an arbitrary artificial boundary imposed by the NCEP grid which happens to bisect Peel. This could introduce an artificial north-south gradient which is not realistic. The preference is therefore to use one of these two cells and apply it equally over the entire Peel region.

An investigation of the projected annual temperature and precipitation change between the northern and southern cells covering Peel demonstrated small, and statistically insignificant differences in these 2 primary variables. Any differences found are well within the range of the entire multi-model ensemble distribution. The greatest 'uncertainty' results not from the selection of the north or south cell, but in the range of actual models. This indicates that use of either of the 2 re-gridded cells over Peel region would result in near identical projections and would in no way alter any of the conclusions of this report. The use of an equally averaged value of the two

cells would generate an even smaller difference. For this reason, a decision was made to apply the northern cell's climate change signal over the entire Peel region study area. Additionally, the slightly smaller climate change signal from the northern cell is more in agreement with the historical greenhouse gas emission pathway we have observed. A more detailed description of this selection process is provided in an appendix to this report (Appendix B).

Step 3. The CMIP5 ensemble future climate is obtained for the NCEP grid cell for each of the required future periods. In this case, every 10 years starting in the year 2011 and ending in the year 2100. From this, average future conditions are obtained for all the models for ten 10 year periods. This required time series retrieved from the following data portals for the CMIP5 results and CLIMDEX extreme climate indicator database:

- CMIP5 Data Portal: http://cmip-pcmdi.llnl.gov/cmip5/guide_to_cmip5.html
- CLIMDEX database: www.cccma.ec.gc.ca/data/climdex/climdex

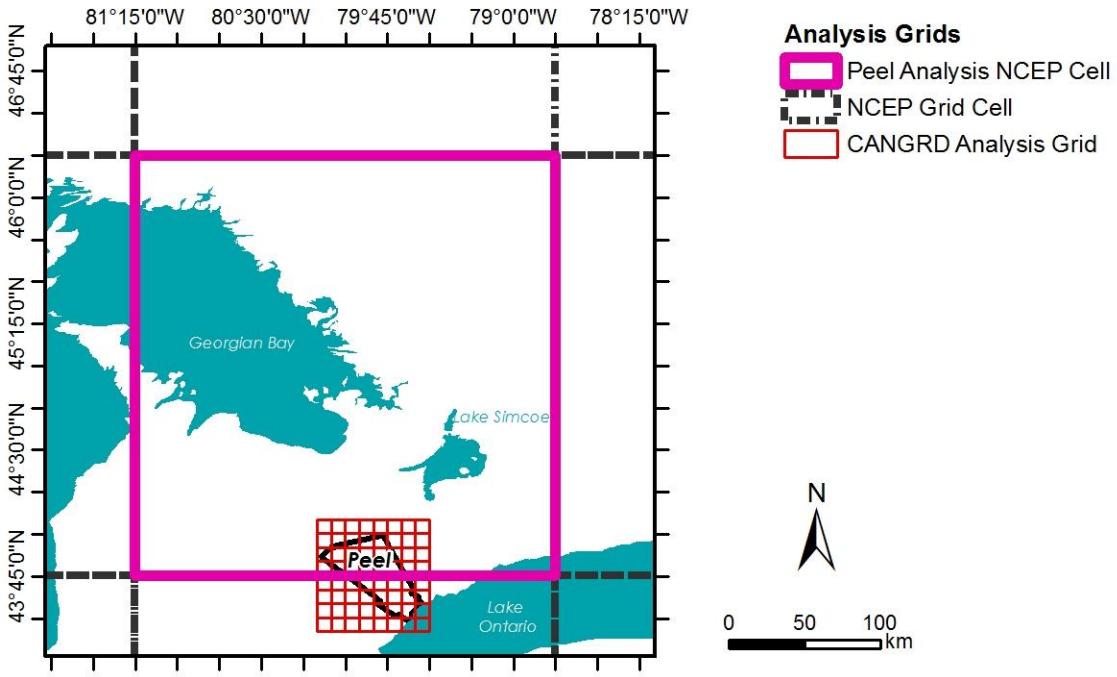

Figure 8: **The CMIP5 GCM re-gridded cell used for this study.**

Step 4. The difference (or 'delta') between the CMIP5 baseline and CMIP5 future periods are computed to represent the change in climate, as determined purely by the model ensemble (Equation 1).

$$\Delta_{i,p} = C_{i,p} - B_{i,p} \quad (1)$$

Where Δ is the delta value, C is the climate model projection value and B is the baseline value for the ensemble statistic, subscript i, and averaging period, subscript p, in question. One delta is produced for each ensemble statistic and each averaging period.

Step 5. The final step is to then add this delta value to the CANGRD baseline period value. This has the effect of correcting for any difference (or bias) between the true measured baseline climate and the CMIP5 baseline climate. After applying the delta to the CANGRD baseline, we have a spatially disaggregated climate average for each of the ten future periods at the local scale.

For this study, CANGRD daily maximum and minimum temperature, along with daily precipitation for the period of 1981-2010 was obtained for the 64 cells covering Peel region. From this data, a baseline 'normal' climate was calculated, representing average conditions for each cell. Baseline calculations at this resolution were calculated from these data except for those variables not available from CANGRD. Variables unavailable include mean windspeed and humidity. Historical data were only available for humidity and windspeed from the Toronto Pearson Airport station. Observations of these two variables at high spatial resolution throughout Peel are not available and it would not be reasonable to interpolate station data for these variables. Thus, historical observations from Toronto Pearson Airport were used to represent the baseline condition for Peel Region.

2.6. Validation of the Ensemble

The use of the CMIP5 ensemble not only allows for the calculation of an average projection of future climate which represents the consensus of all independent models, but it also allows for the estimation of projection uncertainty and statistical distributions which could not be determined from a single model. The projections for the variables in this report represent the 'best estimate' available and are more indicative of the general expectations of climate change over any single model, as was discussed in Section 2.3.

Perhaps the best way to demonstrate the benefit of the ensemble technique is to evaluate the ensemble skill in replicating historical climate. The temperature and precipitation comparisons are shown in Figures 9 and 10, respectively, and in all months, seasons and on the annual basis, the ensemble provides a good reproduction of observations. It is important to note that even the observed data are not in exact agreement (they are generally within 0.5 a degree), as differing interpolation techniques are used. It is not expected that the CMIP5 ensemble value should match the single data point plotted for the Toronto Pearson Airport or Orangeville Station locations, but rather that the historical observed values be contained within the ensemble range. This is indeed the case for these two Environment Canada stations and CANGRD average with respect to temperature (Figure 9). The ability of the CMIP5 ensemble to reproduce the historical temperature gives us confidence that the newest models used in this report are reliable and when grouped in an ensemble, can provide accurate estimates of trends.

Precipitation is not as accurately reproduced by the CMIP5 ensemble based on the comparison of historical model output to the observed datasets, but in almost all months the observed

values lie within the overall ensemble range (Figure 10). Annually, the CMIP5 ensemble does overestimate all observed datasets, but the general pattern of precipitation over the year is well represented by the ensemble median, or mean. It is also notable that precipitation at the Pearson Airport station is also consistently over-estimated by the ensemble and also the CANGRD cell. Finally of note is the larger range of precipitation from the CMIP5 ensemble in the summer months (June-August) versus winter months and an overestimate particularly in March.

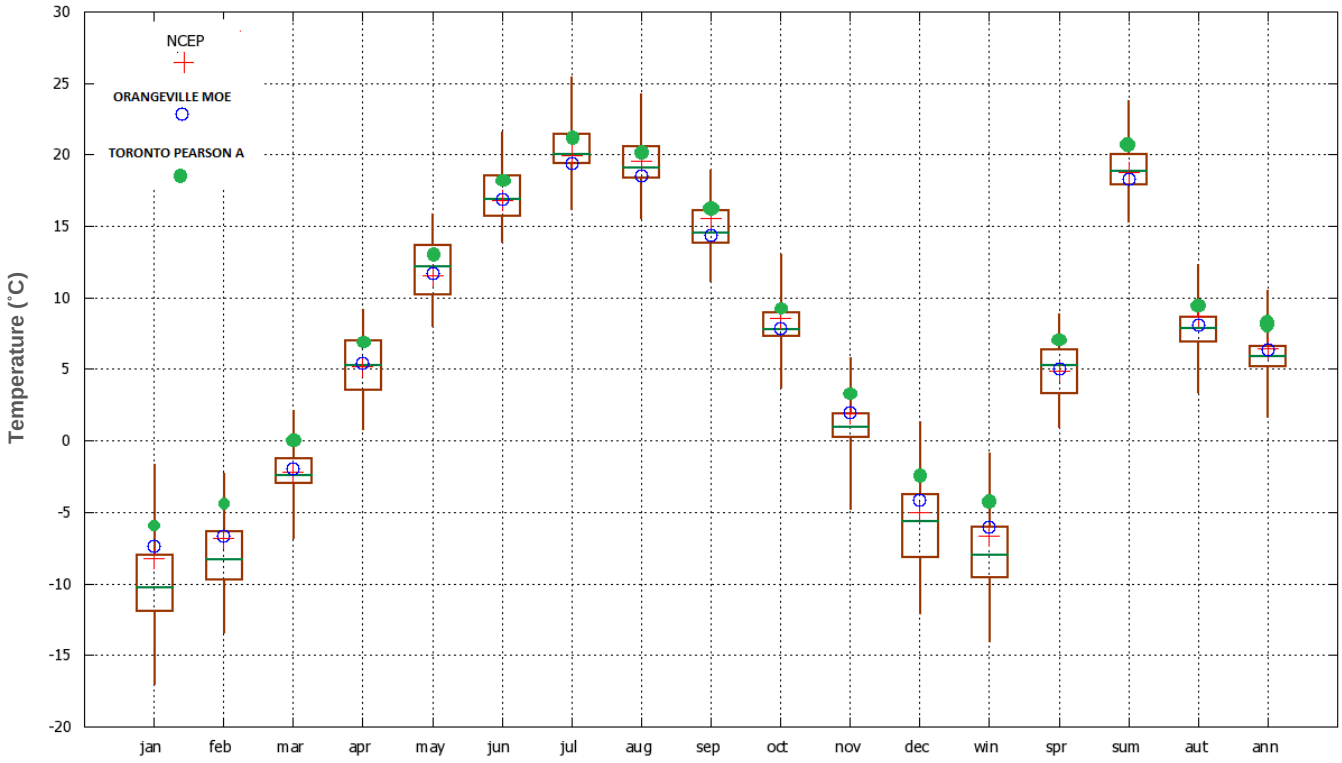

Figure 9: **The comparison between the CMIP5 ensemble temperature and observation datasets (see legend) for baseline period used in this report (1981-2010). The CMIP5 ensemble is represented in the boxplot by the brown box (upper=75th percentile value of the models, lower box =25th percentile, green horizontal line =median of models, brown vertical lines shows the full range of ensemble model projections).**

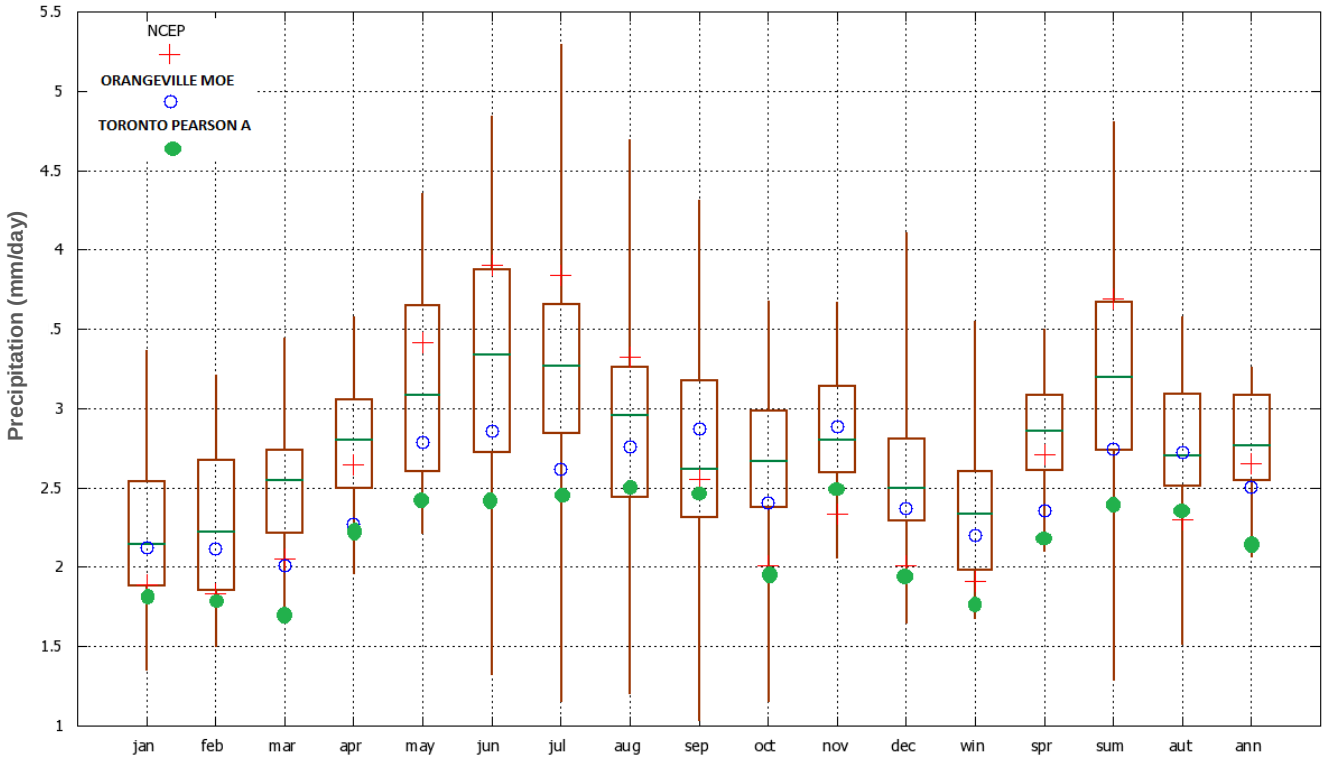

Figure 10: **The comparison between the CMIP5 ensemble precipitation and observation datasets (see legend) for the baseline period used in this report (1981-2010). The CMIP5 ensemble is represented in the boxplot by the brown box (upper=75th percentile value of the models, lower box =25th percentile, green horizontal line =median of models, brown vertical lines shows the full range of ensemble model projections).**

The summertime discrepancy is likely the result of greater convective-type precipitation in the summer and differences between models in handling this precipitation process. Convective precipitation is difficult for models to capture due to its small scale compared to the GCM grid cell size. GCMs employ different parameterizations to estimate convective type precipitation and this can lead to very different estimates from one model to the next. In the winter, precipitation is dominated by larger scale synoptic precipitation 'lows', which are better represented within the models. The causes of the March discrepancy are more difficult to speculate on.

As discussed earlier, the use of the 'delta technique' does not rely on the ability of the models to accurately reproduce historical climate, since what is of interest is the difference between the model baseline and model future time period. It is this difference which is then applied to the historical observed conditions to produce our future estimate of climate. The preceding figures demonstrate that taken as an ensemble, the models can reasonably reproduce the baseline on their own (without bias correction), in this region. The 'delta' technique removes the small bias which does exist in certain months or seasons.

3. FINDINGS

3.1. Summary of Global Trends from the IPCC's AR5

The full IPCC AR5 Working Group 1 Report was released in September 2013 and provides general details of the IPCC position on climate change.[4] Prior to presenting the specific trends in the Peel Region, it is important to present some information on the broader global findings on climate changes and trends, which are summarized from the IPCC's AR5 Summary for Policy Makers, as follows:

- Warming of the climate system is unequivocal, and since the 1950s, many of the observed changes are unprecedented over decades to millennia. The atmosphere and ocean have warmed, the amounts of snow and ice have diminished, sea level has risen, and the concentrations of greenhouse gases have increased.
- Each of the last three decades has been successively warmer at the Earth's surface than any preceding decade since 1850.
- Over the last two decades, the Greenland and Antarctic ice sheets have been losing mass, glaciers have continued to shrink almost worldwide, and Arctic sea ice and Northern Hemisphere spring snow cover have continued to decrease in extent.
- The atmospheric concentrations of carbon dioxide (CO_2), methane, and nitrous oxide have increased to levels unprecedented in at least the last 800,000 years.
- Human influence on the climate system is clear. This is evident from the increasing greenhouse gas concentrations in the atmosphere, positive radiative forcing, observed warming, and understanding of the climate system.
- Human influence has been detected in warming of the atmosphere and the ocean, in changes in the global water cycle, in reductions in snow and ice, in global mean sea level rise, and in changes in some climate extremes. This evidence for human influence has grown since AR4. It is *extremely likely* that human influence has been the dominant cause of the observed warming since the mid-20th century.
- Observational and model studies of temperature change, climate feedbacks and changes in the Earth's energy budget together provide confidence in the magnitude of global warming in response to past and future forcing.
- Climate models have improved since the AR4. Models reproduce observed continental-scale surface temperature patterns and trends over many decades, including the more rapid warming since the mid-20th century and the cooling immediately following large volcanic eruptions.

[4] Please see the following URL for more details: http://climatechange2013.org

- Global surface temperature change for the end of the 21st century is *likely* to exceed 1.5°C relative to 1850 to 1900 for all RCP scenarios except RCP2.6. It is *likely* to exceed 2°C for RCP6.0 and RCP8.5, and *more likely than not* to exceed 2°C for RCP4.5. Warming will continue beyond 2100 under all RCP scenarios except RCP2.6. Warming will continue to exhibit interannual-to-decadal variability and will not be regionally uniform.
- Changes in the global water cycle in response to the warming over the 21st century will not be uniform. The contrast in precipitation between wet and dry regions and between wet and dry seasons will increase, although there may be regional exceptions.
- Continued emissions of greenhouse gases will cause further warming and changes in all components of the climate system. Limiting climate change will require substantial and sustained reductions of greenhouse gas emissions.

With each subsequent assessment report produced by the IPCC, the evidence of climate change builds and increasingly points towards greater confidence that human-kind is having and will continue to influence our future climate, from warming, to extreme events, to sea-level rise to melting sea-ice. So in addition to changes in the mean climate, extreme climate events will also be impacted, and in many cases the changes in the extremes are expected to be greater than mean changes. Of particular interest are some conclusions from the IPCC's "Special Report: Managing the Risks of Extreme Events and Disasters to Advance Climate Change Adaptation" (SREX) (IPCC 2012), as follows:

- It is *virtually certain* that increases in the frequency and magnitude of warm daily temperature extremes and decreases in cold extremes will occur in the 21st century at the global scale.
- It is *very likely* that the length, frequency, and/or intensity of warm spells or heat waves will increase over most land areas.
- It is likely that the frequency of heavy precipitation or the proportion of total rainfall from heavy falls will increase in the 21st century over many areas of the globe.
- Extreme events will have greater impacts on sectors with closer links to climate, such as water, agriculture and food security, forestry, health, and tourism.
- Attribution of single extreme events to anthropogenic climate change is challenging.

Figure 11 provides a graphical example of how changes in temperature increase the likelihood of extreme events through changes in mean, variability and symmetry of the overall probability distribution of the climate.

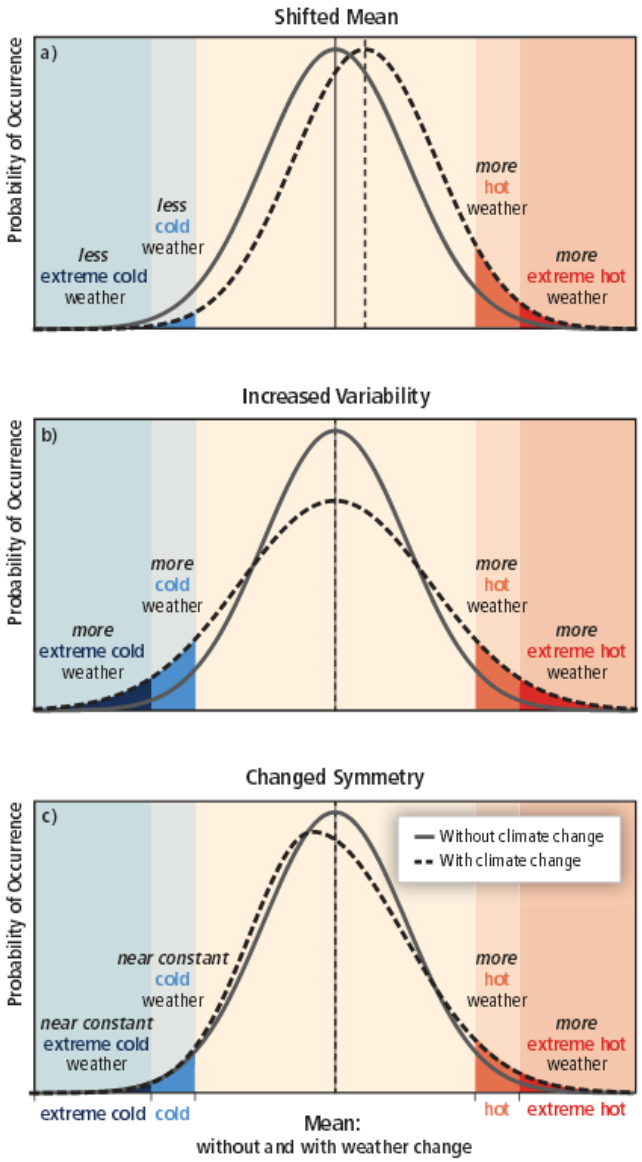

Figure 11: **How changes in temperature distributions can affect extremes (from IPCC, 2012).**

3.2. Confidence in Climate Change Projections

Confidence wording in the IPCC documents is characterized by the use of specific terms such as ‘very likely’ or ‘virtually certain’; where in previous reports changes may have been referred to as ‘likely’ (Table 3). There has been a gradual increase in confidence of the projections from climate models over time. With each report there are more and higher quality observations of the changing climate and improvements in the model equations/parameterizations, and their spatial and temporal detail. The IPCC reports continue to provide the best science-based information on projected climate change assembled from the best climate researchers worldwide. Climate change projections for this report are based upon the same new models

used for guidance in the IPCC AR5 report recently released. Generally, evidence is considered to be more robust when there are multiple, consistent, independent sources of high quality information (IPCC 2012) (see Figure 12).

Table 3: **Confidence terminology employed by the IPCC in their official reports (AR5) (from IPCC 2014)**

Term	Likelihood of the Outcome
Virtually certain	99 – 100% probability
Very likely	90 – 100% probability
Likely	66 – 100% probability
About as likely as not	33 – 66% probability
Unlikely	0 – 33% probability
Very unlikely	0 – 10% probability
Exceptionally unlikely	0 – 1% probability

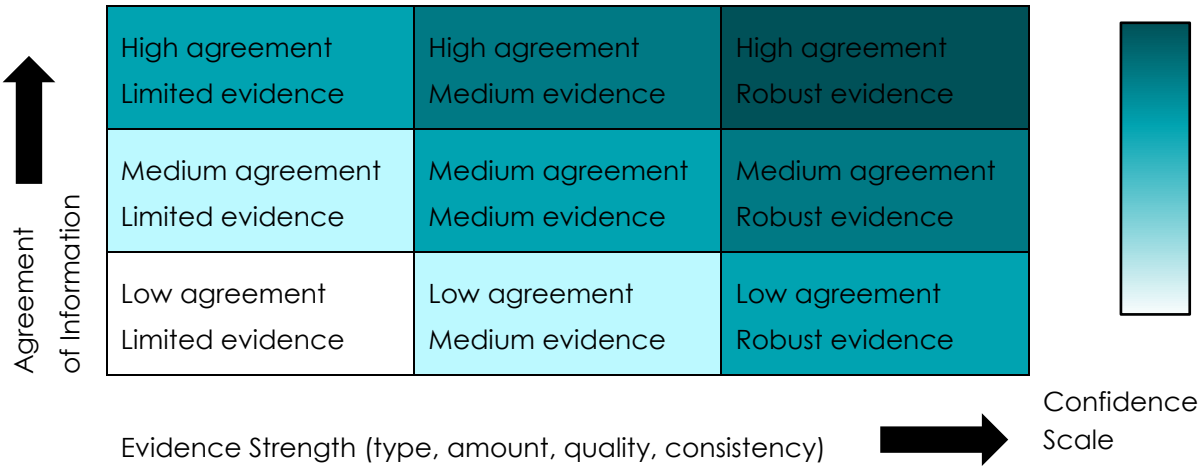

Figure 12: **Conceptual depiction of the relationship between evidence and confidence (adapted from IPCC 2012).**

3.3. Atmospheric Drivers of Climate in Peel

Peel Region's weather and climate is influenced by atmospheric circulations or weather drivers operating on scales ranging from local to continental to the global atmosphere. These main weather and climate drivers include: 1) air masses and weather systems that track into the region from elsewhere (Figure 13); 2) the Great Lakes, and particularly Lake Ontario and distance inland from the Lake; 3) topography and elevation features including the Niagara Escarpment, Oak Ridges Moraine and other higher elevations (see topography in Figure 2); and, 4) urban and rural land uses. The air masses and weather systems are the main drivers of

weather and climate, all transporting moisture, temperature, and other physical and chemical properties to the region (Figure 13).

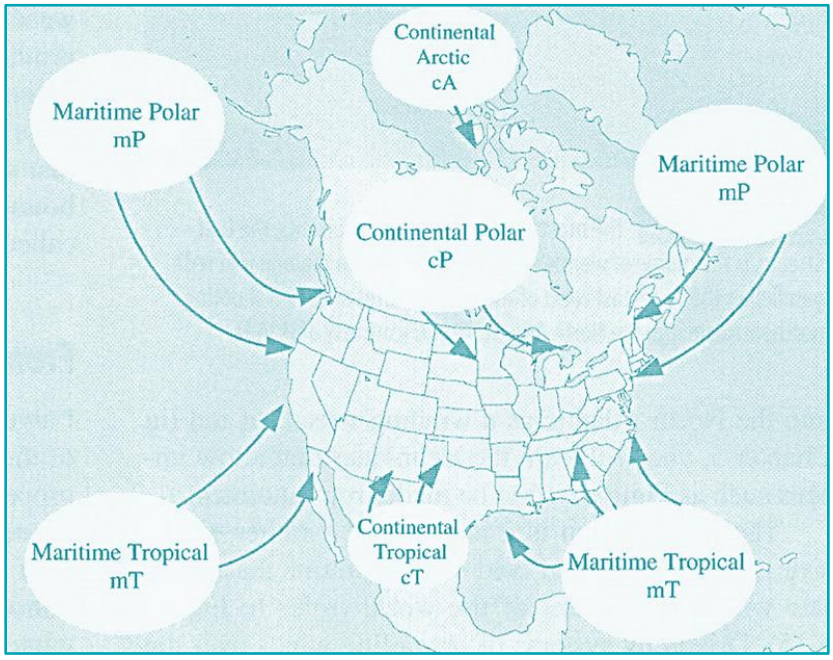

Figure 13: Air masses influencing climate in North America (from: Grenci et al. 2010).

Peel Region, like the rest of south-central Ontario, is roughly located midway in a large continental landmass between the Arctic, subtropics and Atlantic Ocean, and subsequently is impacted by air masses that track from many origins and directions. Air masses form when air stagnates for long periods of time over a uniform surface, with the characteristic features of the air mass defined by the underlying surface where it stagnated. Typically, cold air masses originate in polar or Arctic regions while warm air masses form in tropical or sub-tropical regions. These warm to cold air masses can also be moist or dry, with moist air masses that form over oceans referred to as maritime, while those over drier land surfaces are described as continental. Air masses move from one region to another through weather systems or low pressure and frontal systems. Weather systems can develop and track eastward from the lee of the Rocky Mountain ranges, Arctic and polar regions, the Gulf of Mexico or even from the Atlantic coast, bringing air masses from tropical, polar, cold Arctic and modified origins. The Jetstream that steers these weather systems and air masses in and out of Peel Region brings widely varying day-to-day weather conditions (Eichenlaub, 1979; Phillips, 1990; Angel, 1996; SENES, 2011; U.S. EPA, 2012).

The air masses that impact Peel Region can be described as continental polar (cP), continental arctic (cA), maritime polar (mP), maritime tropical (mT) and in summer, occasionally continental tropical (cT) from the southwestern United States. Peel Region's winters are dominated by the cold and drier air masses, namely the continental Artic and at times the maritime Polar air masses that have lost considerable moisture crossing the mountains in western North America

(Eichenlaub, 1979, SENES, 2011). On occasion, warm and moist tropical systems from the Gulf of Mexico and the southern United States move north, delivering milder temperatures as well as the potential for heavy snowfall, freezing rain or changing precipitation. The most severe snow and freezing rain events often result when these pulses of warm moist Gulf of Mexico air move north and override colder air near the ground (Klaassen et al. 2003). A common winter storm type known as an “Alberta clipper” typically develops in the chinook region in the lee of the Alberta Rocky Mountains and barrels eastwards, bringing modified moist Pacific air to the Great Lakes region and is often followed by cold continental air in its wake. As spring arrives, warmer atmospheric systems, such as the Maritime polar air mass, replace the colder Arctic systems. Spring, like autumn, is characterized by variable weather and rapidly alternating air masses, often resulting in frequent cloud cover, showers and occasional thunderstorms. Summer is characterized by a combination of the Maritime polar air masses from Pacific Ocean origin and Maritime tropical or Gulf of Mexico air masses, bringing warm and moist air. The tropical air masses from the Gulf of Mexico are associated with heat waves, high humidities and frequently with heavy rainfall events and deteriorating air quality conditions in Peel Region. During late summer and autumn, tropical storms and remnants of hurricanes from the Atlantic Ocean and Gulf of Mexico can also bring heavy rainfalls to the area, often accompanied by strong winds. By autumn, Arctic air masses become more common, returning colder air to the region. During the autumn to early winter, the rapid north and south movement of weather systems and air masses are accompanied by stronger winds, increased cloudiness and precipitation as average air temperatures drop gradually (Angel, 1996).

The Great Lakes themselves can moderate the cooler air masses by releasing heat stored in the lakes in the fall and winter months, ensuring that the region enjoys milder conditions than similar mid-continental areas away from the Lakes and at lower latitudes (U.S. EPA, 2012). The same lakes also provide additional moisture to the drier air masses. It is estimated that the Great Lakes can suppress spring and summer precipitation along their shorelines (estimated at 10-20% due to the stabilizing influences of the relatively cooler lake surfaces) while winter precipitation is enhanced by onshore lake-effect snows (Scott and Huff, 1997). Lake effect snowfalls from persistent northerly winds off Lake Huron and Georgian Bay sometimes impact northern Peel while southern Peel shoreline regions occasionally are impacted by lake-effect snow from the east to southeast winds fetching across Lake Ontario. With lake ice cover diminishing over time, it is expected that lake effect snowfall events could be common occurrences for the next few decades over Lake Huron and Georgian Bay (Kunkel et al, 2009a, 2009b).

In spring and summer, the penetration of lake breezes away from Lake Ontario can create narrow boundaries further inland, enhancing cloud generation, severe thunderstorms and convective rainfall events. Studies have linked lake breezes and their inland boundaries with the development of severe thunderstorms and tornadoes. In southern Peel, weather forecasters have long noted the tendency for thunderstorms moving from the west to dissipate as they approach Toronto Pearson Airport in southeastern Peel Region, with different explanations offered (King et al, 2003). Other studies have highlighted the role of the Great Lakes as a

preferred region for wintertime storm development (cyclogenesis) and for its role in altering the tracks of weather systems moving through the region (Scott and Huff, 1997).

Because the Great lakes are slower to warm than the land, they tend to keep the shoreline land areas cooler in spring, prolonging cool conditions well into April and providing a buffer for tender perennial plants. The cooler spring shoreline conditions near Lake Ontario delay the leafing and blossoming of plants and protect tender plants, such as fruit trees, from late spring frosts. This extended state of dormancy allows plants from somewhat warmer climates to survive in the shadow of the lakes by delaying the cold vulnerable blossom period.

Sometimes in spring and early summer, as tropical air from the Gulf of Mexico crosses the Great Lakes, especially in the spring and early summer, the bottom layers remain cool while the top layers are warmed, trapping moisture and airborne pollutants in the cool air below. This "temperature inversion" can result in humid days and cause fog, haze as well as smog in low-lying industrial areas.

Within Peel Region, the dominant local scale drivers of spatial variations in weather and climate are elevated topography in the north due to the Oak Ridges Moraine (ORM) and the Niagara Escarpment as well as Lake Ontario and the more regional influences of Georgian Bay in the north. Local conditions are also influenced by river and valley corridors, which tend to be north-south oriented, and accompanied by more intense urbanization in the south. It is beyond the scope of this report to provide a detailed analysis of the influence of each of these features, however they are explored in more detail as each variable is described in Section 3.4.

3.4. Climate Trends and Projections in the Region of Peel

A summary description of the following main variable categories is presented in the Roman numeral sub-sections within this Section 3.2 of this report, as follows:

- 3.2.i. Temperature
- 3.2.ii Precipitation
- 3.2.iii Snow and Ice
- 3.2.iv Wind
- 3.2.v Humidity
- 3.2.vi Growing Season Variables and Drought

For each of these variables, trends in current and future seasonality are presented, trends in extremes are interpreted, and long term changes are described including historical trends. Table 4 provides an overview of the projected changes for variables analysed. Electronic versions of these data are also available upon request from the report contact(s) in the form of a MS Access database.

Table 4: **Summary of baseline and projected historical and ensemble mean values for key variables analysed for Peel Region. Values represent the ensemble mean and the level of confidence with each variable is indicated in square brackets next to the "variable" name (Continued on the next two pages).**

Variable [Future Projection Trend Confidence]	Future Trend	Baseline Value (1981-2010)	Short-Term: 2020s (2011-2040)		Medium Term: 2050s (2041-2070)		Long Term: 2080s (2071-2100)	
			RCP4.5	RCP 8.5	RCP4.5	RCP8.5	RCP4.5	RCP8.5
Mean Temperature (°C)			**[VERY LIKELY]**					
Annual	↑	7.4	7.8	8.8	9.1	9.4	10.2	12.3
Winter	↑	-4.8	-4.4	-3.2	-2.8	-2.6	-1.5	0.6
Spring	↑	6.1	6.5	7.3	7.7	7.8	8.7	10.4
Summer	↑	19.3	19.8	20.8	20.9	21.3	22	24.3
Autumn	↑	9.1	9.5	10.4	10.7	11	11.6	13.7
Max & Min Temperature (°C)			**[VERY LIKELY]**					
Max. Annual Temperature	↑	12.3	13.6	13.7	14.0	14.2	15.1	17.1
Max. Winter Temperature	↑	-0.97	0.39	0.43	0.82	0.94	1.9	3.7
Max. Spring Temperature	↑	11.3	12.6	12.7	13.0	13.2	14.1	15.7
Max. Summer Temperature	↑	25.1	25.6	26.6	26.8	27.1	28.0	30.3
Max. Autumn Temperature	↑	13.7	15.0	15.2	15.4	15.7	16.4	18.5
Min. Annual Temperature	↑	2.5	3.8	4.0	4.3	4.5	5.4	7.6
Min. Winter Temperature	↑	-8.7	-8.2	-6.8	-6.4	-6.1	-4.9	-2.3
Min. Spring Temperature	↑	0.78	2.0	2.1	2.4	2.6	3.4	5.2
Min. Summer Temperature	↑	13.5	14.7	14.9	15.1	15.5	16.1	18.4
Min. Autumn Temperature	↑	4.4	5.6	5.7	5.9	6.3	6.9	9.0
Extreme Heat Event Frequency (days yr^{-1})			**[VERY LIKELY]**					
Days T_{max} >= 35°C	↑	0	0	0	2	2	4	14
Days T_{max} >= 30°C	↑	12	15	17	23	26	35	62
Extreme Cold Event Frequency (days yr^{-1})			**[VERY LIKELY]**					
Days T_{min} <= -15°C	↓	19	14	14	10	8	9	4
Days T_{min} <= -10°C	↓	44	35	34	27	23	24	13
Days T_{min} <= -5°C	↓	81	68	67	58	50	53	34
Total Precipitation			**[LIKELY]**					
Annual (mm yr^{-1})	↑	852	894	887	919	926	930	951
Winter (mm mo^{-1})	↑	61	66	66	69	71	71	76

Variable [Future Projection Trend Confidence]	Future Trend	Baseline Value (1981-2010)	Short-Term: 2020s (2011-2040)		Medium Term: 2050s (2041-2070)		Long Term: 2080s (2071-2100)	
			RCP4.5	RCP 8.5	RCP4.5	RCP8.5	RCP4.5	RCP8.5
Spring (mm mo^{-1})	↑	68	73	73	77	78	78	84
Summer (mm mo^{-1})	↔	77	79	77	79	78	79	75
Autumn (mm mo^{-1})	↑	77	80	80	82	82	82	82
Dry Days (days yr^{-1})			**[MORE LIKELY THAN NOT]**					
Total Annual	↔	234	225	226	231	231	229	230
Extreme Precipitation			**[LIKELY]**					
Max. 1-day precip. (mm)	↑	37.0	8%	5%	11%	8%	11%	22%
Max. 5-day precip. (mm)	↑	59.2	6%	5%	9%	10%	8%	17%
95th Percentile precip. Amount (mm)	↑	223	13%	13 %	21%	28%	25%	46%
99th Percentile precip. Amount (mm)	↑	79	18%	20 %	33%	51%	42%	90%
SDII (mm day^{-1})	↔	6.5	3%	3%	5%	7%	6%	12%
Growing Season			**[LIKELY]**					
Growing Season Start Date (day of year)	↓[3]	124	119	119	115	112	113	104
Growing Season End Date (day of year)	↑[4]	292	300	**301**	306	314	310	327
Growing Season Length (days/yr)	↑	169	182	183	192	203	198	223
Agriculture Variables			**[VERY LIKELY]**					
Corn Heat Units	↑	3087	3570	3619	3885	4199	4060	4900
Snow and Ice (days/yr)			**[MORE LIKELY THAN NOT]**					
Ice Potential	↔	2.4	2.0	2.1	1.87	1.94	1.88	2.0
Days <= 0°C	↓	147	125	124	109	96	101	71
Days between -2 and 2°C	↓	87	67	63	73	71	65	53
Wind Velocity* (m/s)			**[MORE LIKELY THAN NOT]**					
Mean annual	↔	4.5	4.4	4.5	4.4	4.4	4.3	4.3
Humidity*			**[MORE LIKELY THAN NOT]**					
Mean annual Specific Humidity (kg/kg)[1]	↑	0.0073	0.0081	0.0083	0.0099	0.011	0.012	0.017
Mean annual relative	↓	71.3	70.4	69.8	68.8	67.5	68.4	64.6

Variable [Future Projection Trend Confidence]	Future Trend	Baseline Value (1981-2010)	Short-Term: 2020s (2011-2040)		Medium Term: 2050s (2041-2070)		Long Term: 2080s (2071-2100)	
			RCP4.5	RCP 8.5	RCP4.5	RCP8.5	RCP4.5	RCP8.5
Humidity (%)[2]								

Notes:

*variable was computed using on the CanRCM4 model. Additional detail on the CMIP5 ensemble is provided in section 2.3 of this report

[1]Baseline value provided as an average from the multi-model CMIP5 ensemble (unavailable from historical datasets or CANGRD)

[2]Baseline value obtained from EC historical archive (unavailable from CANGRD)

[3]Decreasing trend implies a shift towards an earlier start date of the growing season

[4]Increasing trend implies a shift towards a later end date of the growing season

i. Temperature

Spatial Trends

On an annual basis, higher mean temperatures are found in the southern portion of Peel than in the northwest regions (see Figure 14). The same trend also holds when temperatures are considered on a seasonal basis (Figure 15). This trend is attributed primarily to the effects of elevation that increase to the north, and the presence of Lake Ontario and intensely urbanized land use in the south. These factors exert influence on the geographic trends in all temperature-related variables during the historical period (e.g., mean, maximum and minimum, number of extreme heat days, etc.). Higher topographic elevation in northern Peel, due to the presence of the Niagara Escarpment and Oak Ridges Moraine, results in cooler temperatures. Additionally, the land use in north Peel consists of farmland, natural forests and some grasslands, which tend to retain less heat energy than the heavily urbanized areas in the south. Urbanization has been found to increase surface temperatures through a process called the urban heat island (UHI) effect, in which solar radiation remains trapped in the environment and more heat is generated or radiated near the ground. Recent mapping of the UHI in Peel Region for a representative hot-day in August has indeed shown that urban areas can significantly warmer than rural areas during such events. An extreme heat dataset from NRCAN (Behan et al. 2011) was used in this estimation of urban heat island for Peel Region. This dataset may exaggerate the effects of UHI given that the measured air temperatures were collected on clear days, which are representative of extreme conditions. Figure 16 illustrates average ground surface temperature in August of 2011 using this dataset with differences between urban and rural areas reaching almost 10°C (see Figure 16).

It is important to note that in addition to the UHI effect, variations in August temperatures may also reflect elevation differences and the lake effect. Lake Ontario can exert either a warming or cooling effect depending upon the season. In colder months, the lake provides a warmer

moderating effect, while in summer months a cooler moderating effect due to the physical interactions of water bodies and the atmosphere. This moderating effect is further enhanced by southerly winds which have travelled over the open lake water. Other UHI mapping exercises in New York City, for example, have shown the effect to be more moderate on less extreme days, with differences between urban and rural areas being up to 3°C. A meta-analysis of UHI by the U.S. EPA estimates that urban heat islands in some cities can be up to 5-8°C warmer than surroundings under special or optimal conditions, with this difference being variable by location and month (U.S. EPA 2014).

Historically, the annual average difference in temperature between the south and the north is approximately 3°C (see Figure 14). This temperature gradient is expected to persist into the projection period, assuming that land cover remains relatively unchanged. Because of the moderating effect of Lake Ontario in the south, the elevation and snow cover differences throughout Peel, and the fact that warming is occurring at the surface and near surface atmosphere, northern Peel can be expected to warm at a faster rate than southern Peel. Figure 17 demonstrates that between the normal periods 1951-1980 and 1981-2010, the areas of northern and eastern Peel within the Humber River watershed have warmed between 0.1 and 0.3 °C faster than the south and western portions.

Lake Ontario also influences in the moderation of climate in the south and changes in long-term climate monitoring stations (or their closures) can also impact detection of trends. Changes in land cover, such as the addition of urban areas or the restoration of natural ecosystems do have the potential to alter local temperature patterns, however these are not explicitly considered in this study. In particular, the addition of treed areas has been shown in previous studies to mitigate the UHI effect (TRCA 2011). The effect of Lake Ontario has likely influenced the slower warming illustrated in the south (see Figure 17), and this influence is expected to remain a critical driver of Peel's temperature into the future. However, the prospect of fewer years with ice coverage and overall warmer summer water temperatures has the potential to reduce this gradient. Ultimately, this may serve to increase local air temperatures in all seasons in both the North and South areas of Peel.

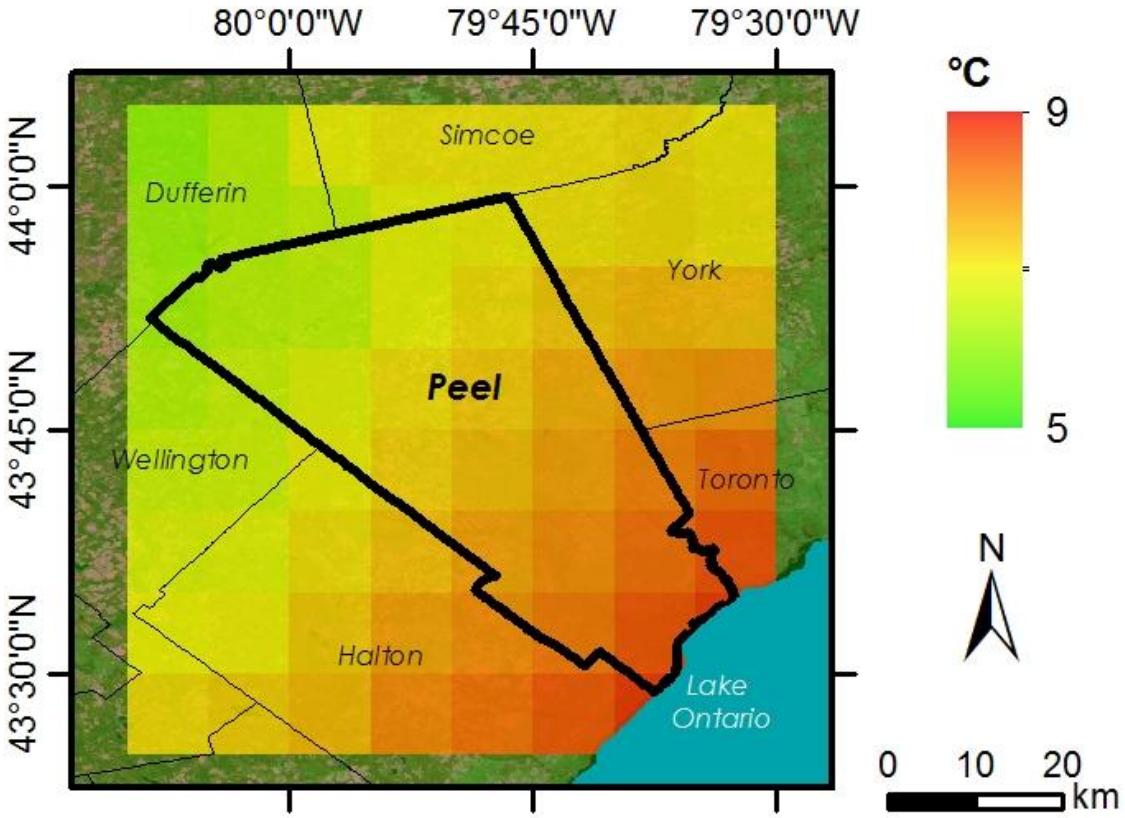

Figure 14: **Annual mean temperature for the baseline period (1981-2010).**

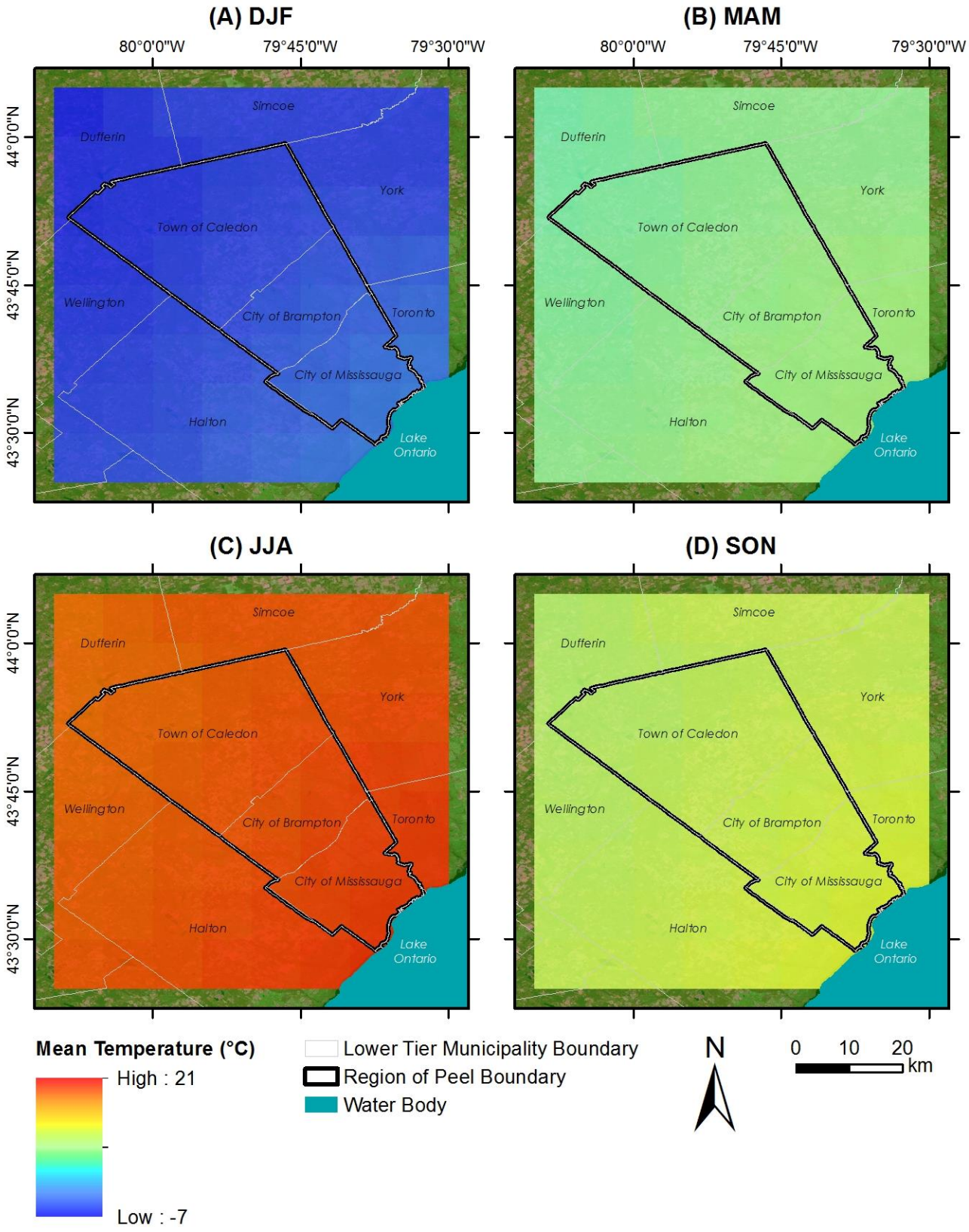

Figure 15: **Seasonal mean temperature for the baseline period (1981-2010).**

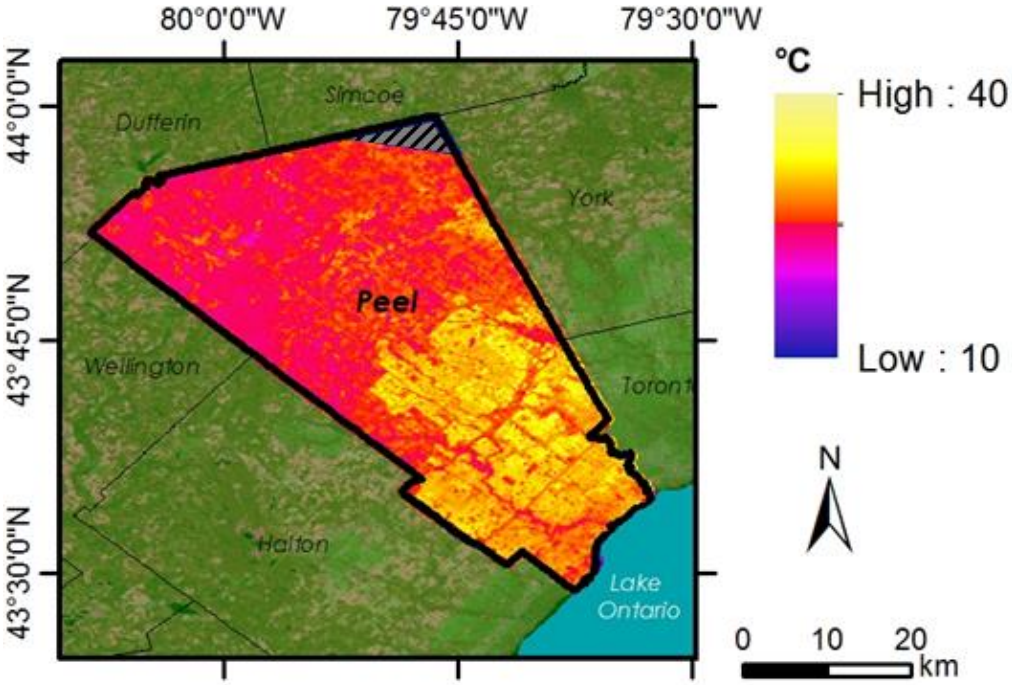

Figure 16: Ground Surface Temperature in August 2011. Shaded grey area indicates data were unavailable (mapping from Behan et. al. 2011)

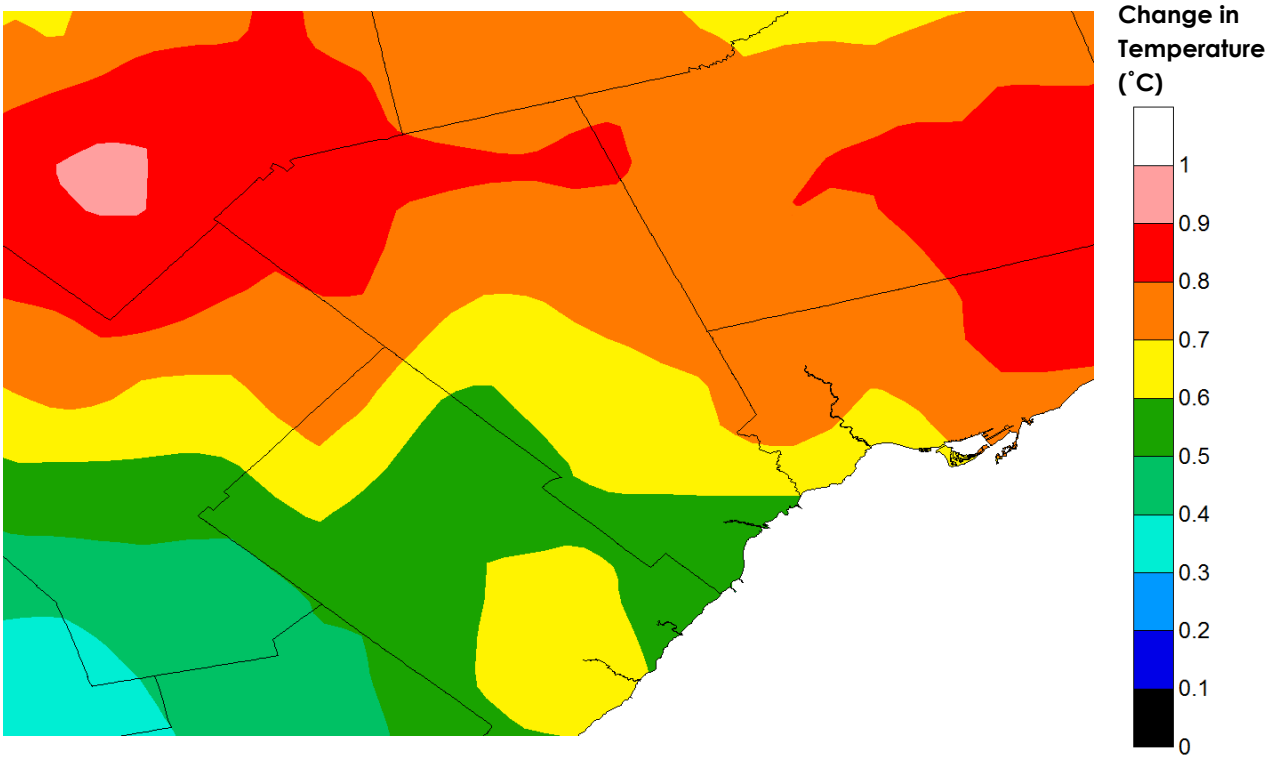

Figure 17: Changes in air temperature between the periods of 1951-1980 and 1981-2010 (˚C).

Seasonal and Inter-Annual Trends

Tables 5 and 6, and Figure 18 provide an overview of the seasonal trends in daily average minimum (T_{min}), maximum (T_{max}) and mean (T_{mean}) temperature for both the historical and future periods over the entire analysis domain for RCP4.5 (Table 5) and RCP8.5 (Table 6). Based on these results, the regional average temperature is projected to increase over all seasons, varying with concentration pathway. Based on the average of both scenarios for the full ensemble, average annual increases by the 2080s in T_{min}, T_{mean} and T_{max} are projected to increase by 4.0°C, 3.9°C and 3.8°C, respectively compared to the baseline period (1981-2010). When broken down by season, the greatest increases are projected for the winter, and particularly for minimum temperatures (Table 5). Increases of 3.9°C, 3.6°C and 3.7°C are projected for the summer, spring and autumn, respectively. Considering a "worst-case" scenario associated with RCP8.5, winter temperature increases are projected to reach up to 5.2°C on average, and 4.3°C, 4.7°C and 4.5°C for the spring, summer and autumn, respectively.

Table 5: **Summary of mean daily temperature changes projected for Peel Region. P10 represents the ensemble 10th percentile, P90 the ensemble 90th percentile and X represents the ensemble *mean change* for the *RCP4.5 scenario*.**

Season	Baseline (°C)	Change by 2020s (°C)			Change by 2050s (°C)			Change by 2080s (°C)		
RCP4.5	X	P10	X	P90	P10	X	P90	P10	X	P90
T_{max}										
ANN	12.3	0.4	1.3	2.3	1	1.7	3.3	1.5	2.8	4.3
DJF	-0.97	0.26	1.36	2.46	0.82	1.79	3.51	1.34	2.89	4.64
MAM	11.34	0.36	1.26	2.29	0.95	1.67	3.16	1.44	2.72	4.02
JJA	25.07	0.55	1.33	2.18	1.19	1.74	3.18	1.64	2.91	4.26
SON	13.74	0.39	1.29	2.18	1	1.68	3.16	1.43	2.68	4.19
T_{mean}										
ANN	7.4	0.4	1.3	2.2	1.1	1.7	3.2	1.6	2.8	4.2
DJF	-4.82	0.37	1.52	2.71	1.14	2.02	3.78	1.67	3.31	5.05
MAM	6.06	0.4	1.22	2.11	0.96	1.61	3.01	1.51	2.65	3.91
JJA	19.3	0.54	1.25	2.03	1.14	1.64	2.93	1.58	2.73	4
SON	9.06	0.45	1.22	2.05	1.06	1.59	2.95	1.45	2.57	3.94
T_{min}										
ANN	2.5	0.4	1.3	2.3	1.1	1.8	3.2	1.6	2.9	4.3
DJF	-8.67	0.43	1.72	3.01	1.39	2.3	4.17	2.1	3.81	5.64
MAM	0.78	0.42	1.22	2.11	1.02	1.61	3	1.52	2.66	3.87
JJA	13.54	0.49	1.19	1.92	1	1.56	2.85	1.39	2.6	3.92
SON	4.38	0.42	1.18	2.03	1.02	1.54	2.93	1.43	2.52	3.82

Table 6: **Summary of mean daily temperature changes projected for Peel Region. P10 represents the ensemble 10th percentile, P90 the ensemble 90th percentile and X represents the ensemble *mean change* for the *RCP8.5 scenario*.**

Season	Baseline (°C)	Change by 2020s (°C)			Change by 2050s (°C)			Change by 2080s (°C)		
RCP8.5	X	P10	X	P90	P10	X	P90	P10	X	P90
T_{max}										
ANN	12.30	0.50	1.42	2.45	1.41	1.94	3.76	3.23	4.77	6.72
DJF	-0.97	0.30	1.40	2.63	1.22	1.91	3.95	2.94	4.67	6.94
MAM	11.34	0.32	1.31	2.36	1.13	1.81	3.67	2.96	4.39	6.02
JJA	25.07	0.81	1.53	2.37	1.77	2.08	3.76	3.69	5.24	7.22
SON	13.74	0.56	1.43	2.45	1.51	1.97	3.66	3.33	4.78	6.69
T_{mean}										
ANN	7.40	0.56	1.42	2.39	1.54	1.97	3.73	3.37	4.86	6.69
DJF	-4.82	0.47	1.60	2.86	1.59	2.20	4.38	3.60	5.42	7.69
MAM	6.06	0.40	1.27	2.24	1.25	1.77	3.59	3.01	4.37	6.01
JJA	19.30	0.80	1.46	2.14	1.75	1.99	3.48	3.50	4.98	6.71
SON	9.06	0.58	1.38	2.31	1.56	1.90	3.48	3.36	4.67	6.34
T_{min}										
ANN	2.50	0.56	1.47	2.43	1.60	2.04	3.87	3.51	5.07	6.86
DJF	-8.67	0.62	1.86	3.20	1.96	2.57	4.90	4.36	6.34	8.56
MAM	0.78	0.38	1.27	2.19	1.30	1.79	3.60	3.08	4.45	6.10
JJA	13.54	0.72	1.39	2.06	1.63	1.92	3.45	3.26	4.82	6.47
SON	4.38	0.54	1.35	2.29	1.50	1.87	3.54	3.32	4.65	6.31

On the daily scale, temperature fluctuates diurnally. Typical practice in climatology is to express nighttime temperature using T_{min} and daytime temperature expressed using T_{max}. The regional average annual T_{max} is projected to increase from a current value of approximately 12°C to between 16 and 18°C by the end of the century depending upon concentration pathway. The regional average annual T_{min} is projected to increase from a current value of 2.5°C to between 6°C and 9°C by the end of the century depending upon concentration pathway. The greatest increases in T_{max} and T_{min} are projected to occur in the summer and winter, respectively (see Table 5). Together these results suggest a uniform pattern of warming in both the average annual daytime and nighttime temperatures. The regional average of annual mean temperature is projected to increase from a current value of 7.4°C to between 10.5 and 13.7°C by the end of the century depending upon concentration pathway.

The results described above are consistent with findings from the IPCC AR5 assessment for projected temperature change and the confidence in this temperature increase is high among models. Figure 19 provides an overview of projected changes in average annual temperature,

broken down by the two emission scenarios, and demonstrates that RCP8.5 projects a higher temperature increase by the 2080s compared to RCP4.5.

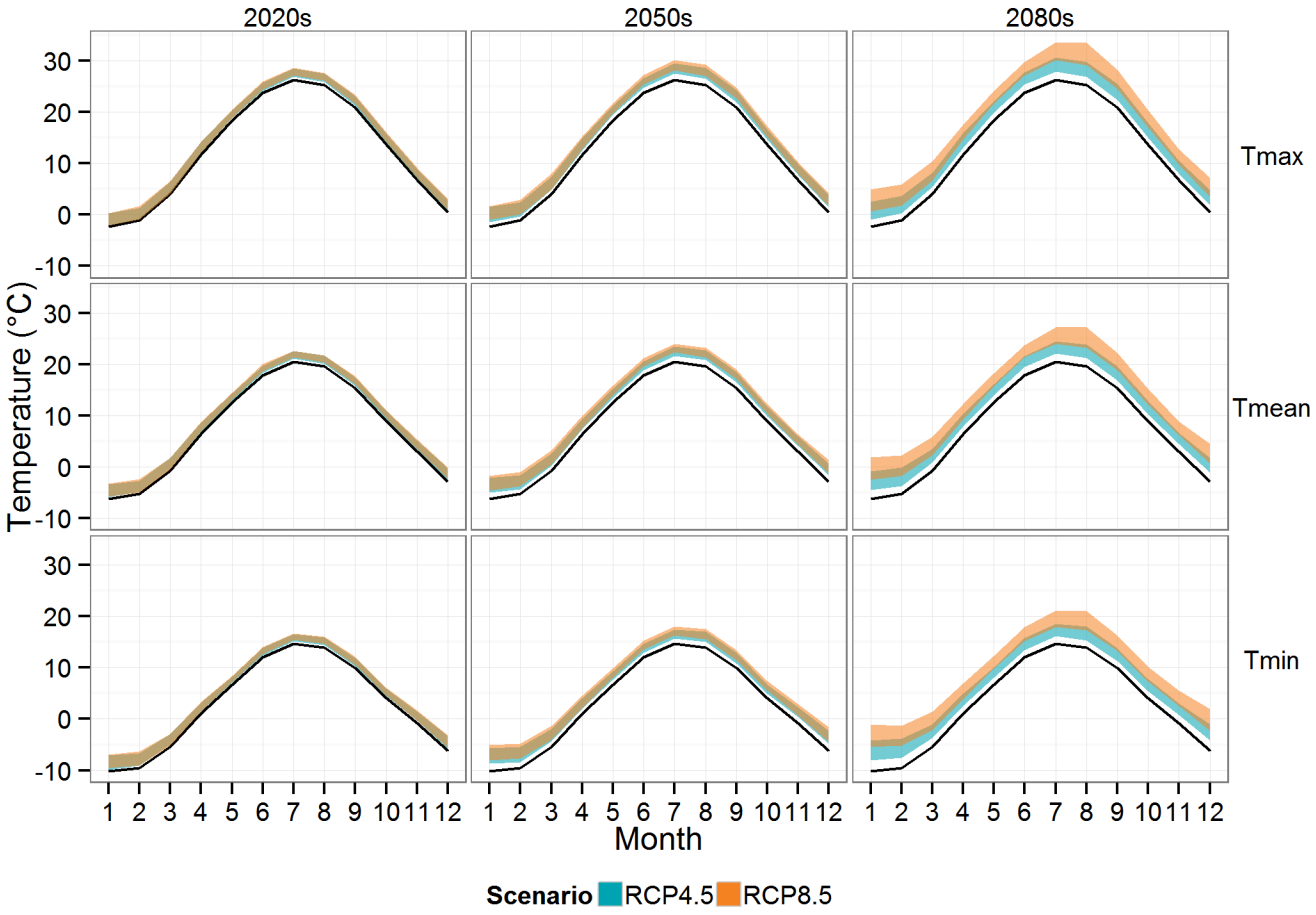

Figure 18: **Seasonal trends for the daily average temperature variables of T_{min}, T_{max}, and T_{mean}. Shaded areas denote the uncertainty bounds for the model ensemble representing 10th and 90th percentile of the ensemble for each scenario. Solid lines represent observed historical means.**

Overall, all historical climate normal (thirty year) periods indicate an upward trend in temperature increases. However, mean annual temperature has varied considerably from year-to-year. If we look at the previous 3 normals periods of 1961-1990, 1971-2000 and 1981-2010, there is an indication that the inter-annual variability has increased at Toronto Pearson Airport (Table 7). These fluctuations are generally the result of larger scale influences such as the North Atlantic Oscillation (NAO), Pacific Decadal Oscillation (PDO) or El Nino (ENSO) for example. More data is required to determine if the increase in interannual variability is to continue. This is an area of active research with contradicting findings. Huntingford et al. 2013 have noted that regionally, greater year-to-year changes recently occurred in much of North America and Europe (1980s and 1990s). However, the frequency of the larger oscillations in climate associated with NAO, PDO and ENSO going forward are not well represented within

climate models, and their effects are hugely speculative. There is also some thought in the literature suggesting that climate change is projected to result in greater instability of large-scale atmospheric drivers, such as the jet stream, which would then translate into greater inter-annual variability in temperature extremes locally as the regularity of global drivers shifts (Kim et al. 2014). Perhaps the best no regrets consideration going forward here would be to operate under the assumption of continued gradual warming with interannual variation at least as large as we have experienced in the past – meaning that average conditions will warm, there will continue to be cycles of warm and cold years, and extreme events may become more variable and more severe.

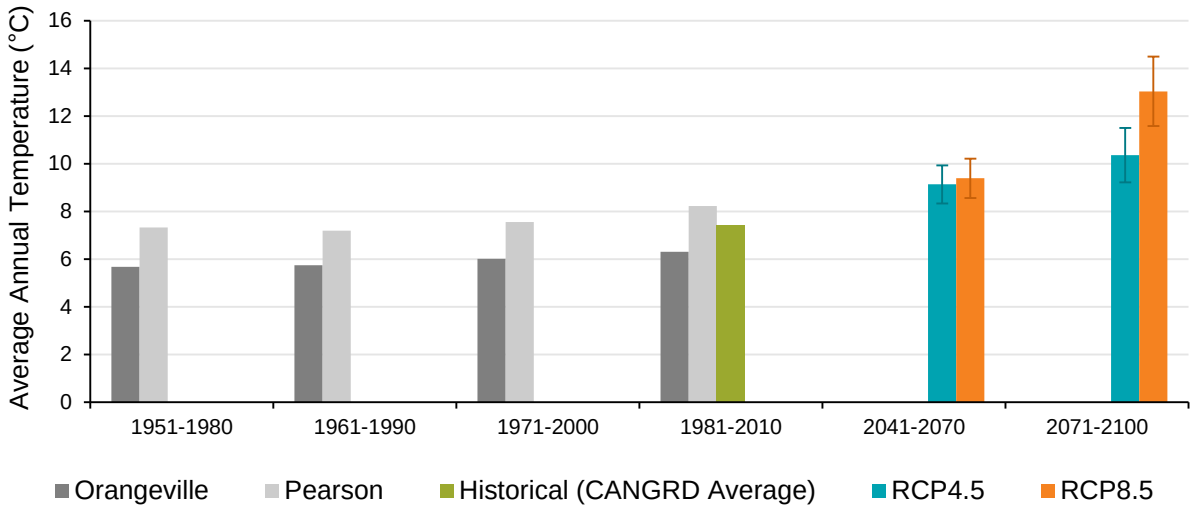

Figure 19: **Summary of average annual temperatures for the historical current and future periods. Error bars denote the standard deviation of the ensemble projections.**

Table 7: **Changes in standard deviation of mean annual temperature for three recent normal periods at Toronto Pearson Airport Station.**

	1961-1990	1971-2000	1981-2010
Standard Deviation of Mean Annual Temperature (°C)	0.64	0.94	0.96

Extreme Temperature

Since the 1960s, the trend in the frequency of extreme heat days has increased slightly. Between the two normal periods of 1961-1990 and 1981-2010, the total number of days with T_{max} greater or equal to the thresholds of 30°C, 33°C, and 35°C during each 30-year period has increased by 40, 43 and 9 days, respectively (see Figure 20). Additionally there has also been a more marked increase in extreme temperatures over the historical period. Figure 21 demonstrates that the long-term trend in the intensity of the 75th, 90th and 99th percentile temperatures in Peel Region have been on the rise. The most marked increase is for the 75th percentile temperature. There have also been marked decreases in the frequency of cold events between the normal periods of 1961-1990 and 1981-2010 for thresholds of -5°C -10°C and -15°C (see Figure 22). Similar to extreme heat trends, there has also been a marked increase in the extreme values of T_{min}, which is consistent with the overall warming trend evident over the last number of normal periods (Figure 23).

As the overall temperature locally increases due to climate change, it is expected with confidence that the frequency and intensity of extreme temperature events will also increase. This projection is directly tied to an increase in the mean temperature that results in a shifting of the climate's statistical distribution, raising the probability that more extreme temperatures will be experienced (as illustrated in Figure 11a). Sillmann et al. (2013a, 2013b) has demonstrated that in Eastern North America, the CMIP5 ensemble is reliable in projecting extreme temperature indicators, such as average seasonal, annual maxima or minima, and number of days exceeding certain extreme temperature thresholds. Other local research using previous IPCC assessments also supports the finding of increases in the daily projected maximum temperature (e.g., see Cheng et al. 2012). Likewise, the regional average minimum temperature is projected to increase over all seasons, varying with concentration pathway. Based on the overall trends in temperature, all seasons will have higher minimum temperatures according to the ensemble projections.

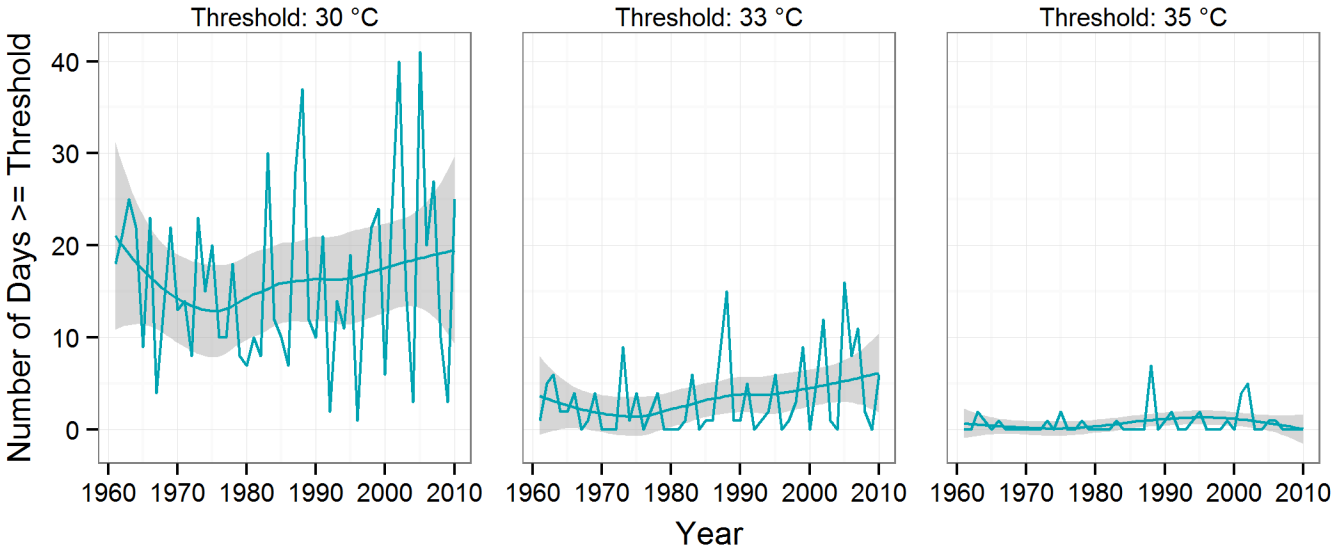

Figure 20: **Inter-annual historical trends in the number of days exceeding extreme high temperature thresholds (T_{max} >= threshold) for the Pearson Airport Station. The smooth line is a Loess nonparametric smoothing curve, and surrounding shaded area denotes the 95 percent confidence interval for that test.**

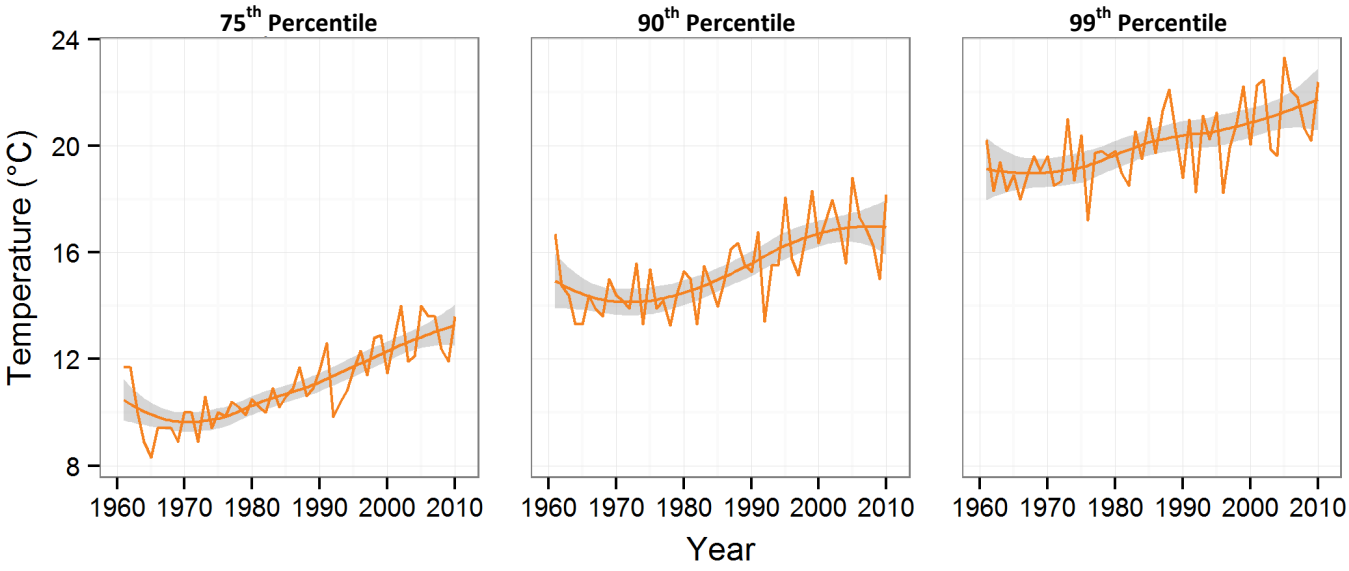

Figure 21: **Inter-annual historical trends for the 75th, 90th and 99th percentile values of T_{max} representing changes in extreme temperature for the Pearson Airport Station. The smooth line is a Loess nonparametric smoothing curve, and surrounding shaded area denotes the 95 percent confidence interval for that test.**

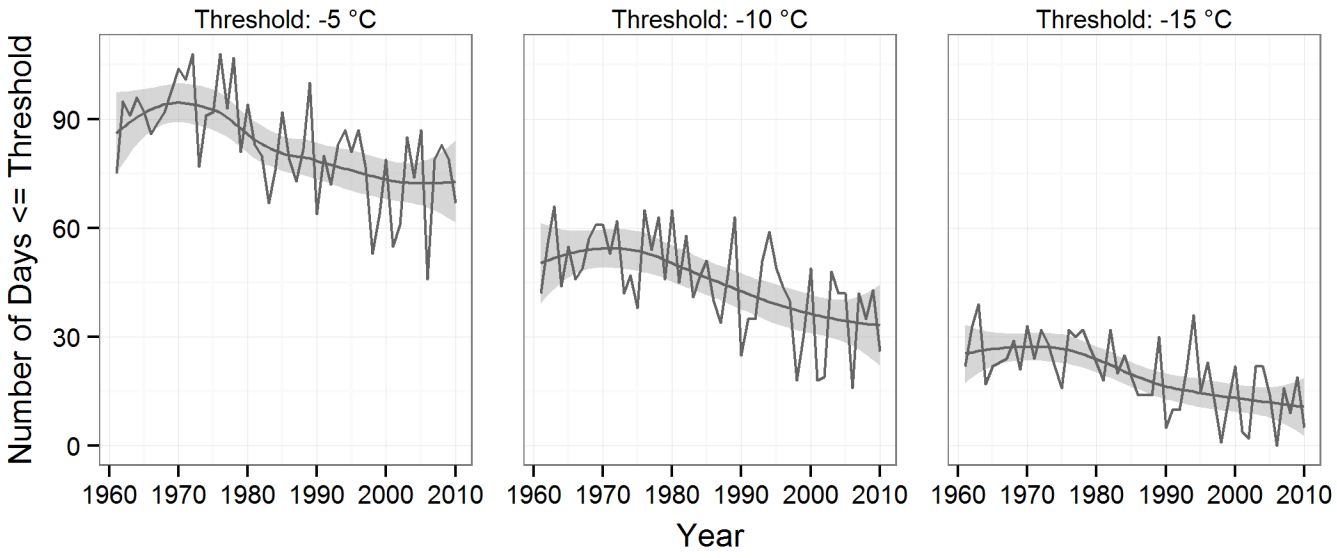

Figure 22: **Inter-annual historical trends in the number of days below low temperature thresholds (T_{min} <= threshold) for the Pearson Airport Station. The smooth line is Loess nonparametric smoothing curve, and surrounding shaded area denotes the 95 percent confidence interval for that test.**

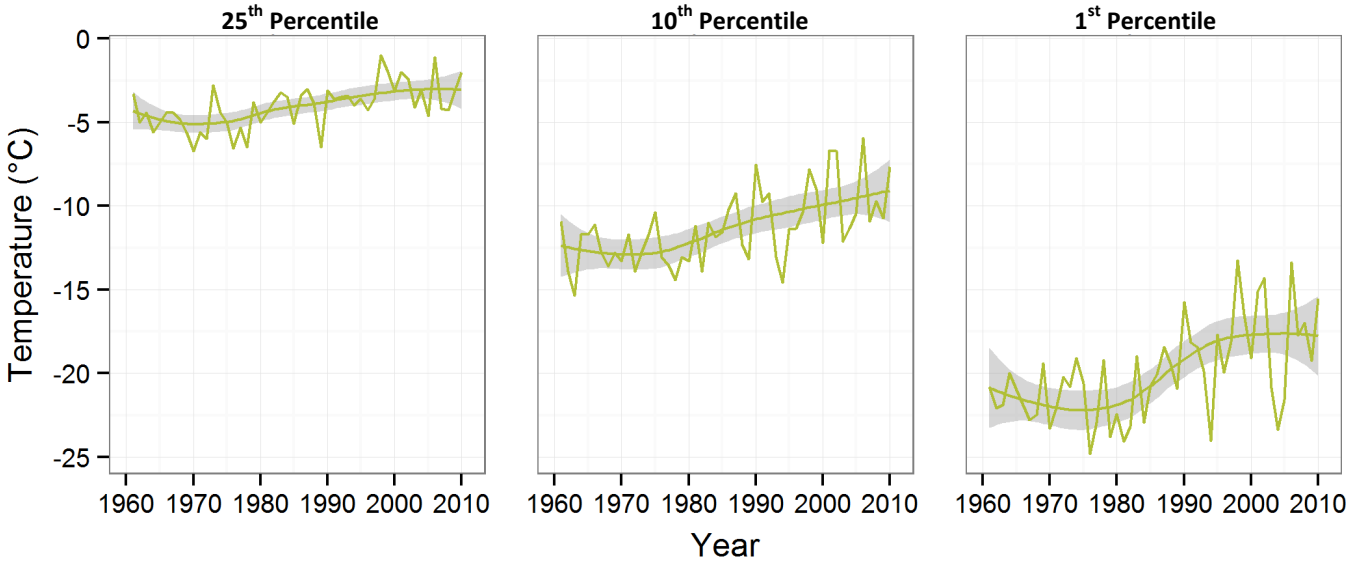

Figure 23: **Inter-annual historical trends for the 25th, 10th and 1st percentile values of T_{min} representing changes in cold temperatures for the Pearson Airport Station. The smooth line is a Loess nonparametric smoothing curve, and surrounding shaded area denotes the 95 percent confidence interval for that test.**

In terms of the frequency of extreme heat events, the regional average for the number of days per year with T_{max} greater than 30°C is expected to increase from 10 to between 40 to 80 days per year by end of the century depending upon concentration pathway (Figure 24). Likewise, regional average annual days with maximum temperature over 35°C will increase from approximately 1 day per year to 5 to 27 days per year by end of the century. These increases in extreme heat events will likely present most in the summer season and potentially in late spring and early fall. Based on the spatial trends in Peel, it is likely that the greatest increase will occur in Mississauga and Brampton (away from the cooler north and cooler lakeshore environments). As was mentioned previously, the UHI effect can exacerbate the intensity and frequency of extreme heat events at intensively urbanized locations throughout the Region.

The regional average annual number of days with temperature less than -5°C is projected to decrease from 80 days per year to 55 to 30 days per year on average by end of the century depending upon concentration pathway. Likewise, the regional average annual days with minimum temperature less than -10°C will decrease from 45 days per year to 25 to 10 days per year on average by end of the century depending upon concentration pathway. Finally, the regional average annual days with T_{min} days less than -15°C will decrease from 20 days per year to 8 to 3 days per year on average by end of the century depending upon concentration pathway. Figure 24 illustrates a comparison of temporal trends of the baseline, RCP4.5 and RCP8.5 until the end of the century for an extreme cold threshold and extreme heat threshold.

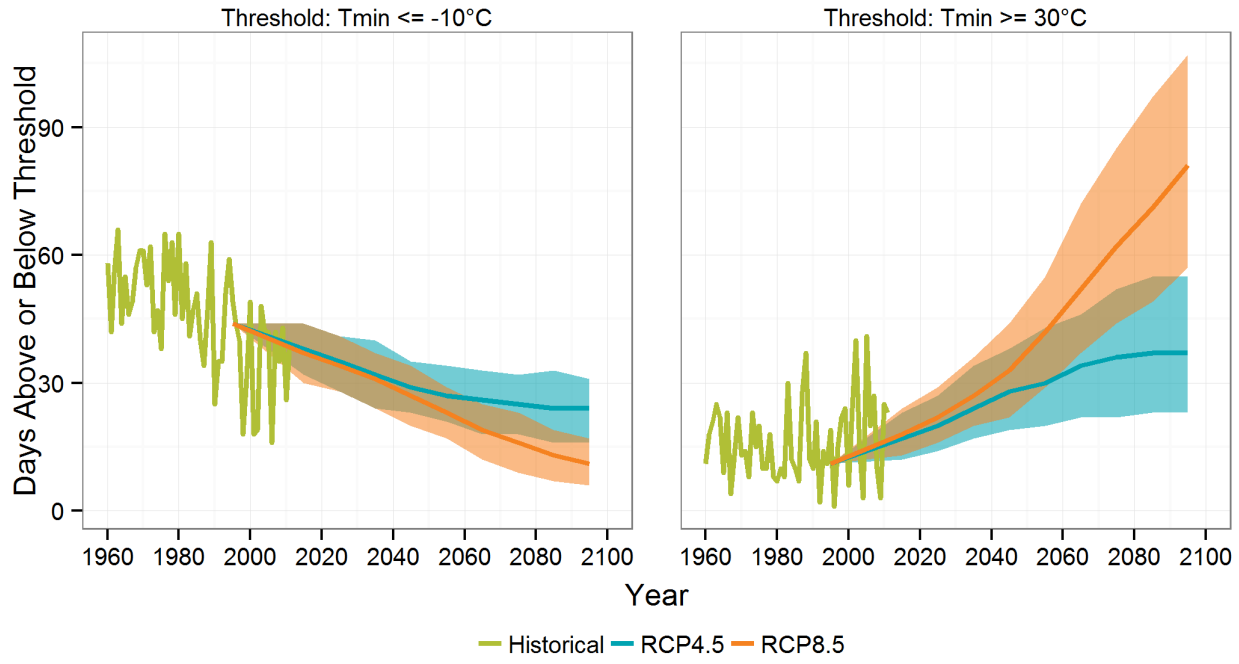

Figure 24: **Comparison of historical and future trends in extreme temperature variables for the frequency of days when T_{min} ≤ -10°C and T_{max} ≥30°C. The shaded area denotes the uncertainty bounds associated with the model ensemble, representing the 10th and 90th percentile of the ensemble.**

ii. Precipitation

Spatial Trends

The north-western portion of Peel is historically the wettest area within the Region on seasonal and annual bases, with the southern portion receiving the least precipitation. Northwest Peel receives an average total amount of precipitation between 835 mm and 925 mm per year and southern area in Mississauga receives between 794 and 836 mm (see Figure 25). Similar trends are also observed when broken down by season (see Figure 26). These ranges represent the 10th and 90th percentile precipitation for each area of Peel (i.e., north versus south) and the maximum difference within the study area is approximately 150 mm annually, based on the CANGRD data. This maximum difference is approximately 18 percent relative to the average mean annual precipitation for the overall study area. The north-south trend in precipitation is driven primarily by the influence of topographic and elevation features of the ORM, Niagara Escarpment and some regional storm track differences. These differences include, but are not limited to, the Great Lakes influences on summertime convective precipitation, the extent of northern progression of tropical air in winter and transition seasons, springtime and fall positions of frontal zones. These features cause a slight rain shadow effect (reduction of precipitation) delivered to Peel compared to other surrounding areas. Frontal systems drive the precipitation regime in the Greater Toronto Area from the west and south-west, causing more precipitation on the windward side of the ORM and Niagara Escarpment in north Peel (Cheng et al. 2011; SENES 2011; Philips 1990; Hoffman and Richards 1953). Conversely, Lake Ontario exerts an influence on the southern Region of Peel and Lake Huron-Georgian Bay on the northern Region of Peel by delivering additional moisture to the area, especially during winter months in the form of lake-effect precipitation, given particular conditions.

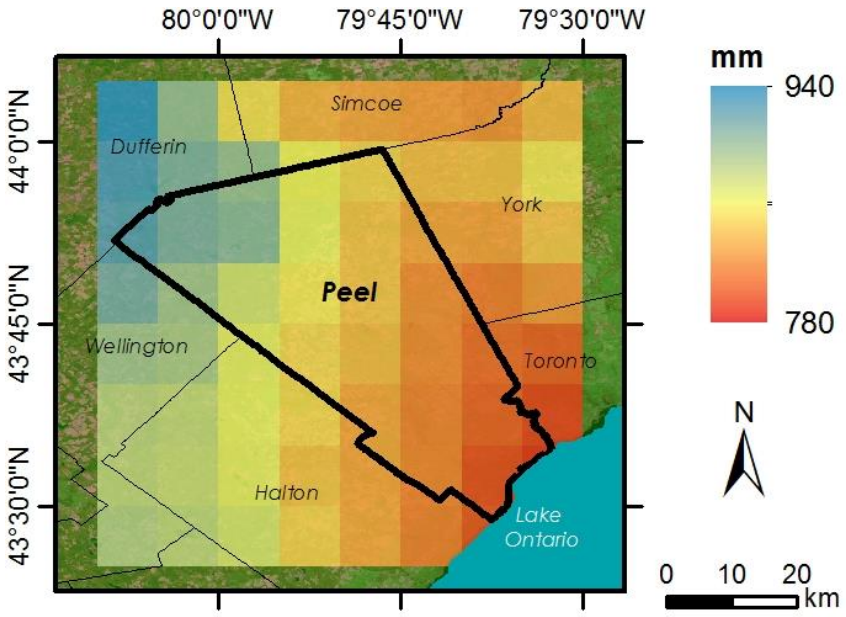

Figure 25: **Maps of total annual precipitation in the Region of Peel for the baseline period of 1981-2010.**

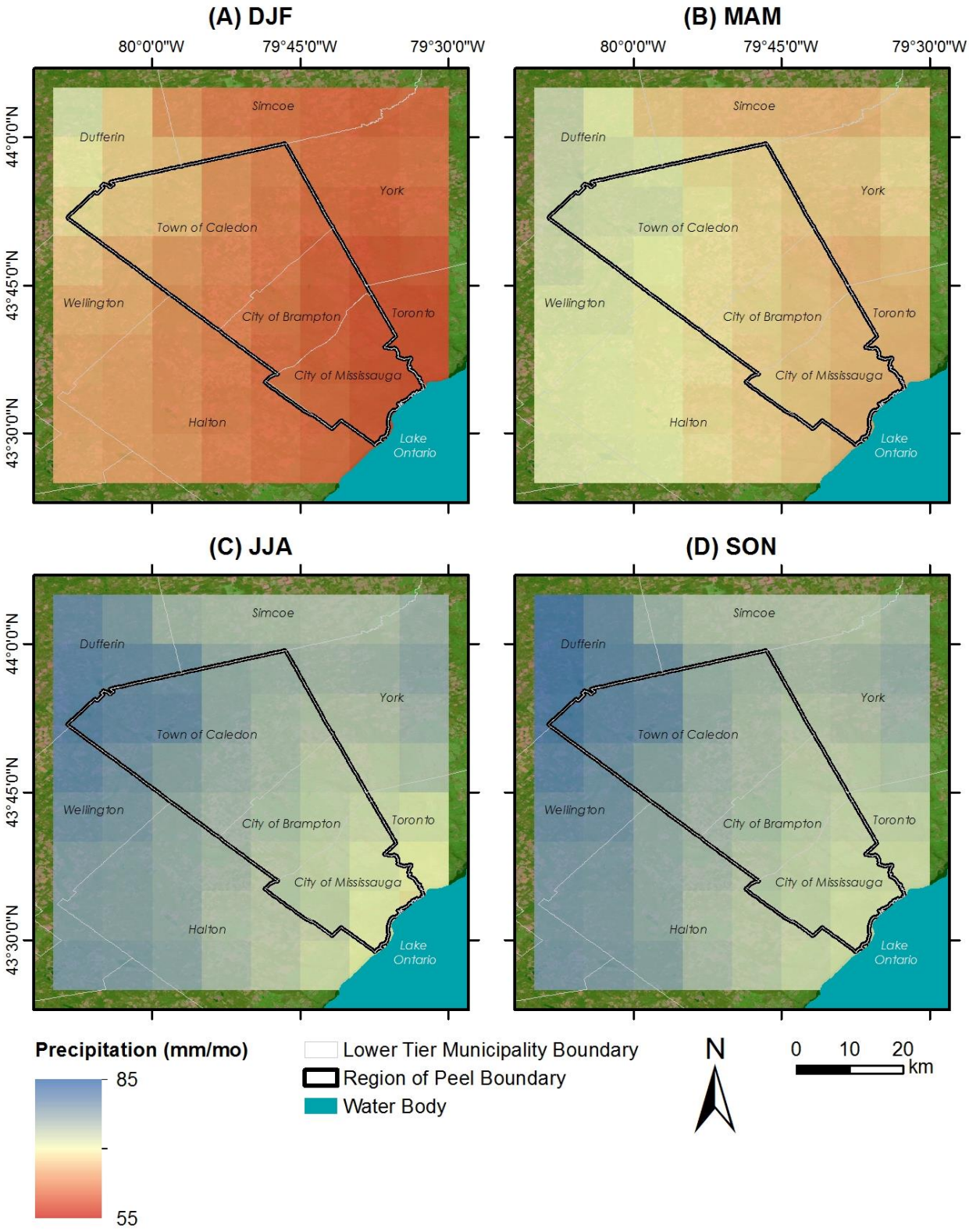

Figure 26: **Spatial trends in seasonal precipitation for the baseline period for (A) Winter, (B) Spring, (C) Summer and (D) Autumn.**

The effect of the UHI, which exerts a strong effect on the spatial trends in temperature, may also influence local precipitation trends in Peel, however the processes and impact associated with land cover differences on precipitation at local scales is not well understood.

Changes in the spatial distribution of precipitation in Peel are not discernible from the CMIP5 ensemble used in this analysis due to the coarse spatial scale of that dataset, however the gridded CANGRD data does show the overall pattern of average historical precipitation shown in the above figures. The ensemble data do, however provide a fair representation of the overall changes that are projected on a regional scale and these trends are broadly applicable to Peel. Additionally, previous studies that have made use of other high resolution downscaling of the A2 scenario from CMIP3 completed by Peltier and Gula (2012), Cheng et al. (2011), SENES (2011) and Wang and Huang (2013) suggest that the overall geographic distribution of precipitation, which is influenced by Lake Ontario, the topography and elevation influences of the Niagara Escarpment and ORM, are not likely to change. A key finding however, from the Peltier and Gula (2012) modeling is that the north-south precipitation gradient in the area around and encompassing Peel is likely to intensify due to an increase in lake-effect precipitation to the north. Additionally, under a scenario of greater local warming, which is projected with confidence by the CMIP5 ensemble, the current distribution of rain/snow would be expected to shift northward with warming, meaning northerly areas would experience greater rain versus snow amounts than they do currently. A complicating factor in the rain-snow ratio is the proximity of the northern portions of the region to areas prone to lake effect precipitation. With greater expected ice-free seasons on the Great Lakes, lake-effect precipitation could increase in the early winter season, and this could be in the form of snow depending on temperatures. The finding of intensified snowfalls in areas already influenced by lake effect snowfall is supported by findings in Peltier and Gula (2012), Wright et al, 2013, and SENES (2011) and in earlier climate trend studies (Burnett et al, 2003; Kunkel et al, 2009a). Open water with cold air outbreaks from the north can lead to increased snowfall, whereas in the past, the lakes would have been iced-over in mid-winter.

Seasonal and Inter-Annual Trends

Due to the seasonality of global and local scale climate drivers discussed in Section 3.1, precipitation in Peel varies throughout the year. In all seasons, precipitation is primarily driven by low pressure systems associated with air masses that deliver moisture from the mid-Atlantic and Gulf of Mexico (SENES 2011). The open water of the Great Lakes can add moisture to the system, especially in the summer when evaporation rates are high.

Precipitation is much more variable from year-to-year compared to temperature, and in fact is more uncertain in its future projections. The historical mean annual precipitation amount for overall Region of Peel, based on analysis of baseline period precipitation recorded at the Pearson and Orangeville stations is between 720 mm and 1042 mm, and 825 mm 1159 mm, respectively (ranges represent the 10^{th} and 90^{th} percentiles). Of note, is that the station-based values represent a larger range compared to the CANGRD data presented in the “Spatial Trends” section. Figure 27 shows a box-plot of the historical annual precipitation for the baseline period and demonstrates that the inter-annual variability expressed as the standard deviation is

approximately 163 mm and 126 mm for the Pearson and Orangeville stations, respectively, or approximately 12 percent of total annual precipitation. The variability of precipitation is even more complicated than that of temperature and depends upon the spatial and temporal scale being considered. Historically, annual precipitation at Pearson has shown increases in variability over time, however there is significant uncertainty in how climate change will influence precipitation variability into the future. Although a generally assumed conclusion of increasing precipitation variability is prevalent on a daily scale (greater extremes, longer dry periods), this will not necessarily lead to increased annual variability. The total amount of annual precipitation may remain the same but be distributed into fewer, more significant events. Sun et al (2012) have in fact demonstrated that global precipitation variability has decreased in the period of 1940 to 2009. These authors show that although some regions do see increased variability, larger regions have undergone decreasing variability. Globally, the overall average is then towards decreasing variability on a longer annual scale.

From a seasonal perspective, Figure 27 shows historical seasonal trends in precipitation and demonstrates a relatively consistent monthly precipitation pattern throughout the year. A key aspect of the seasonality is the amount of precipitation that occurs as rain versus snow. Historically during the baseline period, an annual average of 13 and 17 percent of total annual precipitation occurred as snow for the Pearson and Orangeville stations, respectively, with the greatest amounts occurring during the month of January.

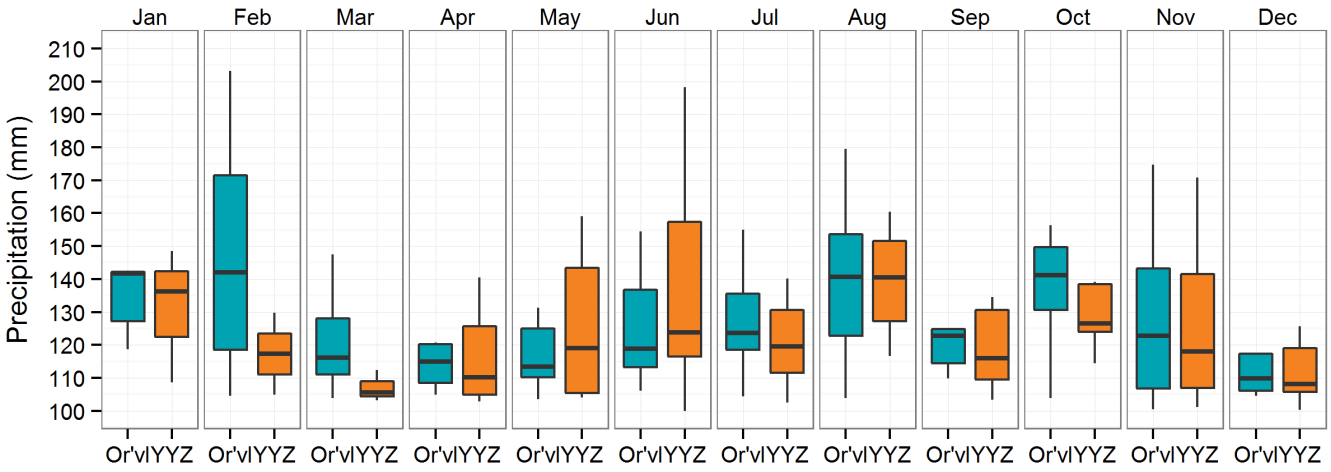

Figure 27: **Box plots of seasonal and annual precipitation for the Toronto Pearson Airport (YYZ above) and Orangeville (Or'vl above) stations for the baseline period.**

Looking ahead to the future, total mean annual precipitation is projected to increase from the 1981-2010 baseline value of 851mm to between 935 to 958 mm by the end of the century (Table 8). This represents an 11% increase in average total annual precipitation, based on the mean of the CMIP5 ensemble for both emission scenarios. Projections in future precipitation, while more uncertain compared to temperature trends, can still be elucidated with greater confidence in the short term for future climate normals (e.g., precipitation amounts projected for

the 2020s have a higher degree of confidence than those projected for the 2050s, and so on, largely due to the numerous possible future decisions made and scenarios of emissions that could occur). The higher RCP8.5 projects a larger total precipitation amount, which is associated with the greater atmospheric temperature and therefore moisture capacity of this scenario. It should be noted, however, that the current inter-annual variability in precipitation is significantly greater than the projected overall increase. Within the global context, the precipitation changes projected for southern Ontario and Peel specifically, are modest, with many areas of the globe projected to have much more significant increases and decreases in precipitation.

A critical finding from the analysis of future trends is that the seasonal distribution of precipitation is likely to shift (See Figure 28). Winter and spring precipitation amounts are projected to increase, while summer and autumn precipitation are projected to either remain steady or slightly decrease. RCP8.5 generates both higher winter and spring amounts and lower summer amounts, compared to RCP4.5. All of these future projections described above are consistent with other studies that have examined changes in precipitation in the GTHA (SENES 2011)

Table 8: **Summary of mean seasonal precipitation changes projected for Peel Region for RCP4.5 and RCP8.5. P10 represents the ensemble 10th percentile, P90 the ensemble 90th percentile and X represents the ensemble mean change.**

Season	Baseline	Change by 2020s			Change by 2050s			Change by 2080s		
	X	P10	X	P90	P10	X	P90	P10	X	P90
RCP4.5										
ANN (mm/yr)	851	-10%	5%	20%	-8%	8%	24%	-7%	9%	26%
DJF (mm/mo)	61	-7%	7%	23%	-6%	9%	28%	-3%	14%	32%
MAM (mm/mo)	68	-7%	7%	21%	-5%	8%	26%	-3%	14%	32%
JJA (mm/mo)	77	-12%	2%	17%	-13%	2%	16%	-14%	3%	19%
SON (mm/mo)	77	0%	4%	19%	-8%	5%	21%	-9%	6%	22%
RCP8.5										
ANN (mm/yr)	851	-11%	4%	19%	-8%	9%	28%	-10%	12%	34%
DJF (mm/mo)	61	-7%	8%	22%	-3%	10%	31%	0%	21%	45%
MAM (mm/mo)	68	-8%	6%	21%	-5%	9%	30%	1%	20%	43%
JJA (mm/mo)	77	-14%	1%	16%	-14%	2%	18%	-21%	-1%	18%
SON (mm/mo)	77	-12%	3%	19%	-11%	4%	21%	-13%	7%	27%

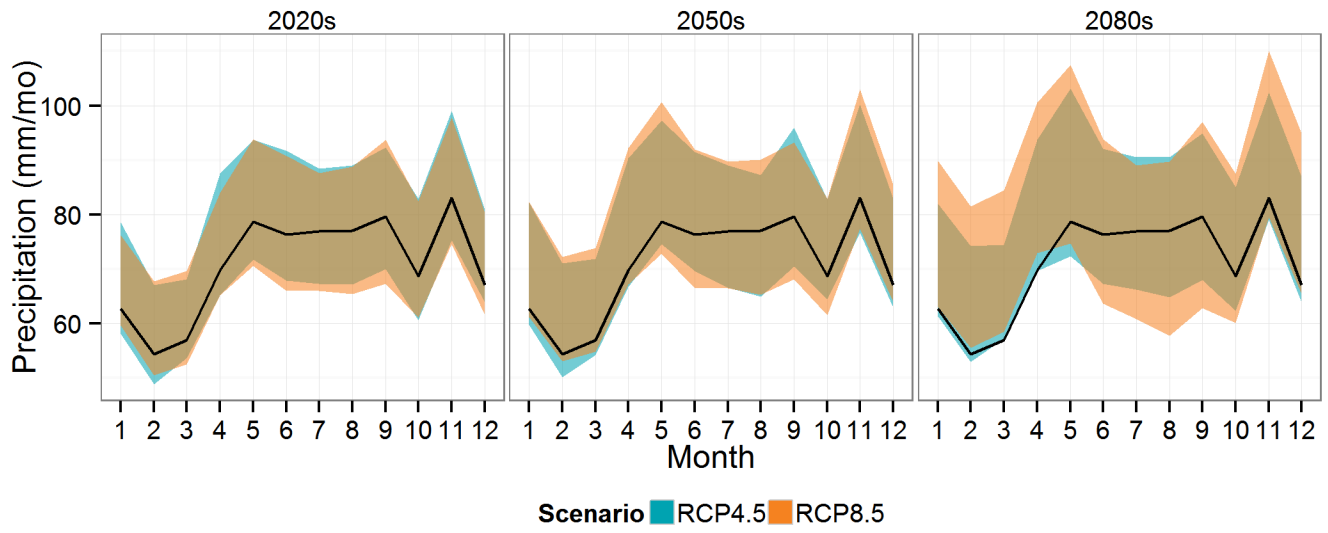

Figure 28: **Trends in monthly precipitation for the baseline 1981-2010 period (solid black line) and two future scenarios. The shaded areas represent the 10th and 90th percentile of the future climate ensemble.**

Extreme Precipitation

In order to understand the impact of climate change on extreme precipitation locally in Peel Region, it is critical to identify and characterize the processes and climate systems that drive this process. Extreme precipitation in Peel is driven by several key meteorological triggers, with the two most common drivers being: (1) large-scale synoptic systems; and, (2) local scale convection driven by meso-scale phenomena (i.e., thunderstorm/orographic/lake-breeze convergence) as well as remnants of tropical storms. Extreme convective events tend to occur with little warning and can be centered on any given localized area within the region. Conversely, large-scale extreme events driven by synoptic systems will tend to have a more broad-scale spatial distribution.

A review of eight major recent rainfall events that have led to reported flooding in the Peel area between 1981 and 2010 was conducted for this study to assist in the characterization of extreme precipitation regimes locally. For this review, eight southern Peel Region flooding events that generated significant basement flooding, as well as other impacts, in the Mississauga area were identified. A forensic investigation of the nature and extent of weather leading up to each event was then conducted to elucidate conditions at play. Results demonstrated that six of the eight events resulted from convective rainfall (i.e. thunderstorms). Most of these were characterized by short duration, extreme rainfall amounts during the summer. While most were not well sampled by standard Environment Canada climate stations (e.g. Pearson Airport) due to the localized nature of the events, many were sampled by other local networks, and it is therefore known that the actual rainfall amounts were far greater. For example, the Cooksville Creek event on August 4th, 2009, produced a 24 hour rainfall total of only 18 mm at Pearson Airport, but other Conservation Authority gauges located within the flood

damage area reported up to 68 mm in *one hour* (Aquafor Beach Ltd. 2012). The study of the eight flooding events indicated the dominant cause of these types of impacts are related to warm season thunderstorms, a trend that has been further borne out by subsequent events (e.g. the July 8, 2013 flood). In a more in-depth forensic analysis of the climatological drivers of the July 8th, 2013 storm that caused significant damage across the GTA, AMEC (2014) described the following major characteristics of the "meso-scale" systems that tend to rapidly produce convective precipitation locally (see box on P.51):

- "Abundant atmospheric moisture is a necessity, with deep moisture adding an additional driver;
- High surface dew points;
- Weak wind shear (direction and speed) resulting in slow moving thunderstorms which increases the probability of extreme local amounts;
- An upper disturbance (short wave) passing through a mean-ridge for upward motion with weak winds aloft; and,
- Frequently nocturnal" (after AMEC 2014, p. 102).

When reviewing antecedent or moisture conditions preceding the extreme events reviewed for this study, two modes were noted: (1) either the antecedent rainfall conditions were already above normal values prior to the extreme rainfall event, or (2) the month preceding the event was characterized by very dry conditions, well below the 30 year average. A much greater sample of events would need to be analysed to determine if these trends are statistically significant.

Prior to discussing the recent and projected trends, it is necessary to discuss some key limitations associated with the analysis in extreme precipitation and how they were addressed in this study. Precipitation observation intervals, periods of record and the spatial coverage of monitoring networks are often inadequate for robustly measuring intense rainfall event trends, particularly convective ones (CSA 2012, TRCA and ESSA 2012). Because of the high spatial and temporal scales at which extreme rainfall occurs in the Peel area, the limited resolution of the historical data networks (for defining the baseline climate) and the coarser spatial resolution and longer time-steps of both GCMs and RCMs, these datasets are often inadequate for definitively drawing conclusions on the physical drivers of convective extreme precipitation. An analogous challenge is the difficultly that forecasters currently have in predicting the specific location and timing of small scale severe thunderstorms during a given convective event. While RCMs are typically regarded as more robust tool for downscaling extreme precipitation than statistical methods because they explicitly capture some of the physical processes if run at high enough resolution spatial and temporal scales, they are still quite limited in accurately projecting extreme rainfall. Studies indicate that the main uncertainties associated with RCMs are due the propagation of systematic errors from the driving global models (IPCC, 2013) and the lack of two-way interactions between regional and the global climate driving model. Finally, because of the significant level of effort and expertise needed to create and run regional climate models, there are fewer available. As such, it is difficult to use them in an ensemble analysis in a way that captures the full uncertainty because of this limitation in available models.

The approach taken in this study was to use a combination of regional extreme precipitation indicators from the GCM ensemble to determine overall trends in extreme precipitation. These indicators were extracted from the CLIMDEX experiment led by the Canadian Centre for Climate Modeling and Analysis. Results from the Fourth Canadian Regional Climate Model (CanRCM4) were also analysed to add additional higher resolution information to the base of evidence for projected changes in extreme precipitation. Within the CanRCM4 runs, only one realization of a dynamically downscaled dataset driven by the Canadian Earth System Model (CanESM2) is represented. The combination of coarser GCM datasets enables a characterization of projection uncertainty using the full GCM ensemble, while additional detail on local trends between north and south Peel are provided by the CanRCM4 model.

DRIVERS OF EXTREME RAINFALL IN THE GTA

From AMEC (2014)

A Forensic Analysis of the July 8, 2013 Storm System

The July 8th storm that occurred in Toronto was not unprecedented, and in fact, did not surpass Canadian record IDF extreme rainfall amounts anywhere (AMEC 2014). This storm was the result of local scale convection driven by meso-scale phenomena. Two weather systems brought moisture and high-energy conditions to the GTA: (1) a cold front over central USA, and (2) a warm front circling clockwise around Bermuda that is often referred to as a "conveyor belt." This conveyor belt brought heat and humidity from the Gulf of Mexico into the Great Lakes region on July 6th. Changing conditions up until the afternoon of July 8th brought in a near-stationary front located just north of the TRCA jurisdiction that was approached by a general trough of low pressure (cold front) extending eastward across the Great Lakes region. Low pressure systems generally have a lot of humidity, and this system brought high amounts of instability on July 8th.

A surface pattern for a typical convective extreme rainfall event is similar to what occurred and is illustrated in the figure (below) over infrared satellite images at 4:45 EDT on July 8th. While heavier rainfall was actually expected over Windsor, the mixing of these particular conditions over the GTA produced extreme rainfall in a few hours in the afternoon. The presence of the slow-moving eastward front acted as a trigger and focusing mechanism, with thunderstorms occurring in the warm sector of the approaching cold front.

How do we Predict Extreme Rainfall Events?

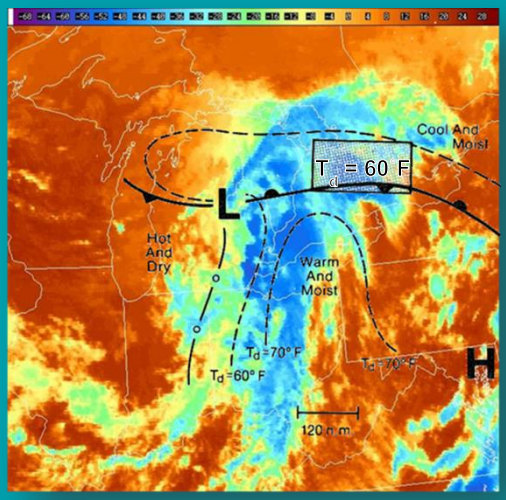

Weather forecasters have two main tools at their disposal: (1) weather models and (2) real-time radar, station data, ground observers and weather balloon observations. Forecasting of total 3-hour rainfall occurs using the Global Environmental Multi-scale Model (GEM) four times daily at The hours of 00 UTC (8pm EDT), 06 UTC (2am EDT), 12 UTC (8am EDT), 18 UTC (2pm EDT). Operational forecasters at Environment Canada interpret wide-ranging numerical weather prediction models to conduct 'nowcasting.' Model outputs are selected and adjusted based on previous historical performance and real-time data to fit the current or short-term meteorological conditions. Long-range forecasts using a regional weather model also provide a snapshot of potential future conditions of precipitation up to 7 days in advance. Situations such as the July 8th storm can occur rapidly, meaning that models may be unable to effectively capture complex conditions and observations may be difficult to make.

A List of Factors that Increase the Likelihood of a Events Like the July 8th Storm:

- Convective weather systems; driven by the interaction of heat and moisture
- High moisture conditions (total precipitable water, dew points)
- Weak, vertical wind shear
- Presence of a trigger mechanism (e.g. an approaching front, topographic features) that has triggered convection in the past
- Evidence of extreme rain bursts produced upstream by the same system
- Shifting atmospheric conditions associated with climate change:
- Warmer, polar air mass boundary shift associated with atmospheric changes
- Decreased pressure gradients at the Toronto latitude
- Slower wind speeds
- Heat and moisture content increase in mid-latitudes, yielding more moisture held in the air

Recent studies on extreme climate indicators have demonstrated that the CMIP5 ensemble CLIMDEX data adequately reproduce historical extreme precipitation trends for key indicators of simple daily intensity index (SDII), maximum 5 day precipitation, maximum 1 day precipitation, 95th percentile precipitation amount, 99th percentile precipitation amount and number of days with precipitation greater than 20 mm at a regional scale in eastern North America (Sillmann et al. 2013a, 2013b). By using several different indicators, confidence in the projections of extreme precipitation can be increased if trends for all indicators behave similarly and consistently. Likewise, divergence in a suite of indicators suggests significant uncertainty in future projections. A multi-indicator approach was used in this study and the specific indicators examined are detailed below. Generally, extreme precipitation indicators examined in this study consistently demonstrate an increasing trend, except perhaps in the daily intensity of future precipitation events, which could remain similar to current conditions. The five indicators used in this study are as follows and were computed only for the RCP4.5 and RCP8.5 scenario. The precipitation indices provided are as follows adapted from Sillmann et al. (2013):

a. Maximum 1 day precipitation (RX1day): This represents the model projected single-day maximum amount of precipitation falling, averaged over the normal period.

$$RX1day_j = \frac{\sum_{i=1}^{n} \left(\max_i Ptot \right)}{n}$$

Where: j = normal (averaging) period in question
i = individual year in question
n = number of years in normal period, j
$Ptot$ = total daily precipitation (mm)

b. Maximum 5 day precipitation (RX5day): This is similar to the previous variable, but with the $Ptot$ variable summed over 5 days.

$$RX1day_j = \frac{\sum_{i=1}^{n} \left(\max_i Ptot5 \right)}{n}$$

Where: j = normal (averaging) period in question
i = individual year in question
n = number of years in normal period, j
$Ptot5$ = total 5-day accumulated precipitation (mm)

c. Simple Day Intensity Index (SDII): This represents the average amount of precipitation in mm which occurs per day on average in a year. This is an index of 'precipitation intensity'. It is simply the total amount of precipitation in a year, divided by the number of days with precipitation. SDII can therefore increase if the same amount of precipitation occurs in fewer days, or if greater precipitation falls in the same number of days. This variable would increase with increasing precipitation intensity (i.e., more precipitation per day).

$$SDII_j = \frac{\sum_{i=1}^{w} (Ptot_i)}{w}$$

Where: j = normal (averaging) period in question
w = number of wet-days in normal period, j, or days with $Ptot > 1\ mm$
$Ptot$ = total daily precipitation (mm)

d. 95th percentile precipitation amount (R95p): This variable expresses the amount of annual precipitation for events in the top 5% of precipitation events during period, *j*, compared the baseline period. For example, using the baseline precipitation data, in the period of 1981-2010, the top daily 5% of events (i.e. 95th percentile) produced on average 223 mm of precipitation annually of the total 851 mm. This is a measure of the extreme precipitation events - the top 5% and how it is projected to change from the models. This value increases as the total amount of precipitation falling as extreme 1-day events increases.

$$R95p_j = \frac{\sum_{i=1}^{w}(P95_i)}{w}$$

Where: j = normal (averaging) period in question
w = number of wet-days per normal period, j, or days with $Ptot > 1\ mm$
$P95$ = total daily precipitation above the 95th percentile daily precipitation value for the baseline period (mm)

e. 99th percentile precipitation amount (R99p): This variable is similar to the R95p indicator, but represents even more extreme events (in the top 1%). This indicator would also increase if extreme events were to become greater.

$$R95p_j = \frac{\sum_{i=1}^{w}(P95_i)}{w}$$

Where: j = normal (averaging) period in question
w = number of wet-days per normal period, j, or days with $Ptot > 1\ mm$
$P95$ = total daily precipitation above the 95th percentile daily precipitation value for the baseline period (mm)

Table 9 provides an overview of current and projected changes in the extreme precipitation indicators examined in this study and demonstrates that instances of extreme precipitation are likely to be more severe and frequent on a regional scale. These findings are consistent with other research in this region (e.g., see Kharin et al, 2013; Peltier and Gula 2012; SENES 2011). Such trends have also been observed regionally from historical analysis conducted in Sillmann et al. (2013a), Alexander et al. (2006), and are consistent with the conclusions presented in IPCC (2012, 2013). Cheng et al, 2011 also undertook a study into extreme rainfall in southern Ontario using a subset of CMIP3 models. Results from Cheng et al. 2011 are not quantifiably comparable to the current study since, in addition to using fewer previous generation models, a much different baseline period was used beginning in 1961, and a statistical downscaling technique was employed (i.e. weather map typing approaches). Nonetheless, the general trend of increasing extreme precipitation was also found in that study. From a meteorological viewpoint, the physical conditions associated with a warmer atmosphere increases moisture holding capacity, making more water available for precipitation events (Oke 1978; IPCC, 2013).

Table 9: A summary of the extreme precipitation indicators for the historical and future periods

Indicator	Baseline	Change by 2020s			Change by 2050s			Change by 2080s		
	X	P10	X	P90	P10	X	P90	P10	X	P90
RCP4.5										
R95p	223 mm	3%	**13%**	26%	4%	**21%**	41%	9%	**25%**	45%
R99p	79 mm	-1%	**18%**	50%	11%	**33%**	82%	16%	**42%**	94%
RX1day	37 mm	-3%	**8%**	18%	1%	**11%**	26%	-1%	**11%**	20%
RX5day	60 mm	-1%	**6%**	13%	-3%	**9%**	18%	-3%	**8%**	20%
SDII	7 mm/day	0%	**3%**	6%	2%	**5%**	10%	2%	**6%**	10%
RCP8.5										
R95p	223 mm	-2%	**13%**	28%	10%	**28%**	43%	16%	**46%**	72%
R99p	79 mm	-3%	**20%**	51%	19%	**51%**	95%	44%	**90%**	147%
RX1day	37 mm	0%	**5%**	17%	1%	**8%**	21%	8%	**22%**	30%
RX5day	60 mm	-5%	**5%**	15%	2%	**10%**	19%	7%	**17%**	26%
SDII	7 mm/day	0%	**3%**	6%	4%	**7%**	12%	4%	**12%**	20%

The frequency of extreme rainfall events is also projected to increase, resulting in shortened return periods associated with current storm intensities. In other words, large events will not only be larger, but will occur more frequently. Kharin et al. 2013 suggest that for every increase of 1°C over the northern hemisphere, return periods for 20 year precipitation events decrease by 10-20%. With projected increases of approximately 2°C by mid-century, this implies events which currently occur every 20 years will occur on average every 14 years. Certainly it is possible that return periods of extreme events will be halved in the latter part of the century from current values (a '100 year storm' becomes a '50 year storm'). There is however, great uncertainly in the magnitude of changes in extreme rainfall frequency estimates, but there appears to be a consensus that return periods will continue to shorten, based on recent trends.

Precipitation extremes are often analysed in terms of the frequency, intensity and duration of rainfall events using intensity-duration-frequency (IDF) curves. These curves are updated by Environment Canada from historical observed precipitation data, and they are not forward-looking. The effect of climate change on these curves is not incorporated in any quantitative fashion as they are based purely on historical event amounts and frequencies. Although there are some future IDF projections, such as quantile mapping that have recently become available, there is very high uncertainty associated with these data and currently no universally accepted method of incorporating climate change projections into the development of future IDF curves. As such, future IDF statistics are not analysed in this study. Table 10 presents the current IDF values for the Pearson Airport station (up to 2007).

Table 10: Intensity-duration-frequency information for the historical period of 1950-2007 at Toronto Pearson Airport station

	Return Period	Intensity Values (mm/hr)					
		2 Year	5 Year	10 Year	25 Year	50 Year	100 Year
Precipitation Event Duration	5min	100	133.2	155.2	183	203.6	224
	± 95% CL	9.2	15.5	20.9	28.2	33.8	39.3
	10min	72.7	97.1	113.3	133.7	148.8	163.9
	± 95% CL	6.8	11.4	15.4	20.7	24.8	28.9
	15min	59.7	80.5	94.2	111.6	124.5	137.2
	± 95% CL	5.8	9.7	13.1	17.6	21.1	24.6
	30min	39.5	53.3	62.4	74	82.5	91
	± 95% CL	3.8	6.4	8.6	11.6	13.9	16.2
	1hr	22.5	30.2	35.3	41.8	46.6	51.3
	± 95% CL	2.1	3.6	4.8	6.5	7.8	9
	2hr	13.2	17.9	21	25	27.9	30.8
	± 95% CL	1.3	2.2	2.9	4	4.7	5.5
	6hr	5.9	8.1	9.5	11.4	12.7	14.1
	± 95% CL	0.6	1	1.4	1.8	2.2	2.6
	12hr	3.4	4.7	5.6	6.7	7.5	8.3
	± 95% CL	0.4	0.6	0.8	1.1	1.3	1.5
	24hr	1.9	2.7	3.2	3.8	4.3	4.7
	± 95% CL	0.2	0.3	0.5	0.6	0.8	0.9

As was mentioned previously, examining trends in recent historical extreme precipitation is a valuable source of information for characterizing and validating future projections. When examining trends in the frequency of extreme precipitation at the Pearson airport station, it is evident that there has been a recent trend of increases in extreme precipitation events, following a decline during the 1980s (Figure 29). Vincent and Mekis (2006) analysed trends in extreme precipitation intensity at the Toronto Downtown station and concluded that both the 95th and 99^{th} percentile precipitation have no statistically significant trend. These trends are highlighted in Figure 30. The detection of trends in extreme precipitation requires long periods of station data record and preferably, a dense network of precipitation monitoring stations to reliably capture the regional extremes of the finer scale events (CSA 2012).

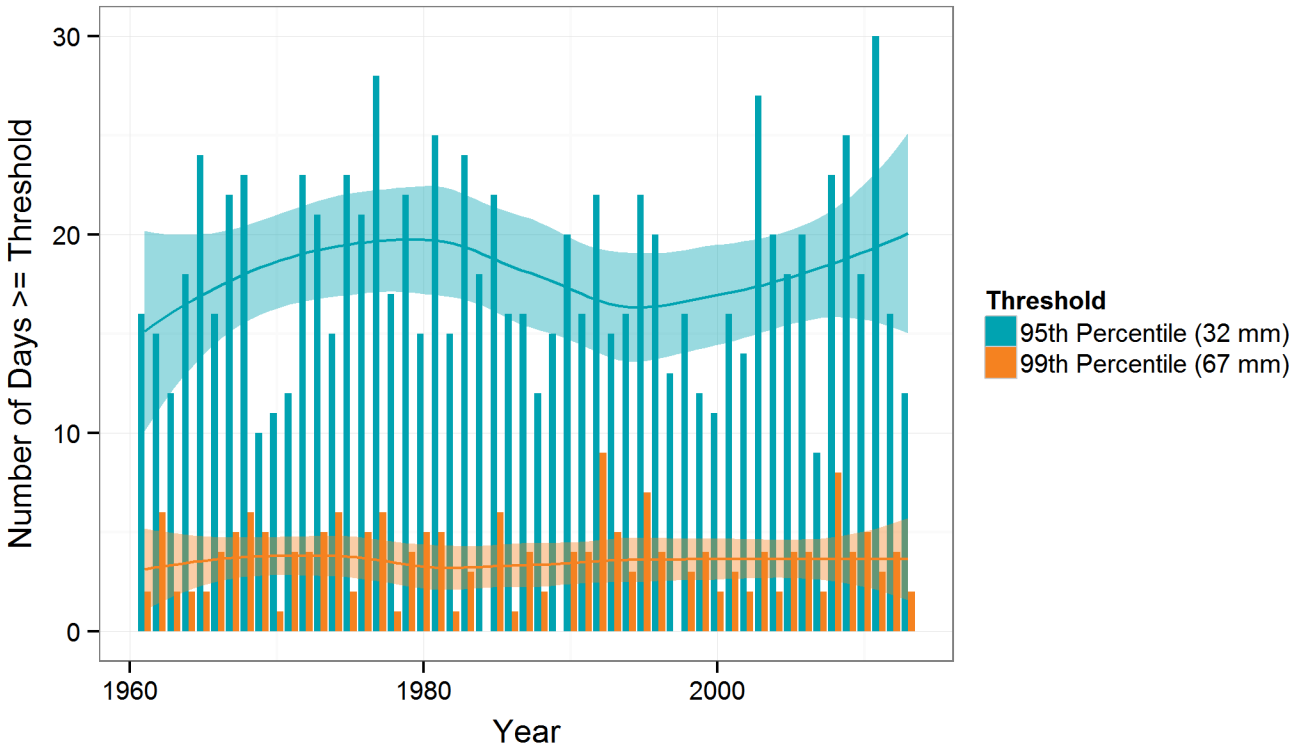

Figure 29: Historical Trend in the number of days per year greater than the 95th and 99th percentile daily precipitation for Toronto Pearson Airport station.

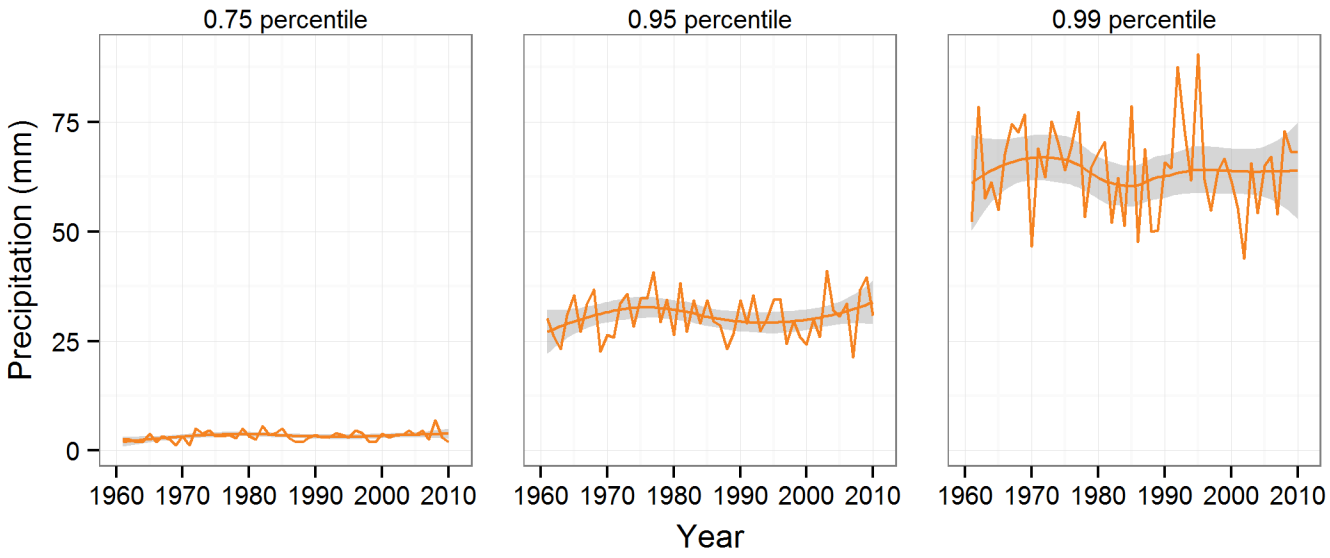

Figure 30: Trends for several percentiles of total daily precipitation expressing the intensity of extreme rainfall at Toronto Pearson Airport Station.

iii. Snow and Ice

Snow Conditions

Snow trends are not analysed directly in this study, however some observations can be made about this variable based on the analysis of trends in Section 3.2.ii by examining winter precipitation. Additionally, several future indicators based on temperature ranges for snow and ice conditions have been analysed. Figure 31 presents a summary of winter precipitation from the 1961 through 2010 period and demonstrates that, aside from isolated heavy snowfall seasons in 2006 and 2008, there has been no discernable change in winter precipitation over time within the historical period analysed. It is evident from Figure 31 that more winter precipitation consistently falls in Northern Peel (as per Orangeville station), compared to Southern Peel and in the 2006 and 2008 seasons, significantly less snow fell in southern Peel. This trend is consistent with the overall drivers of spatial precipitation variability explored in Section 3.2.ii. Based on the trends discussed in Sections 3.2.i and 3.2.ii, it is likely that although more winter precipitation is projected in the future, warmer temperatures will mean that more of this will fall as rain and not snow. This is consistent with other studies that have previously examined future snowfall (Peltier and Gula 2012; EBNFLO Environmental and AquaResource 2010). Figure 32 provides an overview of the ensemble projected location of the zero-degree temperature isotherm compared to baseline conditions and demonstrates a northward the progression of this indicator over time. The zero-degree temperature isotherm represents the approximate location of the boundary between freezing and non-freezing conditions. By the 2080s, northern portions of Peel are still projected to be below freezing at the surface, meaning snow can still be expected, but the area affected has been reduced. Coupled with the possibility of ice-free conditions over Lake Huron and Georgian Bay to the northwest (the predominant wind direction in winter), this would also mean that lake-effect snowfall is still likely. As was discussed in Section 3.2.ii, this trend has been validated through other modeling studies and it has been demonstrated that lake-effect snow in northern Peel may be enhanced in the earlier part of the next century (Peltier et al. 2012).

With respect to winter snowstorms, evidence from sections of the U.S. National Climate Assessment which focused on the Great Lakes highlighted that such events have increased in frequency and intensity since the 1950s, and that their tracks have shifted northward. This is consistent in projections for tropical cyclones, which could shift northward bringing additional precipitation into Peel Region. The amount of rain or snow falling in the heaviest one percent of storms has risen nearly 20 percent, averaged nationally—almost three times the rate of increase in total precipitation between 1958 and 2007 (Melillo et al. 2014). The report notes that heavier-than-normal snowfalls recently observed in the Midwest and Northeast U.S. in some years, with little snow in other years, are consistent with indications of increased blocking (a large scale pressure pattern with little or no movement) of the wintertime circulation of the Northern Hemisphere.

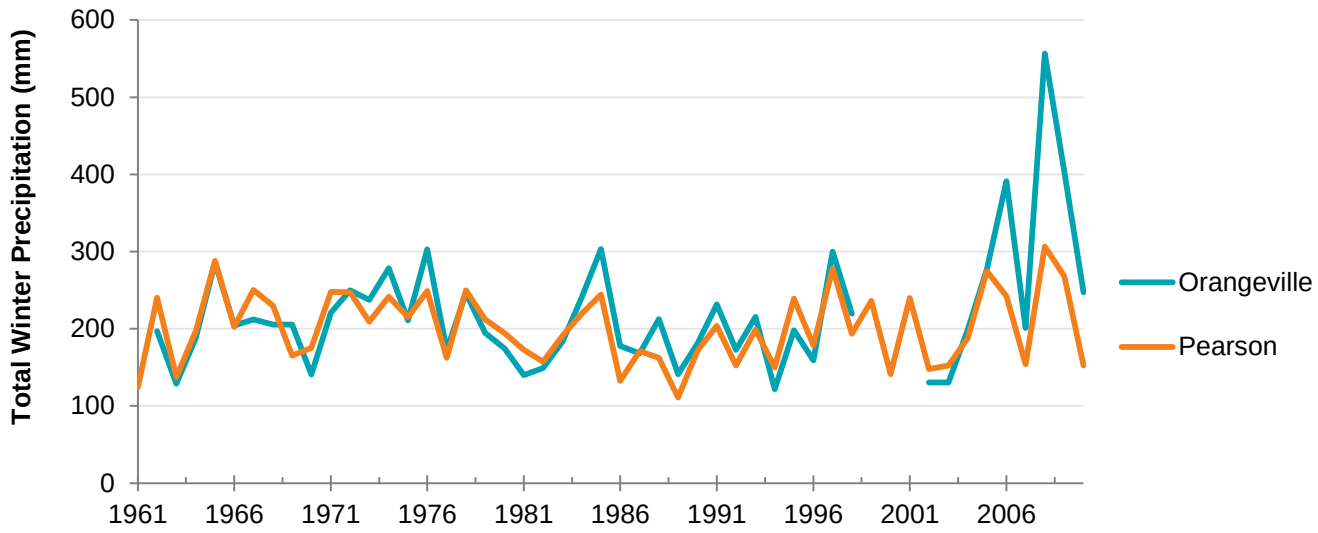

Figure 31: **Total historical winter precipitation at Orangeville and Pearson stations.**

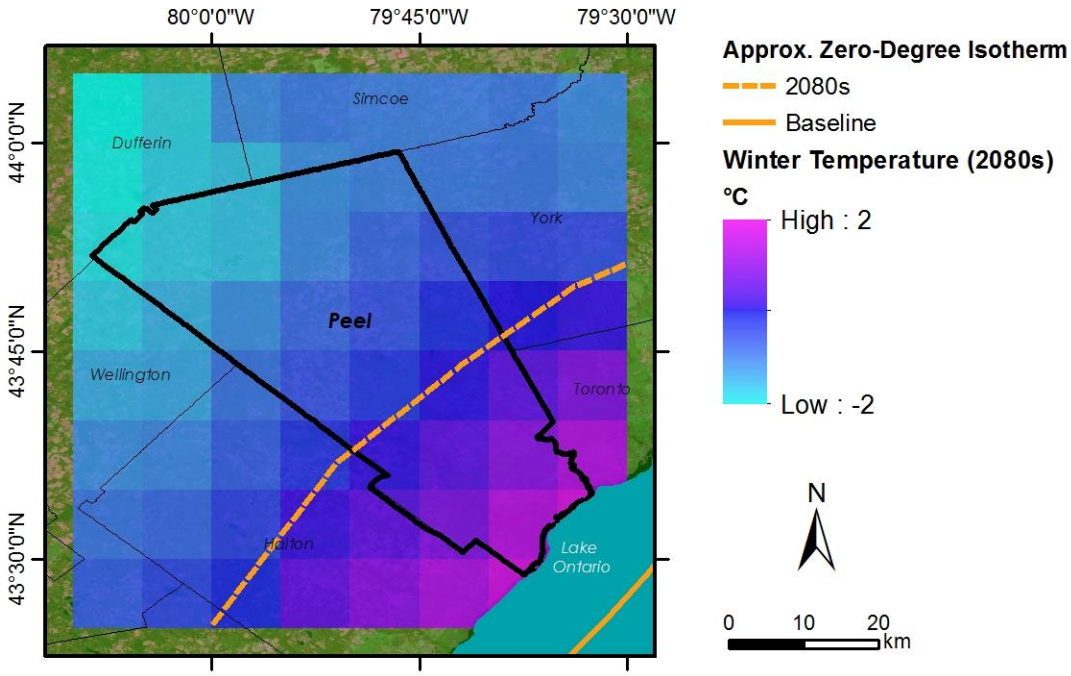

Figure 32: **Approximate location of the air temperature zero-degree isotherm based on the ensemble and emission scenario average for the 2080s.**

Freezing Rain

Typically, the longest lasting severe ice storms in Canada and the U.S. have rich sources of warm moist air from the Gulf of Mexico, sometimes augmented by moisture from the Atlantic Ocean. Some of the most severe ice storms in North America and the greatest losses from ice

storm catastrophes, especially for power lines, have been noted in the northeastern U.S. and in the southeastern U.S. (e.g. Georgia, North Carolina). In southern and eastern Ontario, the majority of the severe ice storms have originated with storm systems tracing north from the southern and south-central U.S.

The Great Lakes have an important influence on the occurrence of freezing rain in southern Ontario. Freezing rain typically occurs when cold winds from the west and northwest cross the Lake waters and are warmed to a few degrees within the 0°C range. These conditions are currently most frequent during the late fall and early winter when the lakes are ice-free. As a result of these dynamics, freezing rain events are slightly shorter in duration near the shorelines compared to locations further inland.

The variable “ice potential” is a proxy indicator for the likelihood of prolonged ice events and was defined as the number of days where the daily maximum and minimum temperatures are within 2 degrees of the freezing point. As seen earlier in the precipitation and temperature discussions, both the winter precipitation amount and mean temperature are projected to increase under both RCP scenarios. Even under the current climate within southern Ontario, the line between a rain event and snow event (zero-degree temperature isotherm) often occurs in the GTHA and this is not expected to change, except for a general trend for this line to shift further north in the region as shown in Figure 32.

The ice potential index calculated for the region indicates that on an annual basis, very little change is expected. Historically there have been 2.5 days on average per year which match this criterion in the 1981-2010 periods and given the large uncertainty bounds no definitive conclusions can be drawn regarding this variable into the future (Figure 33). On an annual basis, the CMIP5 ensemble frequency of ice events is balanced between spring and fall decreases in ice potential versus a mid-winter season increase where previously too cold conditions approach zero. Cheng et al (2007) and Cheng et al (2011b) present results on the impacts of climate change on freezing-rain events of various durations using a four model subset of the previous IPCC AR4 models and statistical downscaling (synoptic or weather map typing procedures). Studies by Cheng et al. (2007, 2011) using weather map typing and climate change downscaling approaches for 4 sets of AR4 GCMs (IPCC 2007) indicated that the frequency of freezing rain events lasting 6 hours or more for the typically coldest months could increase in southwestern and south-central Ontario by 40% by the 2050s (95% confidence interval, CI ± 6%). For the southern Ontario portion of the study area, the seasonal frequency of future freezing rain events is similar to the baseline period (1953-2000) with an increase in January and mid-winter events balanced by decreases during the winter transition periods in December and February (Cheng et. al. 2011b). This is a similar result to the index calculated in this report, where annual occurrences remain relatively unchanged from present conditions, with a projected increase in mid-winter ice events. Historically the number of freezing rain days has also changed very little at Toronto Pearson Airport as shown in Figure 33.

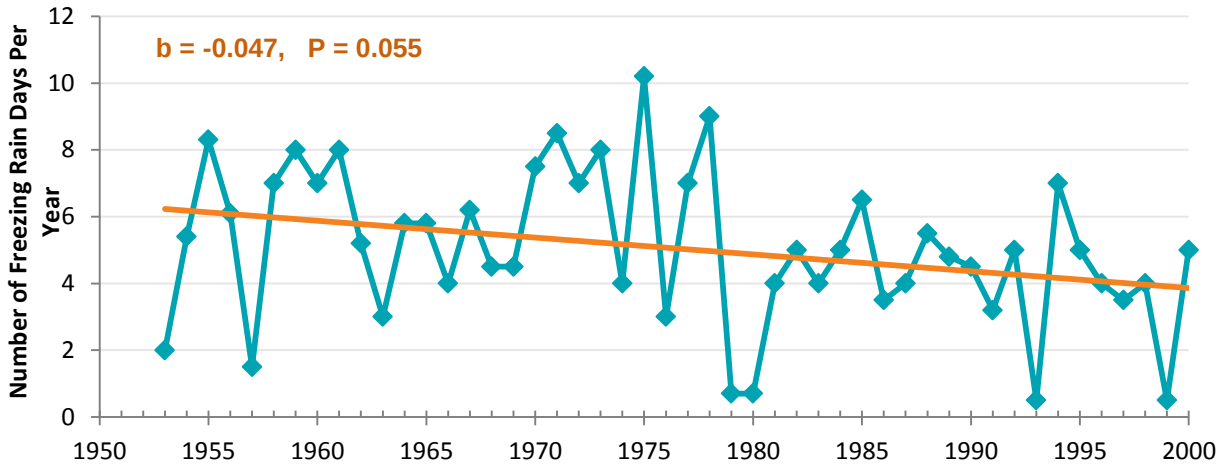

Figure 33: Number of freezing rain days per year at Toronto Pearson Airport (MSC-Hazards, 2011).

Other future variables associated with snow and ice formation show a stronger trend of declining frequency that is associated with the overall warming of the atmosphere locally in Peel. The regional average number of freeze-thaw cycles will decrease from 90 days per year to 65 to 45 days per year by end of the century depending upon concentration pathway (Figure 34). The greatest decreases are found in the spring and fall seasons, while there is a small decrease in wintertime occurrences. A similar trend is projected for the variable of days below zero degrees (see Figure 34).

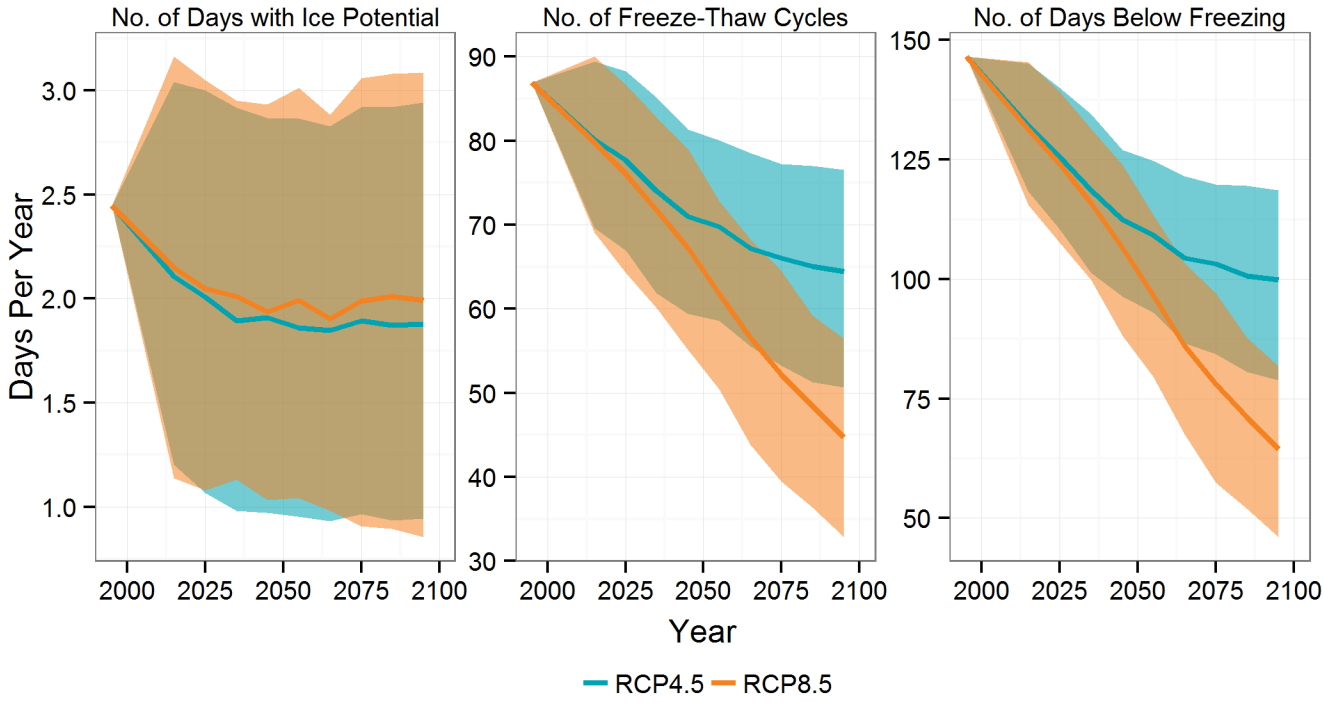

Figure 34: **Future projections for variables pertaining to snow and ice.**

iv. Windspeed

Wind in a given area at a given time is the result of atmospheric pressure and temperature differentials causing air to move from areas of higher to lower pressure. Because air pressure fields can vary over small distances and change rapidly over time, there is significant local variability in wind velocity for an area the size of Peel Region. A key challenge in describing wind trends is the limited availability of robust and good quality observational datasets that cover long enough periods of record with consistent observation instrumentation. Some types of weather stations in Canada with wind observation programs have not been able to capture daily or more frequent extreme wind gusts due to instrument and recording limitations. Records from Toronto Pearson Airport station were analysed for the baseline period, as these represent the only reliable long-term measure of windspeed in Peel Region.

The most frequently recorded wind direction observed at Pearson is from the west, however during the spring and early summer months northerly winds dominate (Figure 35). The highest windspeeds originate from the west and southwest arriving from across Lake Ontario (Figure 35). Average monthly windspeeds tend to be higher during the winter compared to the summer, however this difference is only approximately 5 km/h (Figure 36). Additionally, there is no clear long-term trend in average windspeed (Figure 36).

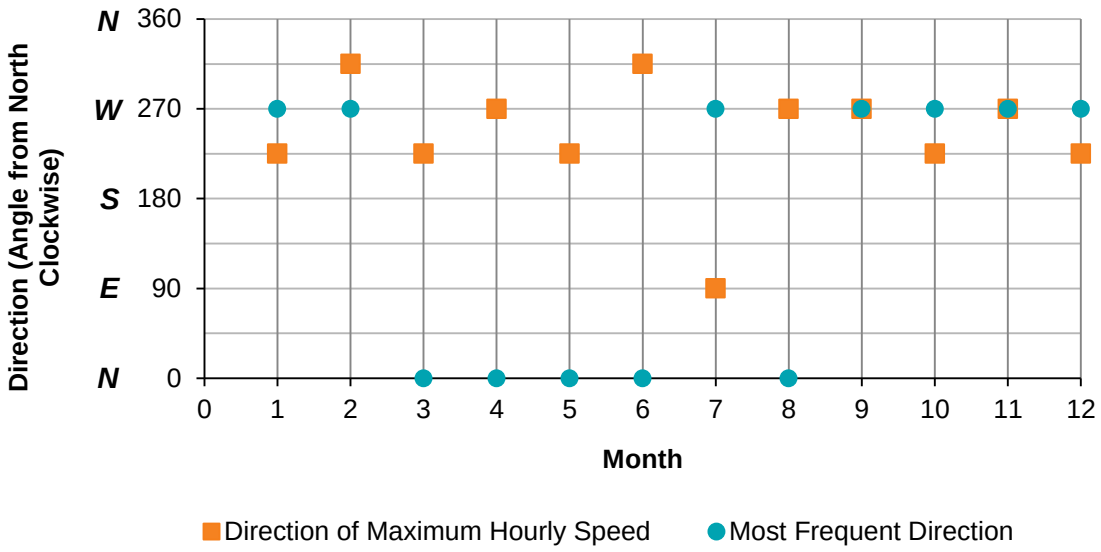

Figure 35: **Most frequently recorded wind directions at Toronto Pearson Airport station.**

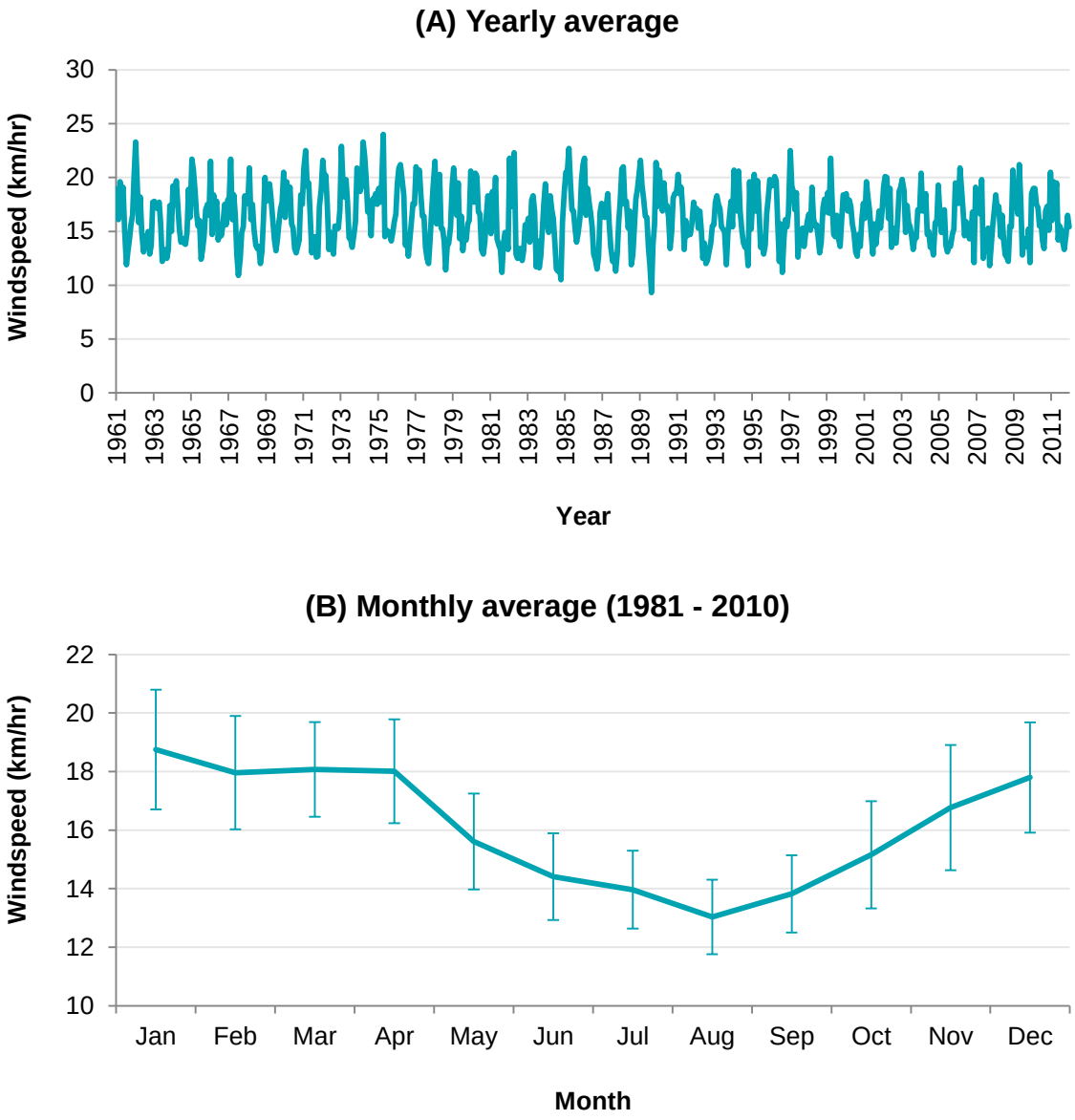

Figure 36: Summary of historical wind speeds at Toronto Pearson International Airport.

There is significant uncertainty with respect to the future projections of wind. The CMIP5 ensemble is inconclusive in its projections, and the changes shown in Figure 37 and Table 11 are well within observed inter-annual variability. Previous studies such as Cheng et. al. (2012b) have shown that eight IPCC AR4 model data projections show a modest decrease in wind gusts between 2 and 5% by mid-century over southern Ontario; however statistical downscaling of the model data projects an increase in the higher gusts. Together, this adds evidence to the finding that wind velocities are very difficult to project into the future with much reliability. Historically, there also appears to be no clear signal in wind speeds or extreme gusts, as shown in Figure 38 (MSC-Hazards, 2011), and this trend is considered to be not statistically significant.

Using 8 GCMs, Cheng et al (2012) projected general increases in hourly or aviation type wind gusts ≥ 70 km/h and ≥ 90 km/h for Ontario. In the more detailed Ontario study (Cheng et. al., 2012), the frequency of wind gusts ≥ 70 km/h using the IPCC AR4 models are projected to increase in the area from Windsor to east of Toronto by about 17% by the 2050s compared to the historical period 1994-2007. While much more difficult to project winds for the higher threshold of ≥ 90 km/h (due to limited events in the historical period and large inter-scenario and inter-model uncertainties), the results indicate that increases would be greater for the higher wind gusts (~ 70% more frequent) compared to the historical period (Cheng et. al., 2012). In general, several studies on climate change impacts on wind regimes from around North America suggest increases in the frequencies of extremes by the 2050s while other studies show little change or decreases, all with large uncertainties that make it difficult to assess trends. Additionally, in a warmer more convective atmosphere, it is not expected that thunderstorm gusts would decrease. There is no reason to believe that current thunderstorm characteristics (strong gusts), would decrease. Cheng et al. (2012) also showed stronger wind events in all seasons during anomalously warm years.

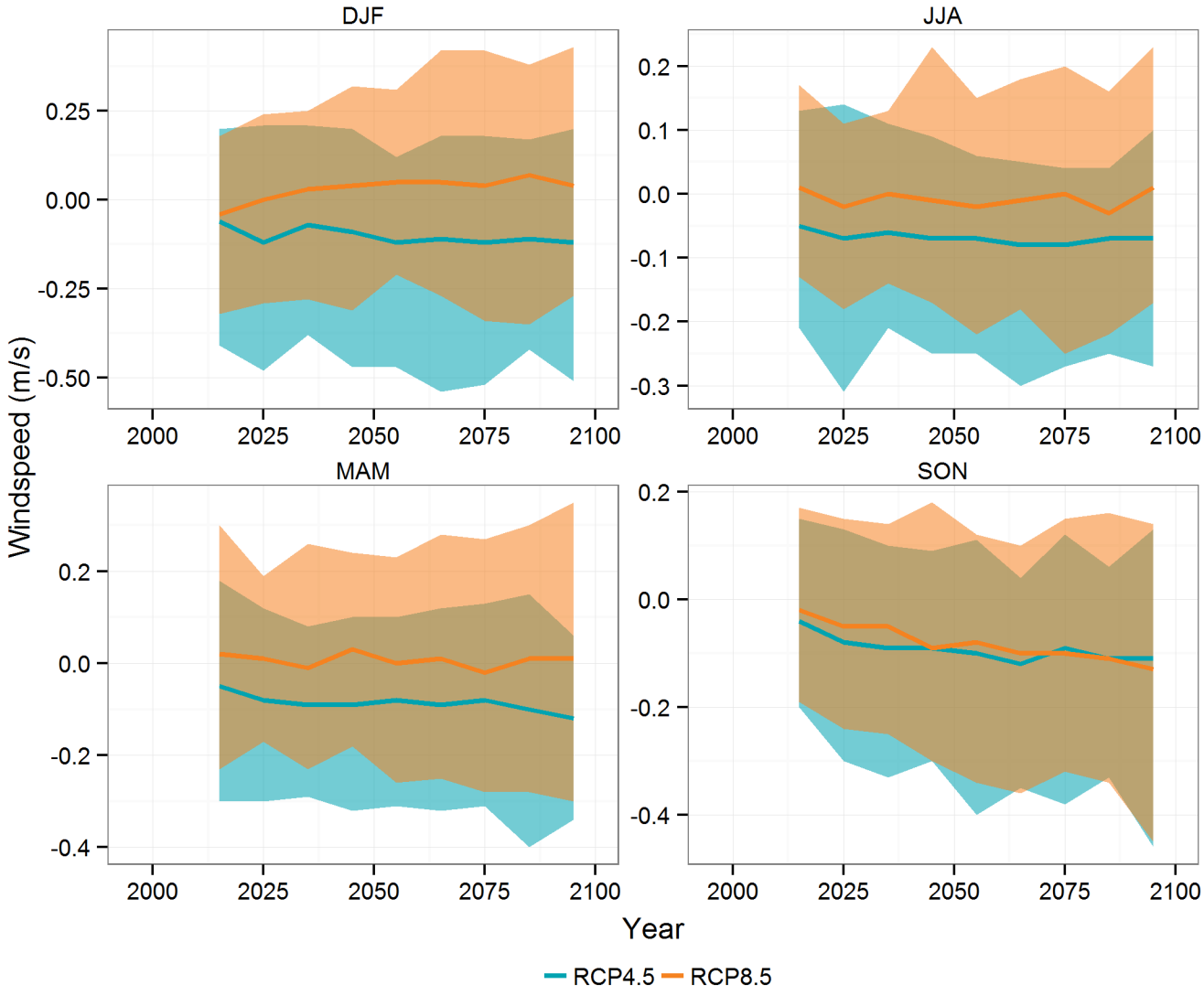

Figure 37: **Projected changes in seasonal mean windspeeds based on the CMIP5 ensemble.**

Table 11: **Summary of mean seasonal windspeed changes projected for Peel Region for RCP4.5 and RCP8.5. P10 represents the ensemble 10th percentile, P90 the ensemble 90th percentile and X represents the ensemble mean change.**

Season	Baseline ($m\ s^{-1}$)	Change by 2020s			Change by 2050s			Change by 2080s		
	X	P10	**X**	P90	P10	**X**	P90	P10	**X**	P90
RCP4.5										
ANN	**4.5**	-0.6	-0.2	0.5	-0.8	-0.3	0.4	-0.8	-0.3	0.5
DJF	**5.0**	-1.3	-0.3	0.8	-1.5	-0.3	0.9	-1.5	-0.4	1.0
MAM	**4.8**	-0.7	-0.2	0.6	-0.8	-0.2	0.5	-0.8	-0.2	0.4
JJA	**3.8**	-0.9	-0.2	0.5	-1.0	-0.3	0.5	-1.1	-0.3	0.6
SON	**4.2**	-0.8	-0.2	0.6	-1.1	-0.3	0.6	-1.2	-0.3	0.6
RCP8.5										
ANN	**4.5**	-0.3	0.0	0.3	-0.4	0.0	0.3	-0.4	-0.1	0.4
DJF	**5.0**	-0.9	0.0	0.6	-0.8	0.1	0.9	-1.0	0.2	1.2
MAM	**4.8**	-0.5	0.0	0.4	-0.6	0.0	0.4	-0.6	0.0	0.5
JJA	**3.8**	-0.6	0.0	0.6	-0.7	0.0	0.6	-0.9	0.0	0.7
SON	**4.2**	-0.7	-0.1	0.5	-1.0	-0.3	0.6	-1.1	-0.3	0.7

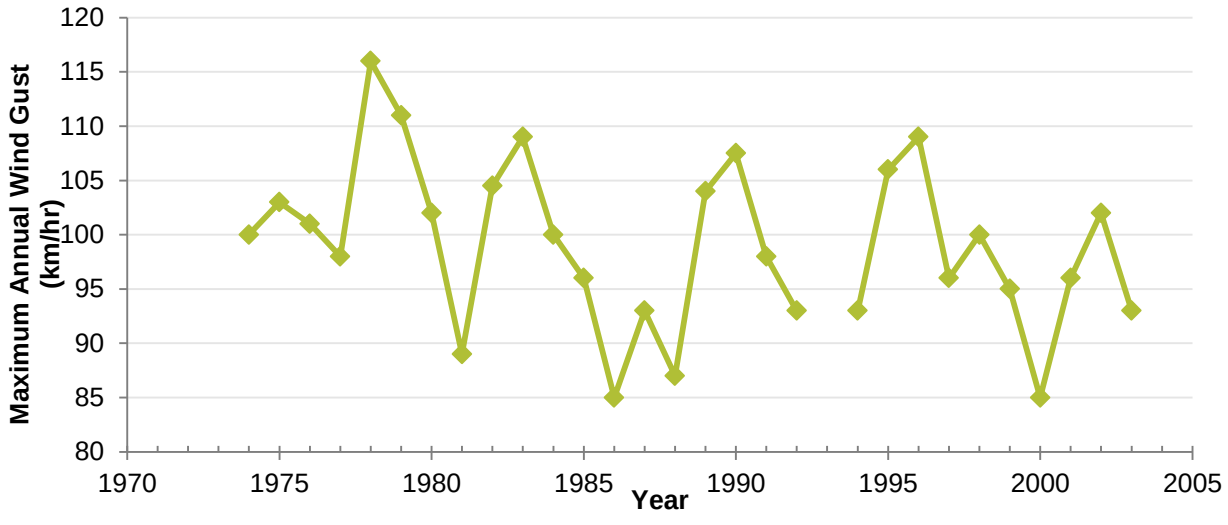

Figure 38: **Historical trend in Toronto Pearson Airport Wind gusts (1974-2003) (Wind monitoring and data quality control programs changed at many airports from the late 1990s onwards with 1.3% missing data).**

i. Humidity

Two humidity variables are analysed in this report: (1) relative humidity, which provides an indication of level of saturation of the atmosphere at a given time, and (2) specific humidity, which indicates the absolute content of atmospheric moisture. The general relationship between these two variables is that as relative humidity decreases, specific humidity increases. This may seem contradictory, but relative humidity is related to temperature (higher temperatures have a greater moisture capacity), while specific humidity is an actual measure of moisture (water mass), in the air. This relationship is governed by the Clausius-Clapeyron relation, a well-established physical law that determines the water-holding capacity of the atmosphere based on temperature (IPCC 2007). It suggests that for every 1°C increase in air temperature, the atmosphere can hold an additional 7% of moisture (IPCC 2007).

For the historical period, only relative humidity was available from Environment Canada's archived climate normal information. Figure 39 demonstrates that relative humidity varies diurnally and seasonally, with the greatest values of daytime humidity in the winter. Early morning relative humidity tends to be much more stable across seasons. Evident from Figure 39 is a slight decrease in relative humidity over time, particularly in the winter months. This is consistent with trends observed in other literature suggesting that the atmospheric water content (specific humidity) in the northern hemisphere has been increasing over time, with the increase being greater in winter than summer (IPCC 2013, Gill et al. 2013).

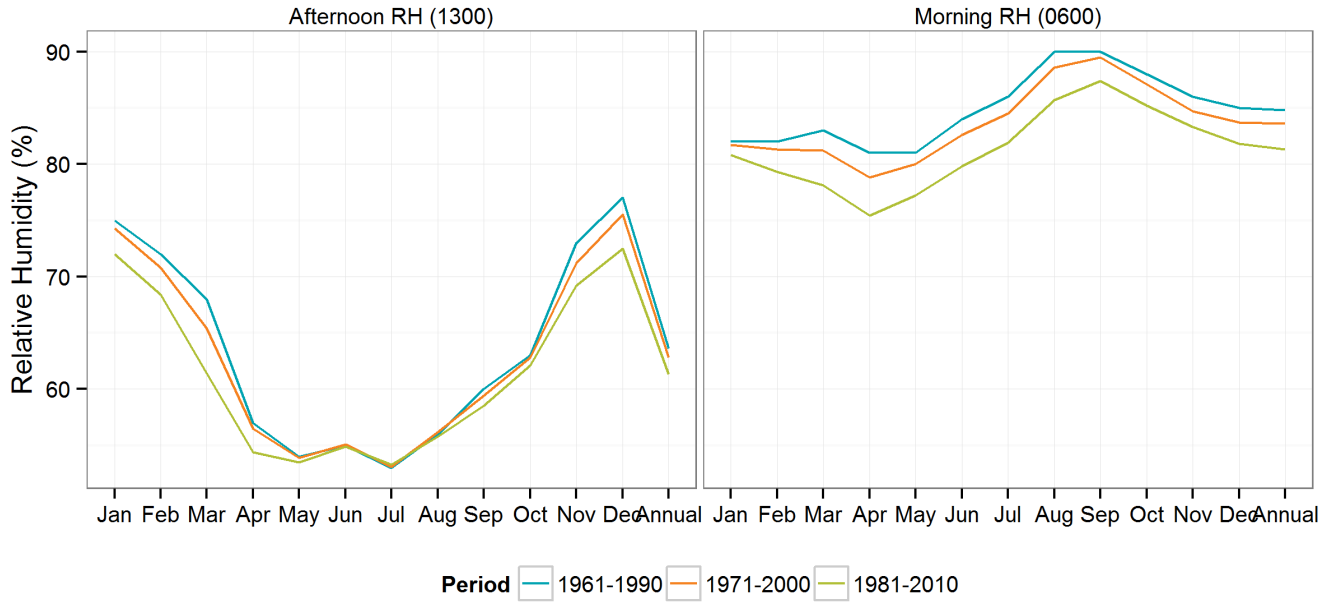

Figure 39: **Historical seasonal and diurnal variability in relative humidity showing three recent normal periods for the Toronto Pearson Airport station.**

Globally, the IPCC concluded in its AR4 report that “observations of trends in relative humidity are uncertain but suggest that it has remained about the same overall, from the surface throughout the troposphere, and hence increased temperatures will have resulted in increased water vapour” (IPCC 2007).

The ensemble analysis conducted for this report shows that relative humidity values are generally projected to decrease, while specific humidity will increase (Figure 40 and Table 12). Based on the projections in temperature and precipitation, CMIP5 models suggest with likelihood that the atmosphere will hold more moisture. Increasing atmospheric temperature increases the available capacity of the atmosphere to hold moisture and overall this increased capacity reduces the relative humidity values through the end of the century (Figure 41 and Table 13). The greater the warming, which is shown by RCP8.5, the greater the moisture holding capacity of the atmosphere. This variable indicates that going forward there will be more moisture available for precipitation events in general.

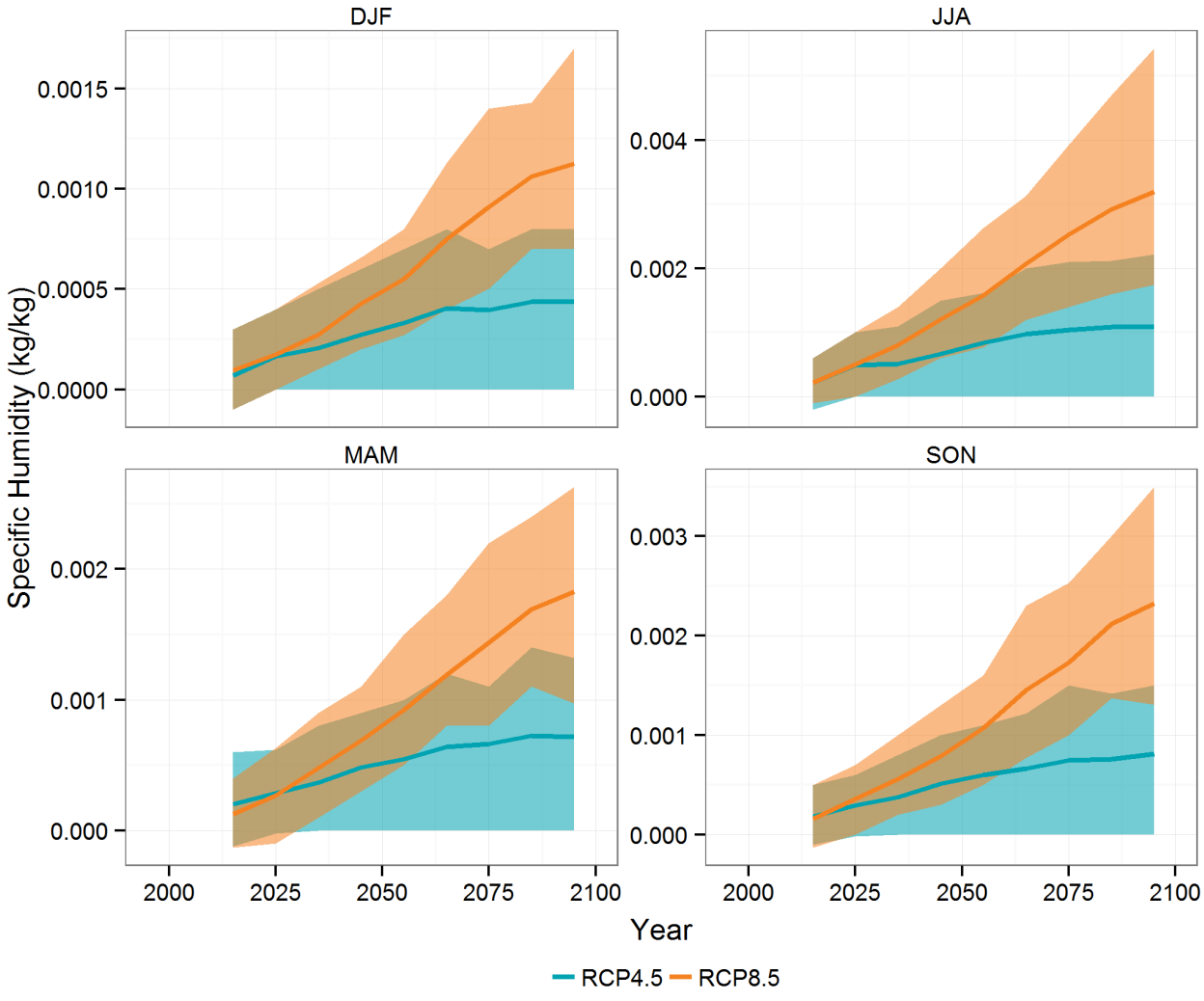

Figure 40: **Projected changes in specific humidity based on the CMIP5 ensemble.**

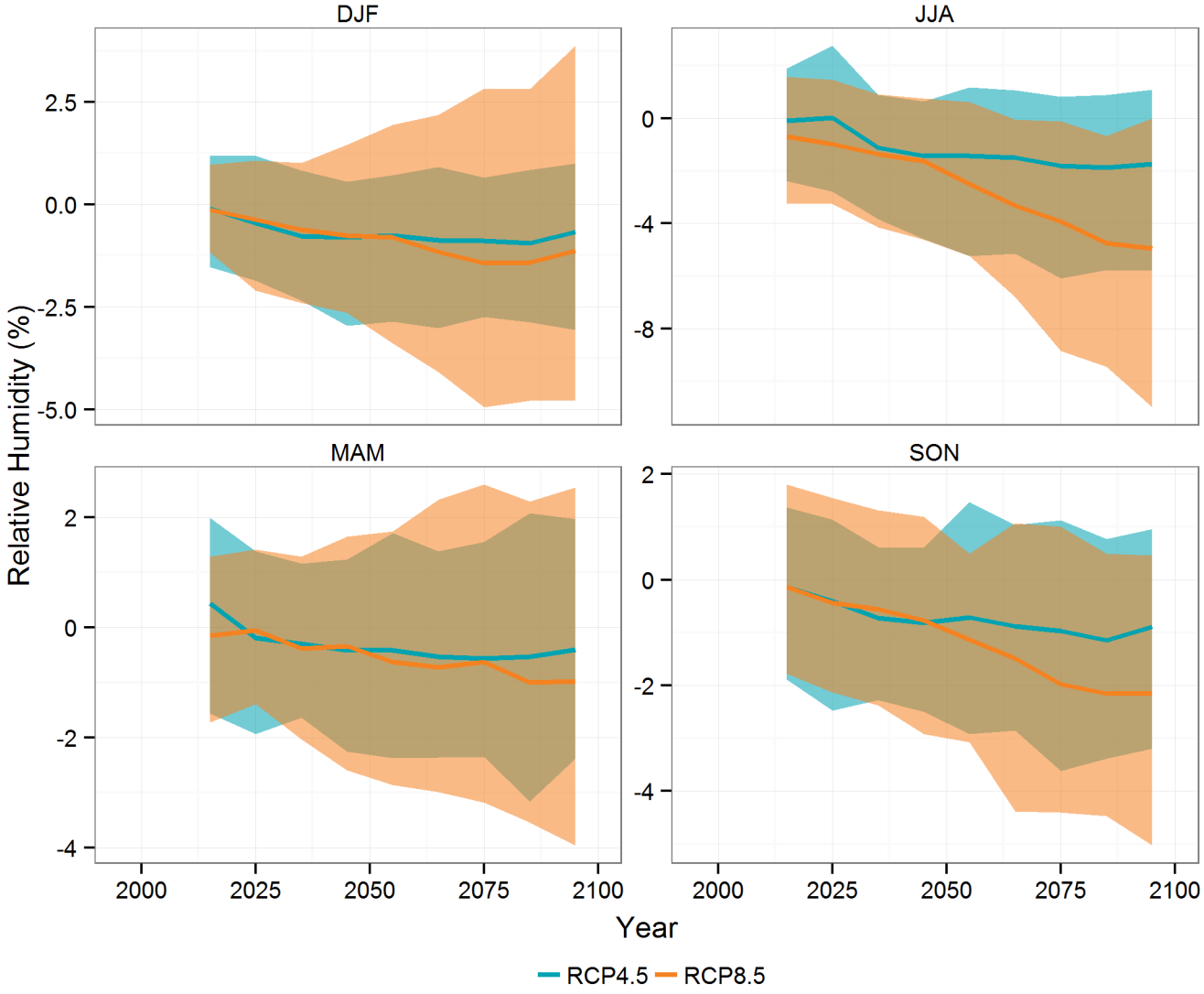

Figure 41: **Projected changes in relative humidity based on the CMIP5 ensemble.**

Table 12: **Summary of mean seasonal changes in specific humidity (kg kg^{-1}) projected for Peel Region for RCP4.5 and RCP8.5. P10 represents the ensemble 10th percentile, P90 the ensemble 90th percentile and X represents the ensemble mean change.**

Season	Baseline	Change by 2020s			Change by 2050s			Change by 2080s		
	X	P10	**X**	P90	P10	**X**	P90	P10	**X**	P90
RCP4.5										
DJF	0.0025	-0.0001	**0.0004**	0.0012	0.0000	**0.0010**	0.0021	0.0000	**0.0013**	0.0023
JJA	0.011	-0.0002	**0.0012**	0.0027	0.0000	**0.0025**	0.0051	0.0000	**0.0032**	0.0064
MAM	0.0053	-0.00014	**0.0009**	0.0020	0.0000	**0.0017**	0.0031	0.0000	**0.0021**	0.0038
SON	0.0066	-0.00012	**0.0009**	0.0019	0.0000	**0.0018**	0.0033	0.0000	**0.0023**	0.0044
ANN	0.0063	0.0001	**0.0008**	0.0016	0.0000	**0.0017**	0.0030	0.0000	**0.0022**	0.0039
RCP8.5										
DJF	0.0025	0	**0.0005**	0.0012	0.0009	**0.0017**	0.0026	0.0019	**0.0031**	0.0045
JJA	0.011	0.00017	**0.0015**	0.0030	0.0026	**0.0049**	0.0078	0.0047	**0.0086**	0.0141
MAM	0.0053	-0.00013	**0.0009**	0.0019	0.0016	**0.0028**	0.0044	0.0029	**0.0050**	0.0072
SON	0.0066	0.00007	**0.0011**	0.0022	0.0016	**0.0033**	0.0052	0.0037	**0.0062**	0.0090
ANN	0.0063	0.0004	**0.0010**	0.0017	0.0020	**0.0031**	0.0046	0.0037	**0.0057**	0.0085

Table 13: **Summary of mean seasonal changes in relative humidity (%) projected for Peel Region for RCP4.5 and RCP8.5. P10 represents the ensemble 10th percentile, P90 the ensemble 90th percentile and X represents the ensemble mean change.**

Season	Baseline	Change by 2020s			Change by 2050s			Change by 2080s		
	X	P10	**X**	P90	P10	**X**	P90	P10	**X**	P90
RCP4.5										
DJF	75.8	-5.7	**-1.3**	3.2	-8.8	**-2.4**	2.2	-8.7	**-2.5**	2.5
JJA	68.6	-9.0	**-1.2**	5.5	-15.0	**-4.4**	2.9	-17.6	**-5.5**	2.8
MAM	66.7	-5.1	**0.0**	4.5	-7.0	**-1.4**	4.3	-7.9	**-1.5**	5.6
SON	74.3	-6.6	**-1.3**	3.1	-8.3	**-2.4**	3.1	-10.2	**-3.0**	2.9
ANN	71.3	-4.8	**-0.9**	2.3	-8.2	**-2.5**	2.1	-9.9	**-2.9**	1.9
RCP8.5										
DJF	75.8	-5.7	**-1.1**	3.1	-10.1	**-2.7**	5.6	-14.5	**-4.0**	9.5
JJA	68.6	-10.7	**-3.0**	3.9	-16.6	**-7.4**	1.3	-29.2	**-13.6**	-0.8
MAM	66.7	-5.1	**-0.6**	4.0	-8.4	**-1.7**	5.7	-10.7	**-2.6**	7.4
SON	74.3	-6.3	**-1.1**	4.7	-10.4	**-3.4**	2.8	-13.9	**-6.3**	2.0
ANN	71.3	-5.4	**-1.5**	2.4	-9.0	**-3.8**	2.4	-14.5	**-6.7**	2.5

Some authors have shown that the atmospheric moisture content should be related to the trend in maximum precipitation (Westra et al. 2013). They have shown that the rate of increase of these events is similar to the rate of increase in atmospheric moisture, roughly following the theoretical relationship between temperature and moisture capacity. These results have been associated with daily events, but not shorter-duration events where precipitation amounts can exceed this relationship. In these cases, changes in atmospheric circulation (horizontal transfer) also play an important role (Westra et al. 2013). The findings of increased atmospheric moisture in the current study further support the likelihood of an increase in extreme precipitation events.

WHY CARE ABOUT HUMIDITY?

Even though humidity impacts our lives on a day-to-day basis, its effects generally go completely unnoticed. Without humidity, there would be no weather, no clouds, no precipitation or fog, and little opportunity for life. Humidity is simply water vapor in the air, which is needed to form rain and hold heat in the air. It is a greenhouse gas that can absorb heat and warm the atmosphere. Humidity or water vapour in the air can store large amounts of energy and release it again during precipitation (e.g. thunderstorms and hurricanes). Due to its properties, humidity in the air stabilizes our climate and prevents large extremes of temperature.

Humans are sensitive to humidity because our bodies use evaporative cooling to regulate internal temperatures. Humans can be comfortable within a wide range of humidities depending on the temperature — from thirty to seventy percent, but ideally between 50% and 60%. For safety reasons, occupational health and safety regulations require limitations on human activities during high humidity situations. Other studies have linked low humidities in winter with flu virus prevalence and transmission, and high humidities in summer with heat related illnesses and with heart attack deaths among the elderly. High humidity levels also influence agricultural crop health, pose risks for animal health both in barns and during grazing and impact crop and post-harvest management (crop storage). Excess humidities and moisture infiltration into buildings can also accelerate mould and decay damage and generally lead to premature deterioration of materials and equipment. Humidity can also disrupt manufacturing processes, with responses needed to prevent condensation, corrosion, mould, warping or other spoilage that are highly relevant for foods, pharmaceuticals, chemicals, fuels, wood, paper, fertilizers, and many other products. Air conditioning, ventilation technologies and associated control systems are often used to control humidity levels, each requiring significant energy to remove or mitigate atmospheric water vapour. High humidity levels also have impacts on transportation through roadway icing risks, poor visibilities in fog restricting our ability to drive, move over water and fly and in requirements for humidity control in transport containers.

i. Growing Season and Drought

The general scientific consensus is that climate change is very likely to result in increased temperature globally (IPCC 2013) however the specific manner in which that trend will affect the local climate in Peel Region is complex. For certain variables, specifically monthly precipitation, winds, humidity, and indices dependent on daily sequences, the specific changes are predicted within large ranges of uncertainty (Schindler et al. 2015; Wilby et al. 2004). That being said, certain trends can be elucidated with higher confidence. In particular, the region will likely see increased temperatures over all seasons, and seasonal changes in precipitation distribution, along with greater probability of extreme temperature and precipitation events. More precipitation is likely during the winter, with slightly greater amounts in the fall and spring. On average, the summer is likely to be drier, but punctuated by heavy rainfall events. While the growing season is projected to increase by between approximately 13 and 34 days on average, because of the difficulty of predicting day-to-day variability in climate models (Schindler et al. 2015), unseasonal frost is still an important climate risk (Holland & Smit 2014). Corn heat units (CHUs) are also projected to increase by between 19 and 38 percent, however if accompanied by a lack of precipitation, this trend may not be beneficial to producers. Additionally, the increased occurrence of extreme heat events during the growing season can compound issues of lacking moisture. The aforementioned trends are summarized in Table 14, and it is evident from the estimates that the uncertainty associated with climate change will make predicting seasonal climate conditions become more difficult.

Many of the changes described previously and highlighted in Table 14 are evident in the recent climatic history. Figure 42: provides an overview of changes in the agroclimatic variables of growing season length and corn heat units and demonstrates trend increases over the three most recent normal periods. With respect to moisture, Figure 43 provides an overview of growing season moisture index based on Environment Canada's homogenized monthly climate data, and demonstrates a trend toward drier growing seasons. Applying the Mann-Kendall trend test reveals that this trend toward drier growing seasons is indeed significant.

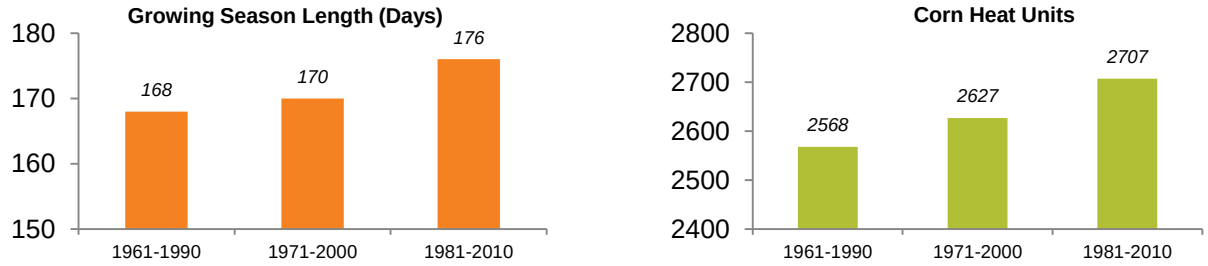

Figure 42: Historical trends in agricultural variables of growing season length, corn heat units and frost-free period for the Orangeville climate station. Results show increases in the each variable over time.

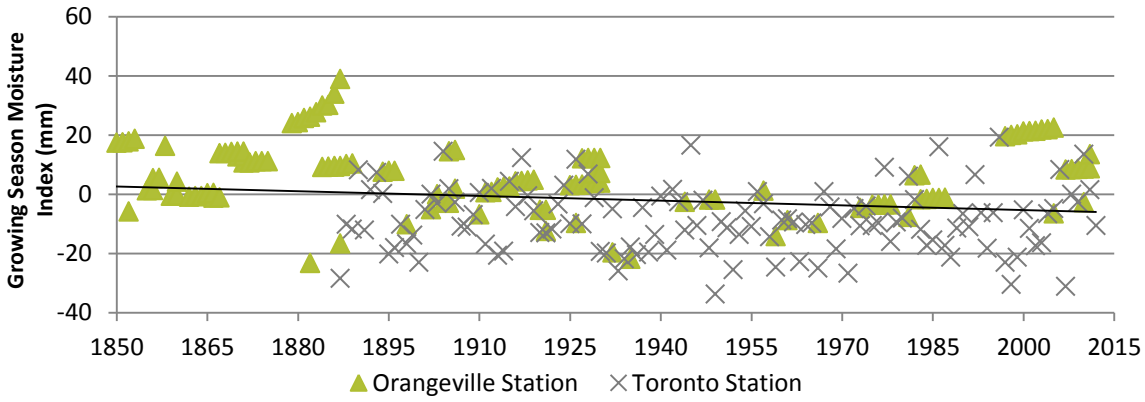

Figure 43: Growing season moisture index record for the Toronto and Orangeville stations since 1850. Application of the Mann-Kendall trend test reveals a statistically significant trend toward a drier climate (tau = -0.135, 2-sided p-value =0.0105 at 0.95 confidence level).

Table 14: Baseline (1981-2010) and future (2041-2070) projected values for agricultural climate indicators, along with interpretation of trends for the future.

Climate Condition / Event	Indicator	Baseline Value	Lower Estimate	Upper Estimate	Lower Estimate Change	Upper Estimate Change	Interpretation
Growing Season Condition	Corn Heat Units [CHU]	3087.2	3674.3	4246.9	19%	38%	Very likely more
	Growing Season Length (frost-free period) [days]	164.5	178.0	197.5	13.48	32.95	Likely longer[b]
	Growing Season Start Date [day of year]	124.3	109.6	118.6	-14.67	-5.68	Likely earlier[b]
	Growing Season End Date [day of year]	287.8	298.9	313.9	11.13	26.12	Likely later[b]
	Growing Season Average Temperature [°C]	15.1	16.8	18.9	1.70	3.80	Very likely warmer
	Growing Season Total Precipitation [mm]	464.5	414.4	573.7	-11%	24%	Likely overall drier season, with more precip. in shoulder months
Frost Risk	Growing Season days per month with daily minimum temperature ≤ 0°C [days]	2.9	0.8	1.9	-2.06	-0.96	Uncertain - assume more frequent
	Growing Season days per month with daily minimum temperature ≤ 2°C [days]	1.5	0.3	0.9	-1.19	-0.61	Uncertain - assume more frequent
	Growing Season days per month with daily minimum temperature ≤ 3°C [days]	5.5	2.4	4.1	-3.09	-1.38	Uncertain - assume more frequent
Extreme Heat Events	Total growing season days with daily maximum temperature > 30°C	10.3	3.1	23.4	-70%	127%	Likely more frequent

Table continued on next page…

Climate Condition / Event	Indicator	Baseline Value	Lower Estimate	Upper Estimate	Lower Estimate Change	Upper Estimate Change	Interpretation
Extreme Precipitation Frequency	Total annual precipitation in the 95th percentile mm]	228.9	223.6	337.5	-2%	47%	Likely more frequent extreme precip.
Extreme Precipitation Intensity	1-day maximum precipitation accumulation [mm]	37.0	35.0	47.0	-5%	27%	Likely more intense extreme precip.
	5-day maximum precipitation accumulation [mm]	59.2	55.9	75.1	-6%	27%	Likely more intense extreme precip.
Drought / Moisture Deficit	Growing season moisture index (precipitation – evapotranspiration) [mm]	9.3	-52.1	13.2	-661%	42%	Likely overall drier season[c]
	Growing season days per month with no precipitation [days]	119.3	116.0	121.6	-3	2	Uncertain – assume overall more dry days with more days of heavy precipitation. [c]

Notes:

a. Interpretation is based on ensemble changes, in combination with expert opinions on the reliability of climate models in simulating the variable in question

b. Overall growing season length is projected to increase, however this does not consider the fact that inter-annual variability may result in more instances of unseasonal frost

c. Projections for Ontario suggest that precipitation during the summer months will be characterized by generally drier conditions interspersed with more frequent heavy rainfall events.

Drought

Drier conditions throughout the growing season are not only important for agriculture but future dry periods, their magnitude, their frequency and their duration are particularly relevant for various sectors across Peel Region (e.g., natural systems conservation and land use planning) when dryness leads to drought. The climate variable 'total number of dry days' provides an indication of the future trend of the days per year that receive no precipitation (or less than 1mm). On an annual basis, no significant trend is found to be either increasing or decreasing from the 1981-2010 baseline conditions, which identify 234 dry days on average per year. This projection is associated with 'more likely than not' confidence, as described in Table 3. However, with daily mean, maximum and minimum temperatures in all seasons projected to increase, evaporation and evapotranspiration rates could likely increase on an annual basis and particularly in the summertime. With an increase in water lost to the atmosphere, it is not entirely certain with a changing climate precisely what the frequency and magnitude of water may be in returning precipitation to the surface. Thus, it is prudent to assume that drought conditions, as they have already been experienced in Peel Region to date, will at least remain similar in frequency, duration and magnitude. A case study conducted in Peel Region as part of the natural systems vulnerability assessment (Tu et al. 2015), examined historical drought occurrences based on the climate record at Pearson Airport station. Table 15 summarizes the worst ten drought events since 1849, on a three year basis, expressed in terms of a moisture index (precipitation less evapotranspiration) using the Thornthwaite equation. A negative moisture index indicates a moisture deficit over a specific period. These represent the top 6.3% of extreme drought events that have occurred in the region. A discussion of the impacts associated with these drought conditions is out of the scope of this report; however, impacts on the natural system in the West Humber are presented in Tu et. al. (2015).

Table 15: Historic drought events since 1849 using the Pearson Airport climate station record.

Three Year Period	Total Moisture Index (mm)				Percentile Rank (since 1849)
	Growing Season	April, May, June	July, August	September, October	
1997 - 1999	-746.95	-220.93	-468.68	-57.34	100.0%
1933 - 1935	-655.26	-186.74	-499.11	30.58	99.3%
1948 - 1950	-611.67	-240.67	-393.30	22.30	98.6%
1934 - 1936	-599.80	-136.08	-537.75	74.03	97.9%
1998 - 2000	-569.40	9.49	-515.71	-63.18	97.2%
1949 - 1951	-543.73	-232.27	-297.93	-13.53	96.5%
1947 - 1949	-538.40	-79.62	-412.86	-45.92	95.8%
1898 - 1900	-534.70	-198.21	-543.20	206.71	95.1%
1969 - 1971	-532.58	-158.18	-288.46	-85.94	94.4%
1932 - 1934	-526.81	-180.20	-375.06	28.46	93.7%

4. CONCLUDING REMARKS

This report was intended to provide a summary of recent trends and projected changes in climate for the geographic area of Peel Region. This analysis was the result of original analysis of climate projections, archived climate data and interpretations of existing findings in the literature and demonstrates conclusively that the climate has been changing rapidly since the 1950s and that such changes are projected with confidence to increase into the future. There is, however, significant uncertainty with respect to the precise magnitudes of changes into the future. This uncertainty is the result of multiple sources of variability resulting from natural variation in the climatic between locations and from year-to-year, the abundance of climate models and downscaling techniques, and multiple plausible future emission scenarios. The following sub-sections provide some recommendations on future research and initiatives related to climate data and science that could be pursued for Peel Region

4.1. Bolster Monitoring Data for Better Adaptive Management

The analysis provided in this report indicates a need for higher resolution meteorological observation networks in Peel Region. Forensic case studies showed that existing long-term climate stations were simply by-passed by high impact events, which were only occasionally well sampled by other networks.

- Observation networks should be included in long term planning to develop long term data sets for proper climate monitoring. Locating representative climate data with sufficiently long periods of record was challenging.
- Particular focus should be placed on monitoring and understanding local dynamics of wind, extreme rainfall and changes to the snowpack.
- The urban heat island is a dominant climate driver in the GTHA and currently, our monitoring programs do not adequately capture this effect on a range of variables, including temperature, wind, precipitation, and air quality.

4.2. Focus on Understanding and Measuring Impacts

The forensic assessment of urban flooding events confirmed that individual high impact weather and climate events will result in multiple types of impacts to numerous infrastructure systems. The nature of these combination events should be understood to better develop response measures, such as alternative surface transportation routes in areas vulnerable to overland flooding, and lightning and wind protection for communication systems.

- Forensic assessments also indicated the potential for identification of antecedent conditions which precede high impact events, again indicating the possibility improved preparation and response.
- Studies of local events are of particular importance in that they can identify region specific characteristics which may not be identified in similar events impacting other geographical locations.
- The identification of convective (thunderstorm) rainfall events as being the major contributor to urban flooding in Port Credit is of particular importance when considering that convection is far

more efficient at producing precipitation than other storm types, suggesting that increases in atmospheric moisture will result in disproportionately greater increases in high impact extreme precipitation events.

- Impact data relating to climatic hazards in Peel region should be consistently collected, stored and analysed periodically; given the localized nature of many atmospheric hazards identified in this study, direct meteorological measurements are often not available, and therefore the effects of a given event on public and private infrastructure are the only available record of their occurrence and severity.

4.3. Be Conservative When Estimating Risk with Climate Information

The current best science suggests that globally, the climate is tracking closes to the RCP8.5 scenario. For planning purposes, particularly where extremes matter, we recommend using RCP8.5 scenario. Of the two RCPs, the historical trend has been following RCP8.5. Even if we do make changes to global GHG emissions today, then we will continue along the same trend for a while.

5. REFERENCES

Alexander, L. V., et al. (2006), Global observed changes in daily climate extremes of temperature and precipitation. Journal of Geophysical Research, 111, D05109, doi: 10.1029/2005JD006290

AMEC Environment & Infrastructure, 2014. *July 8, 2013 Extreme Rainfall Event Climatological Report.* Prepared for Toronto and Region Conservation Authority.

Angel, Jim, 1996. *Cyclone Climatology of the Great Lakes*. Miscellaneous Publication 172. Midwestern Climate Center, Illinois State Water Survey, Champaign, Ilinois, U.S.

Aquafor Beach Ltd. 2012. *Cooksville Creek Flood Evaluation Master Plan EA – Final report.* Prepared for City of Mississauga. 40p.

Behan, K.J., Mate, D., Maloley, M., and Penney, J., 2011. Using Strategic Partnerships to Advance Urban Heat Island Adaptation in the Greater Toronto Area. Geological Survey of Canada, Open File 6865. 1 CD-ROM. doi:10.4095/288755

Bürger, G., Murdock, T.Q., Werner, A.T., Sobie, S.R., Cannon, A.J. 2012. Downscaling Extremes – an Intercomparison of Multiple Statistical Methods for Present Climate. *Journal of Climate*, 25, 4366-4388. DOI: 10.1175/JCLI-D-11-00408.1

Burnett, A. W., M. E. Kirby, H. T. Mullins, and W. P. Patterson, 2003: Increasing Great Lake-effect snowfall during the twentieth century: A regional response to global warming? J. Climate, 16, 3535–3543.

Canadian Standards Association (CSA), 2012. *Technical Guide: Development, interpretation and use of rainfall intensity-duration-frequency (IDF) Information: Guideline for Canadian water resources practitioners.* PLUS 4013 (2nd ed.). Mississauga, Ontario.

Cheng, C.S., H. Auld, G. Li, J. Klaassen, and Q. Li. 2007.Possible impacts of climate change on freezing rain in south-central Canada using downscaled future climate scenarios. Natural Hazards and Earth System Sciences. Vol. 7. Pp. 71-87.

Cheng, C. S., G. Li, Q. Li, and H. Auld. 2011. A Synoptic Weather-Typing Approach to Project Future Daily Rainfall and Extremes at Local Scale in Ontario, Canada. Journal of Climate. Vol. 24. Pp. 3667-3685.

Cheng, C. S., G. Li, and H. Auld. 2011b. Possible Impacts of Climate Change on Freezing Rain Using Downscaled Future Climate Scenarios: Updated for Eastern Canada. Atmosphere-Ocean. Vol. 49:1, pp. 8-21.

Cheng, C.S., H. Auld, Q. Li and G. Li. 2012. Possible impacts of climate change on extreme weather events at local scale in south-central Canada. Climatic Change. Vol. 112, Issue 3-4. pp 963-979.

Cheng, C. S., G. Li, Q. Li, H. Auld and C. Fu. 2012b. Possible Impacts of Climate Change on Wind Gusts under Downscaled Future Climate Conditions over Ontario, Canada. Journal of Climate. Vol. 25. Pp 3390- 3408.

Deidda, R., Marrocu, M., Caroletti, G., Pusceddu, G., Langousis, A., Lucarini, V., Puliga, M., & Speranza, A. (2013). Regional climate models' performance in representing precipitation and temperature over selected Mediterranean areas. Hydrology and Earth System Sciences, 17, 5041-5059.

EBNFLO Environmental AquaResource Inc., 2010. *Guide for Assessment of Hydrologic Effects of Climate Change in Ontario*. For the Ontario Ministry of Natural Resources and Ministry of the Environment in Partnership with Credit Valley Conservation.

Eichenlaub, Val, 1979. *Weather and Climate of the Great Lakes Basin*. University of Notre Dame Press, Indiana.

Flato, G., J. Marotzke, B. Abiodun, P. Braconnot, S.C. Chou, W. Collins, P. Cox, F. Driouech, S. Emori, V. Eyring, C. Forest, P. Gleckler, E. Guilyardi, C. Jakob, V. Kattsov, C. Reason and M. Rummukainen, 2013: Evaluation of Climate Models. In: Climate Change 2013: The Physical Science Basis. Contribution of Working Group I to the Fifth Assessment Report of the Intergovernmental Panel on Climate Change [Stocker, T.F., D. Qin, G.-K. Plattner, M. Tignor, S.K. Allen, J. Boschung, A. Nauels, Y. Xia, V. Bex and P.M. Midgley (eds.)]. Cambridge University Press, Cambridge, United Kingdom and New York, NY, USA.

Fuss, S., Canadell, J. G., Peters, G. P., Tavoni, M., Andrew, R. M., Ciais, P., ... & Yamagata, Y. (2014). Betting on negative emissions. Nature Climate Change, 4(10), 850-853.

Giorgi, F., Jones, C., and Asrar, G. 2009. Addressing climate information needs at the regional level: the CORDEX framework. WMO Bulletin, 58(3), 175-183.

Gill, E., Chase, T., Pielke, R., Wolter, K. 2013. Northern Hemisphere summer temperature and specific humidity anomalies from two reanalyses. *Journal of Geophysical Research: Atmospheres*. DOI: 10.1002/jgrd.50635

Gleckler, P. J, K. E. Taylor, and C. Doutriaux (2008) Performance metrics for climate models. Journal of Geophysical Research. Vol. 113. D06104.

Grenci, L. M., Nese, J. M., & Babb, D. M. (2010). *A World of Weather: fundamentals of meteorology*. Kendall/Hunt Publishing Company.

Hoffman, D. W., & Richards, N. R. (1953). *Soil Survey of Peel County*. Guelph, Ontario.

Holland, T., Smith, B. 2014. Recent climate change in the Prince Edward County winegrowing region, Ontario, Canada: Implications for adaptation in a fledgling wine industry. *Regional Environmental Change,* 14(3), 1109-1121. DOI: 10.1007/s10113-013-0555-y

Hopkinson, R., M. F. Hutchinson, D. W. McKenney, , E. Milewska, E., M.F., Papadopol (2012). Optimizing Input Data for Gridding Climate Normals for Canada. Journal of Applied Meteorology and Climatology. American Meteorological Society. Vol. 51. Pp 1508-1518.

Huntingford, C., Jones, P.D., Livina, V.N., Lenton, T.M., Cox, P. 2013. No increase in global temperature variability despite changing regional patterns. *Nature,* 500, 327-350. DOI: 10.1038/nature12310

IPCC (2007). Working Group I Contribution to the IPCC Fourth Assessment Report on Climate Change 2007: The Physical Science Basis. Online: http://www.ipcc.ch/publications_and_data/ar4/wg1/en/contents.html

IPCC (2013). Working Group I Contribution to the IPCC Fifth Assessment Report on Climate Change 2013: The Physical Science Basis. Online: http://www.ipcc.ch/report/ar5/wg1/

IPCC-TGICA (2007). *General Guidelines on the Use of Scenario Data for Climate Impact and Adaptation Assessment.* Version 2. Prepared by T.R. Carter on behalf of the Intergovernmental Panel on Climate Change, Task Group on Data and Scenario Support for Impact and Climate Assessment, 66pp.

IPCC-SREX. (2012). *Managing the Risks of Extreme Events and Disasters to Advance Climate Change Adaptation*. A Special Report of Working Groups I and II of the Intergovernmental Panel on Climate Change. Aka: 'SREX report'. [Field, C.B., V. Barros, T.F. Stocker, D. Qin, D.J. Dokken, K.L. Ebi, M.D. Mastrandrea, K.J. Mach, G.-K. Plattner, S.K. Allen, M. Tignor, and P.M. Midgley (eds.)]. Cambridge University Press, Cambridge, UK, and New York, NY, USA, 582 pp. Access: http://ipcc-wg2.gov/SREX/

Kharin, V. V., F. W. Zwiers, X. Zhang and M. Wehner (2013) Changes in temperature and precipitation extremes in the CMIP5 ensemble. Climatic Change. Vol. 119. No.2. pp 345-357.

Kim, B. M., Son, S. W., Min, S. K., Jeong, J. H., Kim, S. J., Zhang, X., ... & Yoon, J. H. (2014). Weakening of the stratospheric polar vortex by Arctic sea-ice loss. *Nature communications*, *5*.

King, Patrick W. S., Michael J. Leduc, David M. L. Sills, Norman R. Donaldson, David R. Hudak, Paul Joe, and Brian P. Murphy, 2003. Lake Breezes in Southern Ontario and Their Relation to Tornado Climatology. *Weather and Forecasting*, 18: 795-802.

Klaassen Joan, Shouquan Cheng, Heather Auld, Qian Li, Ela Ros, Malcolm Geast, Guilong Li, Ron Lee, 2003. *Estimation of Severe Ice Storm Risks for South-Central Canada. Meteorological Service of Canada, Toronto*. For Office of Critical Infrastructure Protection and Emergency Preparedness, Ottawa, Ontario, Minister of Public Works and Government Services, Catalogue No.: PS4-6/2004E-PDF, ISBN: 0-662-37712-5

Kunkel, K.E., L. Ensor, M. Palecki, D. Easterling, D. Robinson, K.G. Hubbard, and K. Redmond, 2009a. A new look at lake-effect snowfall trends in the Laurentian Great Lakes using a temporally homogenous data set. *Journal of Great Lakes Research*, 35: 23-29.

Kunkel, K.E., M.A. Palecki, L. Ensor, D. Easterling, K.G. Hubbard, D. Robinson, and K. Redmond, 2009b Trends in twentieth-century U.S. extreme snowfall seasons. *Journal of Climate*, 22: 6204-6216.

Melillo, Jerry M., Terese (T.C.) Richmond, and Gary W. Yohe, Eds., 2014. *Climate Change Impacts in the United States: The Third National Climate Assessment*. U.S. Global Change Research Program, 841 pp. doi:10.7930/J0Z31WJ2.

McKenney, D. W., Hutchinson, M.F., Papadopol, P., Lawrence, K., Pedlar, J., Campbell, K., Milewska, E., Hopkinson, R., Price, D., Owen, T. (2011). Customized spatial climate models for North America. American Meteorological Society-BAMS December: 1612-1622).

MSC-Hazards. 2011. Environment Canada. Canadian Atmospheric Hazards Network. Adaptation and Impacts Research, Environment Canada, Toronto, Ontario, Canada.

Oke, T.R. 1987. Boundary Later Climates (2nd Ed.) New York, NY: Published by Menthuen & Co. Ltd. 435 pp.

Peltier, R.W., Gula, J. 2012. Dynamical Downscaling over the Great Lakes Basin of North America Using the WRF Regional Climate Model: The Impact of the Great Lakes System on Regional Greenhouse Warming. *J. Climate*, **25**, 7723–7742. DOI: http://dx.doi.org/10.1175/JCLI-D-11-00388.1

Peters, G., R. Andrew, T. Boden, J. Canadell, P. Ciais, C. Le Quéré, G. Marland, M. Raupach, C. Wilson (2012a), "The challenge to keep global warming below 2ºC" *Nature Climate Change*, http://dx.doi.org/10.1038/nclimate1783, DOI:10.1038/nclimate1783.

Phillips, D. 1990. *The Climates of Canada*. Canadian Government Publishing Center, Ottawa. Available online from: http://climate.weather.gc.ca/prods_servs/historical_publications_e.html

Schindler, A., Toreti, A., Zampieri, M., Scoccimarro, E., Gualdi, S., Fukutome, S., Xoplaki, E., Luterbacher, J. 2015. On the Internal Variability of Simulated Daily Precipitation. *Journal of Climate***,** 28, 3624–3630. DOI: http://dx.doi.org/10.1175/JCLI-D-14-00745.1

Scott, R.W. & Huff, F.A. 1997. *Lake Effects on Climatic Conditions in the Great Lakes Basin*. Research Report 97-01, Mid-Western Climate Center. Illinois State Water Survey, Atmospheric Sciences Division, Champaign, Illinois, U.S.A.

SENES, 2011. *Toronto's Future Weather and Climate Driver Study*. Accessed November 10, 2014 from:
http://www1.toronto.ca/wps/portal/contentonly?vgnextoid=b8170744ee0e1410VgnVCM10000071d60f89RCRD

Sheffield, J, Langenbrunner, B., Meyerson, J.E., Neelin, J.D., Camargo, S.J., Fu, R., Hu, Q. Jiang, X., Karnauskas, K.B., Kim, S.T., Kumar, S.,Kinter,J.,Maloney, E.D., Mariotti, A., Pan, Z., Ruiz-Barradas, A., Nigram, S., Seager, R., Serra, Y.L.,Sun,D.,Wang, C., Yu,J., Johnson, N., Xie,S., Zhang, T., Zhao, M. (2013). North American Climate in CMIP5 Experiments. Part II: Evaluation of Historical Simulations of Intra-Seasonal to Decadal Variability. Journal of Climate, 10.1175/jcli-d-12-0593.1.

Sillmann, J., Kharin, V.V., Zhang, X., Zwiers, W.; Bronaugh, D. (2013a). Climate extreme indices in the CMIP5 multimodel ensemble: Part 1. Model evaluation in the present climate. *Journal of Geophysical Research: Atmospheres*, 118, 1716-1733.

Sillmannn, J., Kharin, V.V., Zhang, X., Zwiers, W.; Bronaugh, D. (2013b). Climate extreme indices in the CMIP5 multimodel ensemble: Part 2. Future climate projections. *Journal of Geophysical Research: Atmospheres*, 118, 2473-2493.

Sun, F., Roderick, M., Farquhar, G. 2012. Changes in the variability of global land precipitation. *Geophysical Research Letters: Hydrology and Land Surface Studies.* DOI: 10.1029/2012GL053369

Taylor, K.E., Stouffer, R.J., Meehl, G.A. (2012). An Overview of CMIP5 and the Experiment Design. Bulletin of the American Meteorological Society, 93, 485-498. Doi: http://dx.doi.org/10.1175/BAMS-D-11-00094.1

Tebaldi, C. and R. Knutti (2007). The use of the multimodel ensemble in probabilistic climate projections. Philosophical Transactions of the Royal Society (special issue on Probabilistic Climate Change Projections), Vol. 365, pp. 2053-2075.

Toronto and Region Conservation Authority (2011). Peel Region Urban Forest Strategy.

Toronto and Region Conservation and ESSA Technologies (TRCA and ESSA) (2012). Mainstreaming Climate Change Adaptation in Canadian Water Resource Management: The state of practice and strategic directions for action. Toronto and Region Conservation Authority: Toronto, ON. pp 79.

Tu, C., Milner, G., Lawrie, D., Shrestha, N., Hazen, S. (2015). Natural Systems Vulnerability to Climate Change in the Region of Peel. Toronto, Ontario: Toronto and Region Conservation Authority and Ontario Climate Consortium Secretariat.

U.S. EPA, 2012. *The Great Lakes: An Environmental Atlas and Resource Book*, Chapter Two. Available online. United States Environmental Protection Agency and Government of Canada, ISBN 0-662-23441-3. Accessed November 10, 2014 at http://www.epa.gov/greatlakes/atlas/glat-ch2.html

U.S. EPA, 2014. *Heat Island Effect.* Retrieved December 1, 2014 from http://www.epa.gov/heatisland/

Vincent, L.A. and É. Mekis, 2006 (updated; trends 1950-2007). Changes in daily and extreme temperature and precipitation indices for Canada over the twentieth century. Atmosphere-Ocean, 44(2): 177-193.

Westra, S., L. V. Alexander, and F. W. Zwiers. 2013. Global Increasing Trends in Annual Maximum Daily Precipitation. Journal of Climate. Vol. 26. Pp. 3904- 3818.

Wilby, R.L, S.P. Charles, E. Zorita,B. Timbal, P. Whetton, L.O. Mearns. (2004). Guidelines for Use of Climate Scenarios Developed from Statistical Downscaling Methods. Intergovernmental Panel Climate Change (IPCC). Access: http://www.ipcc-data.org/guidelines/dgm_no2_v1_09_2004.pdf

Wright, D. M., Posselt, D. J., & Steiner, A. L. 2013. Sensitivity of Lake-Effect Snowfall to Lake Ice Cover and Temperature in the Great Lakes Region. *Mon. Wea. Rev.*, **141**, 670–689.

Zwiers, F. W. 2001. (Regional) Climate Model Validation. Canadian Centre for Climate Modelling and Analysis, Atmospheric Environment Service, Presentation. Victoria, BC.

6. APPENDIX A: CLIMATE MODELS COMPRISING THE CMIP5 ENSEMBLE

Model Name	Organization	Country	Organization Details
ACCESS1-0	CSIRO-BOM	Australia	CSIRO (Commonwealth Scientific and Industrial Research Organisation, Australia), and BOM (Bureau of Meteorology, Australia)
ACCESS1-3	CSIRO-BOM	Australia	CSIRO (Commonwealth Scientific and Industrial Research Organisation, Australia), and BOM (Bureau of Meteorology, Australia)
BCC-CSM1-1	BCC	China	Beijing Climate Center, China Meteorological Administration
BCC-CSM1-1-M	BCC	China	Beijing Climate Center, China Meteorological Administration
BNU-ESM	GCESS	China	College of Global Change and Earth System Science, Beijing Normal University
CanESM2	CCCma	Canada	Canadian Centre for Climate Modelling and Analysis
CCSM4	NCAR	US	National Center for Atmospheric Research
CESM1-BGC	NSF-DOE-NCAR	US	National Science Foundation, Department of Energy, National Center for Atmospheric Research
CESM1-CAM5	NSF-DOE-NCAR	US	National Science Foundation, Department of Energy, National Center for Atmospheric Research
CMCC-CESM	CMCC	Italy	Centro Euro-Mediterraneo per I Cambiamenti Climatici
CMCC-CM	CMCC	Italy	Centro Euro-Mediterraneo per I Cambiamenti Climatici
CMCC-CMS	CMCC	Italy	Centro Euro-Mediterraneo per I Cambiamenti Climatici
CNRM-CM5	CNRM-CERFACS	France	Centre National de Recherches Meteorologiques / Centre Europeen de Recherche et Formation Avancees en Calcul Scientifique
CSIRO-Mk3-6-0	CSIRO-QCCCE	Australia	Commonwealth Scientific and Industrial Research Organisation in collaboration with the Queensland Climate Change Centre of Excellence
FGOALS-g2	LASG-IAP	China	LASG, Institute of Atmospheric Physics, Chinese Academy of Sciences
FGOALS-s2	LASG-IAP	China	LASG, Institute of Atmospheric Physics, Chinese Academy of Sciences
FIO-ESM	FIO	China	The First Institute of Oceanography, SOA, China
GFDL-CM3	NOAA GFDL	US	Geophysical Fluid Dynamics Laboratory
GFDL-ESM2G	NOAA GFDL	US	Geophysical Fluid Dynamics Laboratory
GFDL-ESM2M	NOAA GFDL	US	Geophysical Fluid Dynamics Laboratory

Model Name	Organization	Country	Organization Details
GISS-E2-H	NASA GISS	US	NASA Goddard Institute for Space Studies
GISS-E2-H-CC	NASA GISS	US	NASA Goddard Institute for Space Studies
GISS-E2-R	NASA GISS	US	NASA Goddard Institute for Space Studies
GISS-E2-R-CC	NASA GISS	US	NASA Goddard Institute for Space Studies
HadCM3	MOHC	UK	MetOffice Hadley Centre (additional HadGEM2-ES realizations contributed by Instituto Nacional de Pesquisas Espaciais)
HadGEM2-AO	MOHC	UK	MetOffice Hadley Centre (additional HadGEM2-ES realizations contributed by Instituto Nacional de Pesquisas Espaciais)
HadGEM2-CC	MOHC	UK	MetOffice Hadley Centre (additional HadGEM2-ES realizations contributed by Instituto Nacional de Pesquisas Espaciais)
HadGEM2-ES	MOHC	UK	MetOffice Hadley Centre (additional HadGEM2-ES realizations contributed by Instituto Nacional de Pesquisas Espaciais)
INMCM4	INM	Russia	Institute for Numerical Mathematics
IPSL-CM5A-LR	IPSL	France	Institut Pierre-Simon Laplace
IPSL-CM5A-MR	IPSL	France	Institut Pierre-Simon Laplace
IPSL-CM5B-LR	IPSL	France	Institut Pierre-Simon Laplace
MIROC-ESM	MIROC	Japan	Japan Agency for Marine-Earth Science and Technology, Atmosphere and Ocean Research Institute (The University of Tokyo), and National Institute for Environmental Studies
MIROC-ESM-CHEM	MIROC	Japan	Japan Agency for Marine-Earth Science and Technology, Atmosphere and Ocean Research Institute (The University of Tokyo), and National Institute for Environmental Studies
MIROC4h	MIROC	Japan	Atmosphere and Ocean Research Institute (The University of Tokyo), National Institute for Environmental Studies, and Japan Agency for Marine-Earth Science and Technology
MIROC5	MIROC	Japan	Atmosphere and Ocean Research Institute (The University of Tokyo), National Institute for Environmental Studies, and Japan Agency for Marine-Earth Science and Technology
MPI-ESM-LR	MPI-M	Germany	Max Planck Institute for Meteorology (MPI-M)
MPI-ESM-MR	MPI-M	Germany	Max Planck Institute for Meteorology (MPI-M)

Model Name	Organization	Country	Organization Details
MRI-CGCM3	MRI	Japan	Meteorological Research Institute
NorESM1-M	NCC	Norway	Norwegian Climate Centre
NorESM1-ME	NCC	Norway	Norwegian Climate Centre

7. APPENDIX B: A COMPARISON OF THE NORTH VS. SOUTH REGRIDDED GCM ENSEMBLE CELLS

Considering the re-gridding process to the NCEP standard resulted in two cells bisecting Peel region, a detailed analysis was undertaken to investigate what, if any, effect the use of the northern or southern cell would have on the final outcomes of this report. Many variables were calculated for this report, and clearly not all could be tested, but two of the primary variables (temperature and precipitation) were compared for the cells to determine if there was any significant difference. As indicated in the report text, it is not advisable to use two separate cell values for Peel since this could introduce an artificial gradient which is based purely upon the artificial boundary of the NCEP grid, rather than a real climate gradient.

Annual average temperature and precipitation value change are then checked for the northern and southern cells. The results are found in the table below.

This table compares the north/south cells and their change from the 1981-2010 baseline so we can compare the differences directly.

Variable	North RCP4.5	South RCP4.5	North RCP8.5	South RCP8.5
Ann Temp Change 2020s	1.3	1.3	1.4	1.4
Ann Temp Change 2050s	2.4	2.3	3.4	3.2
Ann Temp Change 2080s	2.9	2.8	5.6	5.3
Ann Precip Change 2020s(%)	3.5	3.2	2.8	2.8
Ann Precip Change 2050s(%)	6.5	6.0	7.5	6.8
Ann Precip Change 2080s(%)	7.7	6.6	10.4	9.9

Cell differences on the order of 3/10ths of a degree or precipitation changes of even 2% between the north and south cells are not significant in our calculations because the uncertainty in the model projections totally overwhelm the spatial differences found. Differences are on the order of tenths of degrees (largest difference found out near the end of the century). Differences between cells increase (as expected) towards the end of the century as all projections become more uncertain across emission pathways.

Additionally, if a 50/50 blend of the two cell values were to be used, the resulting value would be the straight average of the two cells and the resulting value would fall between the values shown above and be even closer to the northern cell value which was used.

It may prove illustrative to show the spread of the model ensemble between the two cells for mean annual temperature and mean annual temperature for the two RCPs. For each cell, we use all available GCMs and all available runs. What this illustrates is the ensemble mean delta (the value we use for further analysis) for the northern and southern grid cells is well within the +/- 1 standard deviation of the models themselves. **The greatest 'uncertainty' lies not in the selection of either the north or south grid cell in this area of the continent, but in the range of the actual GCM model projections.** Emission scenarios (RCPs) also have a significant effect, but we separate out this effect in the examples shown below – showing RCP4.5 and RCP8.5 on their own. These projection differences are related to different model formulations or 'physics'. This latter range far outweighs the north vs. south grid cell selection.

Grid cell selection would become significant if say, one cell was oceanic vs continental, or one cell represented a high-altitude vs low-altitude location, but in the Peel region these are not factors. In the Peel case, the selection of the north or south cells lead to near-identical projection conclusions which statistically are insignificant, and certainly are insignificant for decision makers. A decision maker would not alter his/her actions based upon these differences.

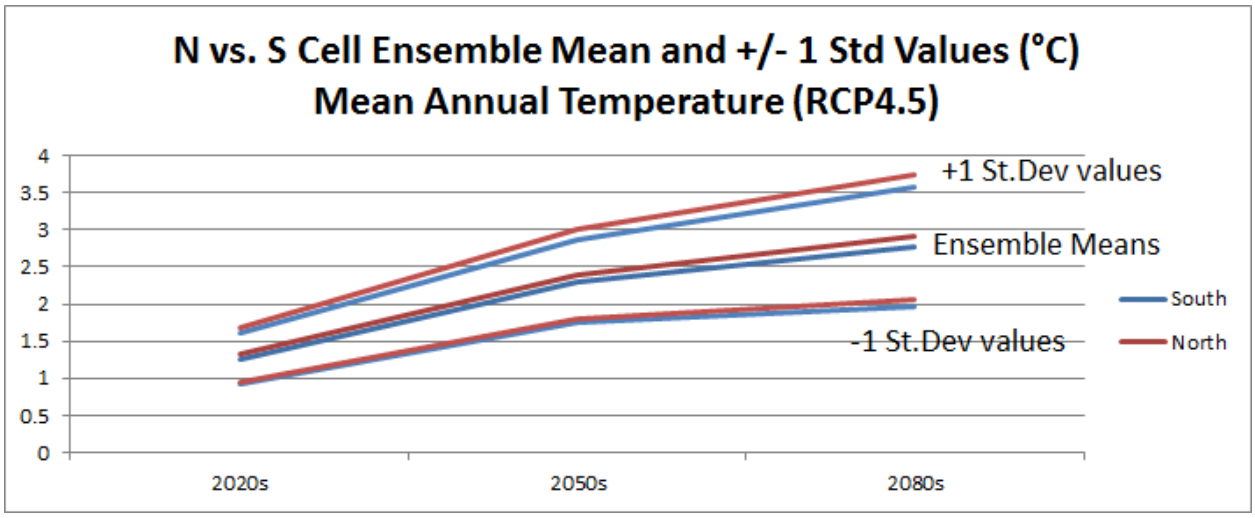

RCP4.5: This shows that for the North and South Cells, the projected change in mean annual temperature (the centre 2 lines) are well within the plus/minus 1 standard deviation values (top 2 and bottom 2 lines respectively for each cell).

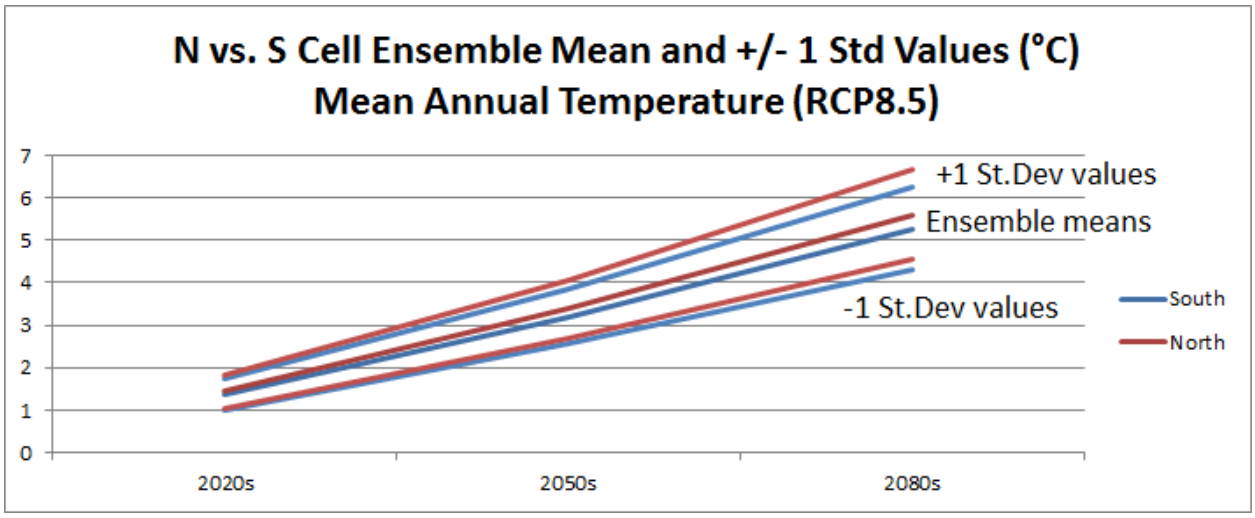

As above, except for RCP8.5 (the higher emission pathway), which results in greater temperature change for both grid cells. Again, although there are differences between the two cells, even at the end of the projection period, the difference is well within the model ensemble standard deviation.

The following similarly looks at cell differences in average annual precipitation.

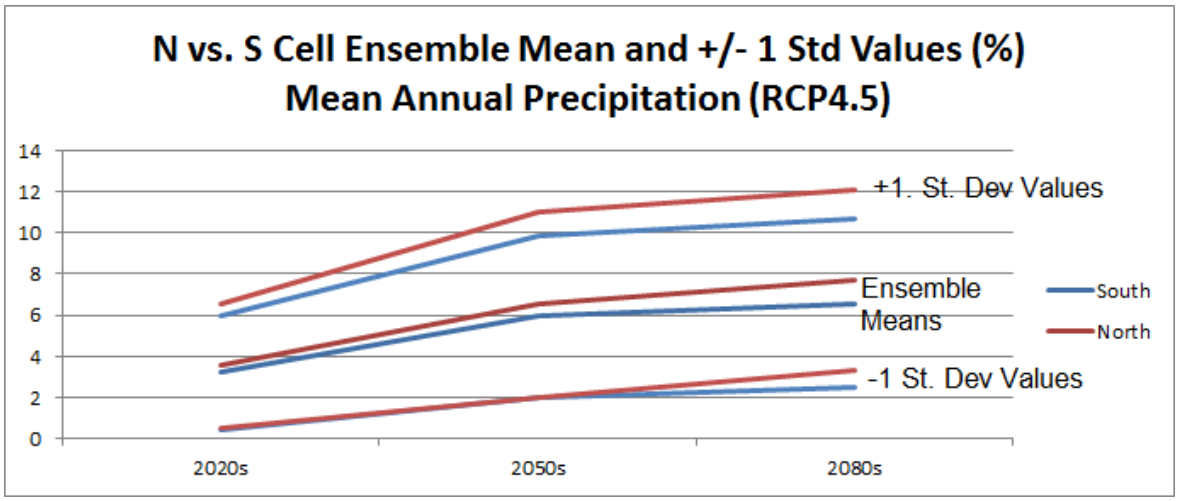

Again, for this RCP, ensemble mean differences between N and S cells are well within the ensemble standard deviations.

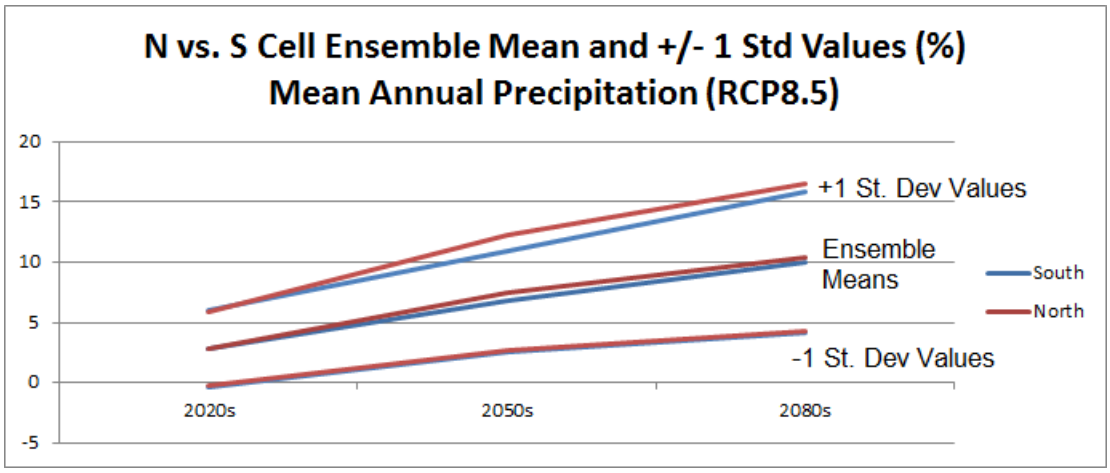

For this higher RCP8.5, ensemble means are near identical.

In the charts shown above, the plus and minus 1 standard deviations of the models are shown. The actual range of model output is much larger than the standard deviations. For example, although the mean ensemble projected annual increase in precipitation for the 2080s is near 10% for RCP8.5, the maximum value of all model runs is 29% and the minimum value of all models is -5% - a huge range. This indicates the selection of model can have a tremendous effect on outcomes versus the north or south grid cell issue considered here. By using many, many model runs a climate change signal is computed which is considered in literature to be the most desirable – the ensemble.

Additionally, the use of the northern cell produces the very slightly greater signal which is consistent with the observed trend historically of GHG emissions and the fact that globally we are always tending towards the 'high' side of projections. The northern cell generates the stronger of the two climate signals. The stronger CC signal of the northern cell used represents the best and most likely of the two cells given historical emission pathways.

For the reasons above, the use of the northern cell for the AR5 ensemble calculations for Peel was made. Indeed, the intention of the GCM ensemble was to provide a wide-range of estimates from many dozens of models from which conclusions of future projection uncertainty could be considered. The results provided in the climate report based upon the ensemble of the northern cell are representative as they stand and the inclusion of the second southern grid cell in the analysis would not alter the report findings in any meaningful manner.